Universität Bremen

# Exploring the Role of Excitatory-Inhibitory Dynamics in Synaptic Plasticity, Memory Stability, and Neural Coding

Mohammad Dehghani-Habibabadi

November 2023

# Exploring the Role of Excitatory-Inhibitory Dynamics in Synaptic Plasticity, Memory Stability, and Neural Coding

Vom Fachbereich für Physik und Elektrotechnik
der Universität Bremen

zur Erlangung des akademischen Grades eines
Doktor der Naturwissenschaften (Dr. rer. nat.)
vorgelegte Dissertation

von
Mohammad Dehghani-Habibabadi, M.Sc.

1. Gutachter: Prof. Dr. Klaus Pawelzik
2. Gutachter: Prof. Dr. Stefan Bornholdt

Eingereicht am: 30.11.2023
Datum des kolloquiums: 27.05.2024

# Abstract

This thesis provides an exploration of the brain's neural dynamics, shedding light on the mechanisms underlying learning, memory retention, neural synchronization, and sensory processing. Through a comprehensive series of studies, we explore how neurons adjust their connections in response to specific patterns, a fundamental aspect of memory and learning. This synaptic plasticity demonstrates a tight balance between different neural adaptations, allowing the brain to retain old memories while continuously forming new ones.

The Investigation proceeds with an investigation of collective neural behavior, in particular the transitions between different firing states within networks of neurons. Our results characterize the critical points that govern these transitions, contributing significantly to the understanding of large-scale neural coordination. This insight highlights the importance of maintaining a balance between excitatory and inhibitory neurons, which directly impacts the brain's ability to process information and maintain functional states.

Delving deeper into the mechanisms of sensory processing, our study examines the brain's response to visual stimuli, specifically under circumstances that generate gamma oscillations in the visual cortex. The interaction between external stimuli and brain wave activity shows layer-specific effects, providing a detailed insight into the neural basis of perception and cognition.

In conclusion, this thesis presents a focused view of neural function, from synaptic alterations to network dynamics and sensory processing. It highlights the brain's remarkable capacity for stability amidst constant change, a foundational aspect underpinning the continuity of memory and the adaptability of learning. The collective findings of study offer profound implications for both neuroscience and the development of advanced artificial neural systems, emphasizing the necessity of intricate balancing in both natural and artificial learning environments.

# Contents

# Chapter 1

# Introduction

The balance between excitatory and inhibitory neural activities, commonly referred to as the excitation/inhibition (E/I) balance, is a fundamental mechanism governing the functioning of neural networks. This balance has been shown to participate in several functions of neural networks.

The concept of dynamic stability is directly related to the balance between excitation and inhibition. This stability can be examined in terms of two main aspects. Initially, it refers to the network's ability to maintain a consistent, balanced level of neural activity under steady internal and external inputs, thereby establishing a baseline of predictable neural activity. Furthermore, dynamic stability includes the network's ability to self-adjust and adapt, specifically its ability to return to a balanced state after facing perturbations. Perturbations can range from external stimuli like sensory input to internal changes, such as changes in neural connectivity or changes in the levels of neurotransmitters.[32,59,129]

The maintenance of dynamic stability is essential to prevent the network from going into a problematic mode of operation, such as hyperactivity or complete inactivity. Hyperactivity is an undesirable state where there is excessive neuronal activity, potentially leading to problems such as neuronal fatigue. Conversely, total inactivity indicates that the neural network is unable to respond to external stimuli and is not functioning optimally for information processing. Therefore, dynamic stability functions as a protective mechanism, ensuring that the neural network remains both robust and adaptable. This enables the system to maintain a well-balanced level of activity despite any external or internal disturbances it may encounter.[1,24,69,75,150]

This balance serves as a crucial factor in optimizing synaptic gain modulation, signal-to-noise ratios, and modulation of neuronal responsiveness to heterogeneous stimulus input. Through these regulatory mechanisms, neural circuits achieve an operational state.In this highly selective period of responsiveness, the network employs salience-based signal amplification to prioritize the processing of behaviorally or cognitively relevant stimuli. In addition, a suppression mechanism is invoked to reduce or filter out non-salient stimuli, thereby reducing computational noise and allowing for a more focused distribution of neural resources. This dynamic interplay between enhancement and attenuation mechanisms allows the network to adapt its functional architecture, effectively adapting its computational performance to the specific demands imposed by varying external and internal conditions.[11,17,25,83,113,123]

Last but not least, the role of the balance between excitatory and inhibitory signals in facilitating information processing is crucial for encoding, transmitting, and decoding neural signals, as well as effectively organizing and integrating them. The balance ensures that the network can perform complex computational tasks such as pattern recognition, memory storage and retrieval, and decision-making with high accuracy and efficiency.[153]

Therefore, it is important to note that the E/I balance is not only static but a dynamic state that is fundamental to the computational capability, adaptability, and accuracy of the neural network. Furthermore, this dynamic equilibrium is essential for achieving strong dynamic stability, finely modulating neural responses, and enabling effective data processing.
In addition, this synaptic balance is critical in defining neuronal responses to sensory inputs, which are fundamentally linked by cause-and-effect relationships in neural pathways. It functions as a modulation mechanism, finely adjusting the impact of incoming sensory data within the neural network. The balance between excitatory and inhibitory synaptic currents enables neurons to respond to sensory input with both precision and adaptability. This ability is crucial for performing complex neural functions like identifying objects, navigating space, and consolidating memories. This state of synaptic homeostasis is essential to ensuring the adaptability, precision, and overall functional efficacy of neural systems. In fact, synaptic homeostasis functions as a self-regulating mechanism that adjusts synaptic strength to maintain overall network stability, a phenomenon known as preventing the nervous system from collapsing into chaos.[19,42,81,90,120,135,138,151]
However, dysregulation of the cortical E/I balance has emerged as a critical etiological factor underlying several neurological disorders characterized by perturbations in the structural, functional, or biochemical substrates of the nervous system. Such imbalances can lead to a range of cognitive, emotional, and motor impairments, such as epilepsy, Parkinson's disease (PD), Tourette's syndrome, autism spectrum disorders (ASD), and schizophrenia.[125] In the following, the relationship between these conditions and the E/I balance will be further explained.
In the case of seizures, the balance between excitatory and inhibitory neural activity tends to heavily shift toward the excitatory side, resulting in a high E/I ratio. This imbalance leads the brain's neuronal networks to become hyperexcitable, contributing to sudden and recurrent seizures. The risk of seizures increases not simply due to an increase in excitation but also because of the ratio of excitatory to inhibitory activity. A slight shift in this ratio can significantly change the stability of neuronal networks, increasing their sensitivity to external stimuli that could trigger a seizure. Medicines called anti-convulsants aim to restore both balance and a more stable E/I ratio by suppressing excitatory activity or enhancing inhibitory signals.[30,45,85,87]
In contrast to the seizures, Parkinson's disease exhibits an opposite trend. In areas like the basal ganglia, the E/I balance often leans more towards inhibition, leading to a decreased E/I ratio. As a consequence of this distorted balance and ratio, motor control is diminished, leading to symptoms such as muscle rigidity and slowed movements (bradykinesia). In the context of PD, enhancing excitatory signals or reducing inhibitory ones can aid in recalibrating the ratio and bringing back a more favorable E/I balance, subsequently enhancing motor functions. For example, dopaminergic therapies aim to modulate this balance.[51,71,140,145]
In Tourette's syndrome, a neurodevelopmental disorder characterized by repetitive, involuntary motor and vocal tics, there is typically an elevated E/I ratio. This ratio is defined as an excess of excitatory activity relative to inhibitory activity. This increased excitatory state disrupts the normal balance, leading to spontaneous, uncontrolled motor tics and vocalizations. For individuals with Tourette's, the frequency and intensity of tics often hinge on this imbalance. Treatment strategies for Tourette's aim to decrease this excitatory activity, using medication such as antipsychotics or behavioral interventions, to return the E/I ratio to a more balanced state.[39,61,104,114]
In autism, the E/I balance and ratio can also be variable, partially explaining the broad nature of the disorder. In some cases, there is a higher ratio of excitatory to inhibitory activity, making sensory stimuli overwhelming and potentially leading to social difficulties. In such instances, medications like antipsychotics or mood stabilizers may be prescribed to modulate

the excitatory activity. On the other hand, there may be an abnormally low E/I ratio in some cases, resulting in reduced responsiveness to social cues and dampened emotional responses. In these situations, treatments might include stimulant medications or selective serotonin reuptake inhibitors (SSRIs) to address the low excitatory activity. Both extremes of the E/I ratio can contribute to the wide range of symptoms seen in autism, making treatment particularly demanding.[5,7,22,72,100,101,110,132,143]

In schizophrenia, the balance and ratio of excitatory and inhibitory signals in key brain regions, such as the prefrontal cortex, can have a significant impact on cognitive and emotional functioning. For example, an elevated E/I ratio, characterized by excessive excitation, could lead to cognitive overload, impairing attention and working memory. Conversely, a reduced ratio could result in neural network hypoactivity, affecting the ability to process information and make decisions. In the same way, emotional regulation can be disturbed by these imbalances in the E/I ratio, resulting in a wide range of emotional symptoms, from heightened sensitivity to emotional numbness.[10,55,76,78,94,95]

Therefore, it is very important to understand the balance and ratio of excitatory to inhibitory neural activity in order to fully comprehend the complicated pathophysiology of these various neurological disorders. A more focused and effective approach to treating these disorders may be possible by targeting these specific imbalances and imbalanced ratios.

Recent theoretical and empirical research increasingly emphasizes the importance of the balance between excitatory and inhibitory (E/I) synaptic inputs in the functioning of neurons. This balance is not just a byproduct of neural architecture; it serves as an active mechanism that enables diverse neural computations and dynamics. Thus, an understanding of this balance is not only essential for unraveling the fundamental mechanisms that govern neuronal behavior but also for developing a coherent picture of the broader functionality of neural networks.

Following the former studies, in this research, I have conducted three sets of studies in three primary areas of Neuroscience and Physics. My initial efforts focused on identifying the biological foundations that enable neural networks to perform self-supervised learning of spatiotemporal embedded patterns. In this context, I concentrated on inhibitory and excitatory synaptic plasticity. I investigated the hypothesis that synaptic plasticity might support a balance between excitatory and inhibitory mechanisms while facilitating the learning of embedded patterns that are robust to different noises. In the following investigation, I did not focus on the origin of the balance between excitatory and inhibitory neuronal activities. Instead, I manipulated the ratio of excitatory to inhibitory neurons to study its influence on scale-free dynamics and to find out if and how this affects the dynamic range. In the last study, I investigated the role of excitatory neurons in modulating gamma oscillations in the visual cortex, specifically under the influence of optogenetic and visual stimuli. I investigated the effect on gamma oscillations by varying the intensity of optogenetic laser activation of excitatory neurons, which indirectly shows how inhibition and excitation work in different areas of the visual cortex.

## 1.1 Learning of Spatio-Temporal Spike Patterns

One of the goals of this research project was to find out if combining realistic learning mechanisms can contribute to the emergence of a balance between excitation and inhibition, like what is seen in the brain's cortex.[49,92] The answer to this question has substantial implications for comprehension of neural networks and brain functioning.

Firstly, the modeling highlights the importance of synaptic plasticity in the learning process and in encoding specific patterns within the neural network. This understanding carries substantial

implications for both basic neuroscience and the advancement of efficient machine-learning algorithms and artificial neural networks. Secondly, the study highlights the essential function of plasticity in maintaining a balanced membrane potential among neurons. A balanced membrane potential is crucial for optimum neural circuit operation, impacting factors ranging from information processing to the efficiency and speed of neural computation.[32]
Therefore, the computational model serves as an essential tool for studying the dual function of plasticity, providing insights that are highly relevant to both neuroscience and the wider field of computational biology.
In this context, it is generally assumed that the neuron and its synapses are the primary focus and that the input received by the neuron is crucial.

However, it should be noted that although early sensory cortex areas primarily represent stimuli via spike rates, experimental evidence demonstrates that time-based information is also processed carefully. Evidence from a diverse range of sensory cortices, including visual, auditory, olfactory, and somatosensory, suggests that neurons can respond deterministically to incoming stimuli, suggesting the possibility of precise spike codes.[23,28,58,62,107,108,133,137]
This level of precision could be reached by changing the rate of spikes in large groups of neurons, but it is an interesting idea that responses from individual neurons may be especially important in higher-order cortical areas like the frontal cortex where firing rates are particularly low, suggesting a unique role for single-neuron dynamics in supporting complex cognitive functions. This concept expands our understanding of neural encoding and decoding mechanisms and provides an opportunity to further explore the complex mechanisms of neural activity.[18,53,60,89,109]
In the fields of neuroscience and computational biology, significant attention has historically been given to the biological plausibility of synaptic plasticity and the balance between excitation and inhibition. However, a number of theoretical studies have set aside these realistic constraints to focus simply on understanding mechanisms that could enable precise encoding of spatiotemporal patterns within neural networks.
These theoretical studies show that even simple neural models, called ”integrate-and-fire” neurons[20,21], can detect and respond to complex spatiotemporal input spike patterns when they possess suitable synaptic weights. To explain further, an integrate-and-fire neuron integrates input signals until a certain threshold is reached or exceeded; at that point, it fires an action potential, or ”spike”.
The Tempotron model is a primary example of this type of neuron.[46] The Tempotron was developed as an advanced version of the classic Perceptron model.[89] It was designed to classify and detect complex spatio-temporal patterns by generating a spike in response to a given set of inputs and no spikes for some other spatio-temporal patterns. The model implements a supervised algorithm to adjust the weights of the neuron’s input signals, also known as afferents, to either enhance (strengthen) or attenuate (weaken) them.
An additional example is the Chronotron, which focuses on time-based rather than label-based learning, and was introduced on the basis of the Tempotron. The Chronotron, like the Tempotron, aims to achieve precise temporal encoding, but with the specific goal of pinpointing the timing of the neuron’s response.[35,36,88] The Chronotron objective can be achieved by several more or less realistic synaptic mechanisms.[6,149]
In summary, the Tempotron and Chronotron models are pioneering theoretical studies that challenge and extend our current understanding of neural dynamics, specifically in the areas of pattern recognition and temporal coding. These models take a different approach from most traditional research in neuroscience, which aims to match biological plausibility closely. They suggest that without relying on the exact mechanisms observed in real neural systems, it is possi-

ble to achieve intricate and subtle forms of pattern recognition. These models imply that neurons are not just simple signal transmitters; rather, they may have the computational capacity to perform complex tasks involving precise timing and complex pattern recognition. They provided a foundation for new directions in computational neuroscience and artificial neural networks. They have opened the path for innovative research that could change our understanding of both biological brains and artificial systems and invite us to reconsider the computational complexity that neurons can possess. The development of multi-layer neural networks, which use spike timing and bio-inspired computing, represents an extension of these studies. This development might enable these networks to potentially perform tasks more efficiently than algorithms that are not based on bio-inspired computing.[68]

However, in fact, the Tempotron and Chronotron models are supervised learning algorithms, a feature that raises questions when trying to adapt these models to biological systems. This is because a biological neuron receives input that is not labeled exactly as it is in supervised learning models. The input is continuous, subject to temporal biases, and often embedded in a noisy background. This variation raises fundamental questions about the applicability of these models to real neural systems.

In more detail, the challenge is how these theoretical models, which rely on labeled data, would map onto the real mechanisms of synaptic plasticity. In the context of these models, it is unclear how neurons, within a biological context, would understand which aspects of an input to focus on when the ”label”—or meaningful context—may not appear until much later. The traditional theories of synaptic plasticity do not easily explain such delayed labeling. For example, Hebbian plasticity relies on the nearly simultaneous firing of connected neurons, as expressed in the phrase ”neurons that fire together wire together”, but does not explain how labels are introduced later on.[50]

The challenge is to introduce timing into models of synaptic plasticity in a biologically plausible way. Moreover, these theoretical models assume a clean learning environment, which is far from the noisy real-world conditions in which neurons function. In contrast, real neurons must perform reliably in the face of noise and variability, raising the question of how these models can be adapted to more closely resemble these conditions.

Therefore, although the Tempotron and Chronotron models offer valuable theoretical insights, applying them to biological systems in a straightforward manner is not without challenges. Their dependence on supervised learning and labeled data introduces gaps that need to be bridged for these models to be considered truly reflective of biological neural learning.[128]

The challenge of combining the supervised nature of models like the Tempotron and Chronotron with the unsupervised learning environment of biological neurons has recently been addressed in a novel way. Robert Gütig demonstrated that neurons can recognize spatio-temporal patterns, even when these are embedded in noisy backgrounds. This recognition was achieved through ”weak supervision”, which relies on optimizing synaptic efficacy based on a known number of pattern repetitions rather than explicit labeling of data.[47]

The study’s findings are based on the features of the N-methyl-D-aspartate (NMDA) receptor, a well-researched element in synaptic plasticity.[8,27,82]

This model provides a connection between the domain of theoretical models based on supervised learning and the actual circumstances of biological neurons, which function through unsupervised learning processes. The study based on weak supervision brings us closer to a model that more accurately represents the biological mechanisms of neural pattern recognition. Moreover, the study emphasizes the role of the NMDA receptor in synaptic plasticity, reinforcing its importance as a key mediator in the learning process. The learning rule proposed based on the NMDA receptor offers a biologically plausible mechanism that aligns well with observed neural

behaviors. This not only enhances the validity of the model but also offers a potential pathway for integrating it into broader theories of neural function and learning. Finally, the study provides an area for further research to enhance our understanding of how weakly supervised or even unsupervised learning mechanisms might work in both biological and artificial neural networks. Indeed, by getting closer to the biological mechanisms that govern neural activity and learning, we might be able to develop more plausible models that could have applications in fields ranging from neuroscience to machine learning and artificial intelligence.[47]

Although Gütig's study addresses some of the problems associated with applying supervised learning models to biological models, it does not fully address the biological plausibility concerns. The model deviates from Dale's rule, which states that a synapse can only be either excitatory or inhibitory, not both. This deviation from Dale's rule raises questions about the biological accuracy of the model.

Furthermore, the model operates under weak supervision. The questions arising from such weak supervision are particularly interesting. In particular, how would this mechanism manifest itself in a biological context where labeling and even the concept of a "known number of repetitions of embedded patterns" may not be clearly defined?

Additionally, the model requires precise fine-tuning of synaptic weight changes, suggesting that only a small subset of possible weight changes would lead to the desired learning outcome. This selection of candidate weights does not fit biological variability and complexity, raising further questions about the biological plausibility of the model. Therefore, this question remains unanswered: can mechanisms of synaptic plasticity be identified that enable neurons to autonomously specialize in detecting statistically dominant patterns in their input? If so, the identification of such mechanisms would advance our understanding of neural plasticity and learning and would provide a bridge between theoretical models and biological reality. Identifying or developing such a mechanism is a vital area for future research in both computational neuroscience and the broader field of machine learning.

I address this issue in paper 2.1. The research employs basic Hebbian mechanisms to facilitate the plasticity of excitatory and inhibitory neurons. This approach is similar to the functioning of NMDA receptors in excitatory synapses. In addition, the study follows Dale's principle by ensuring that neurons maintain their specific inhibitory or excitatory roles without switching between the two during the learning process.

We employed three realistic mechanisms that appeared to be sufficient for the self-organization of pattern recognition in single neurons. First, we imposed limits on synaptic effectiveness to control the instability of Hebbian mechanisms. Second, we considered homeostatic plasticity, which is applied to excitatory synapses. This plasticity regulates the firing rate to match the biological firing rate.[131,134] If the actual firing rate exceeds the target rate, each synapse will be down-scaled, and if the firing rate falls below the target rate, it will be up-scaled. This synaptic scaling is crucial for maintaining system stability. Third, in this methodology, we utilized post-synaptic hetero-synaptic plasticity, which induces a competition for resources provided by the post-synaptic neuron (e.g., receptors) to result in negative changes in efficacy (i.e., long-term depression; LTD).

The algorithm supports the emergence of a balance between excitation and inhibition, which is in line with the findings of the global and detailed balance of excitation and inhibition in the cortex. During periods without a pattern, excitatory and inhibitory inputs are in global balance. At times when a learned pattern is present, excitatory and inhibitory inputs cancel each other out in temporal detail, showing detailed balance.[32,59,92]

In 2.1 we showed that pattern recognition is more reliable when it learns from patterns that include timing changes and Poisson-distributed rate modulation instead of exact repetitions. This

suggests that the proposed mechanisms are adaptable to patterns that are not strictly timed or have a temporal rate code. However, robust pattern recognition resistant to temporal jitter and noise is demonstrated when the algorithm is applied to strictly timed patterns.

On the other hand, the capacity to acquire new information while maintaining memory characterizes functional neural systems. This dual ability presents a dilemma for scientists: how can synapses combine plasticity with the ability to change and learn at the same time? This question is important not only for understanding basic brain function but also for developing effective machine learning systems, which often struggle with the same duality.[93]

The processes underlying the balance between stability and plasticity in neural networks can provide insights into the pathophysiology of neurological and psychiatric conditions such as Alzheimer's disease, Parkinson's disease, and Schizophrenia, which are associated with disruptions in synaptic plasticity and stability. For instance, in Alzheimer's disease, amyloid beta accumulation and tau pathology cause a loss of synaptic plasticity, leading to synapse loss and disruption of neural networks. In Parkinson's disease, the degeneration of dopaminergic neurons disrupts the stability of motor control networks, leading to the characteristic symptoms of tremors and rigidity. These networks cannot compensate for plasticity because of the progressive loss of neurons. In a similar way, schizophrenia is characterized by a disruption in the neural circuitry underlying cognitive functions and emotional responses, suggesting an underlying problem with synaptic stability and plasticity. It has been hypothesized that NMDA receptor hypofunction in schizophrenia impairs synaptic plasticity and may contribute to the cognitive deficits and negative symptoms observed in schizophrenia patients.[26,38,65,77,84,99,127]

Moreover, the brain's ability to be plastic, allowing it to learn and adapt to new situations, is vital. Understanding how neural networks maintain consistency amidst continuous plasticity is critical to understanding processes such as learning, memory consolidation, and retrieval. Note that this adaptability is a continuous process, with neurons constantly adjusting their synaptic connections to achieve optimal biological firing rates, highlighting the perpetual nature of neural plasticity.[131,134]

Furthermore, a more detailed understanding of how stability and plasticity are balanced within neural networks could pave the way for the development of stronger and more effective artificial neural networks. Specifically, networks that are overly stable may struggle to learn new data, while those that are overly sensitive to changes may experience information loss, a phenomenon in which new learning overwrites previously stored data.[2,37,67]

Therefore, it is critical to address the mechanisms necessary for a neural network to maintain both stability and adaptability. This is often referred to as the stability plasticity dilemma, which is a prominent challenge in understanding both natural and artificial neural functionalities. Identifying solutions to this problem is essential for the advancement of cognitive science and neural network technology.[93]

It is important to note that the brain appears to use multiple levels of memory storage and consolidation, from the cellular to the network level, to manage this balance between plasticity and stability. It has been proposed that several mechanisms, including immediate early genes, long-term potentiation, and the integration of new neurons into existing circuits ( e.g., in the hippocampus), contribute to this balancing process.[15,142]

Taken together, the capacity of neural systems to learn while preserving past data presents a critical issue that pertains to the formation and maintenance of memories. However, the mechanisms that allow this delicate balance between plasticity for learning and stability for memory maintenance are not fully understood. This represents a significant gap in our understanding of brain function and a pressing challenge for the field of neuroscience.

In 2.1, we studied this issue for a single neuron and a network of neurons. The results showed ex-

tremely long memory persistence for a single output neuron when learning continues with noise input. For the network of output neurons, the question is whether the mechanism supports incremental learning, where patterns occur rarely and are intermingled with random activity and/or different patterns. This incremental learning of sets of patterns in neural populations is supported by including competition for patterns induced by pre-synaptic hetero-synaptic plasticity.[130] Within this neural architecture, individual output neurons are tuned to recognize specific groups of input patterns, resulting in a collective system that accurately encodes the ”what” and ”when” of those patterns. This organized specialization allows for an accurate mapping of the information presented to the input.

However, the model in 2.1 faces a challenge with sequential learning: when a new embedded pattern is introduced after the initial pattern has been learned, the system experiences a profound memory disruption, where the memory of the previous pattern is overwritten by the new one. This results in the loss of the first learned pattern as the system adapts to recognize the newly presented information.

In the second study in 2.2, we showed that when training spikes are subject to both jitter (temporal variability) and randomness (stochasticity), previous memories are preserved even as new learning occurs. This variety of input ensures that only a specific subset of synaptic weights are selected for adjustment, pushing them toward a state where synaptic scaling-adjustment of the strength of connections based on activity levels-promotes stability.

## 1.2 Excitatory / Inhibitory Ratio and Dynamic Range

In 2.1, it is shown that synaptic plasticity can balance a neuron's input.[41] However, an excess of excitatory neurons can lead to over-excitation, which can ultimately lead to neuronal fatigue or excitotoxicity, a pathological state in which neurons are damaged or destroyed by excessive stimulation. On the other hand, an excess of inhibitory neurons can diminish the activity of the network to such an extent that its functional capacity is reduced. Therefore, achieving a suitable balance between these two types of neurons is crucial for maintaining the proper health and efficient functioning of the nervous system.[12,59,112,121,125]
Moreover, experimental evidence shows that approximately $20\%$ of neurons are inhibitory GABAergic neurons in the cortex. This number has significant implications for the structure and function of neural networks. The presence of this subset of inhibitory neurons helps regulate the excitatory activity of the remaining $80\%$, preventing the network from becoming either hyperactive or too inhibited. These GABAergic neurons have a vital role in shaping neural responses, perfecting neural codes, and therefore contributing to the general stability and adaptability of the network.[29,32,52,56,64,86,122,126]
While inhibitory neurons are fewer in number, they have a significant impact on the behavior of the neural network, providing both the flexibility to learn and the stability to retain information.[43,59]
Therefore, understanding the role and optimal ratio of excitatory to inhibitory neurons is crucial not only for unraveling the functioning of biological brains but might also be crucial for designing effective and balanced artificial neural networks.
Although the importance of the E/I ratio in network dynamics, especially at high levels of connectivity, has been emphasized in previous research[13], an intriguing bridge between these concepts lies in how this ratio in neural networks directly influences the network's dynamic range. In this context, "dynamic range" characterizes the network's ability to adapt and respond to diverse conditions and stimuli, and the question is how this dynamic range is linked to the specific ratio of inhibitory to excitatory neurons.
On the other hand, experimental evidence indicates that the dynamics of neural avalanches, a phenomenon where a series of correlated neuronal firings propagate through a neural network, is closely related to the balance between excitatory and inhibitory neuronal activity (E/I balance). This relationship has been observed in experiments in cortical cell cultures, anesthetized rats, and awake monkeys.[14,97,116,146] Typically, the activation of a single neuron or a small number of them starts this cascade of neuronal activity. Specifically, a neural avalanche is not merely the haphazard firing of neurons but a highly organized sequence where every neuronal activation is related to its preceding activations. This pattern of activations may extend across various clusters of neurons, producing intricate connections within the neural network.[14,33,111]
The emergence of these avalanches is not a random occurrence; instead, it is strongly linked to the balance between excitatory and inhibitory neuronal activities within the system. Several experimental studies have provided substantial evidence for the central role of the E/I balance in governing the dynamics of neural avalanches. For example, cortical cell cultures provide a simplified and highly controlled environment to observe the initiation and propagation of neural avalanches, aiding in isolating the influence of E/I balance from other potential variables. In vivo studies of anesthetized rats and awake monkeys further emphasize the importance of this balance by enabling the examination of neural avalanche phenomena in more complex and naturalistic settings.[97,116,146] In more detail, research has found neural avalanches displaying global behavior within neuronal activity patterns both *in vitro* and *in vivo*.[14,40,96,146] Studies have shown that optimal brain function, including phase synchrony[146], information storage[124], communica-

tion, information transition[14], computational power[16], and dynamic range[66,117], occurs when the brain is operating at or near criticality. At the critical point, a boundary is established between an ordered and a less ordered state that exhibits distinct scaling behaviors.[40] At this point, neural networks exhibit a power law distribution in a statistical collective behavior of the system, such as a neural avalanche. Studies have shown that avalanche size and lifetime distributions are indicators of long-range correlation.[14]

The distribution of neural avalanche size exhibits a widely varying profile, but is described by a single universal scaling exponent, $\beta$, in size, $P(S) \sim \bar{S}^{\beta}$, and a single universal exponent in duration, $\tau$, $P(T) \sim \bar{T}^{\tau}$, where $S$ and $T$ denote the size and duration of the avalanches, respectively. Power-law distributions were observed in neuronal avalanches present in cortex slice cultures of rats in vitro, in the cortical layer 2/3 of rats during the first and second week postnatal[44], Local Field Potentials (LFPs) of anesthetized cats[48,102], newborn rats[146], and monkeys[96,102].

In the context of neural avalanches, the use of the physics of critical phenomena analysis offers a convincing methodological approach for quantitative investigations. This enables an extensive study of phase transitions in neural systems, including the characterization of the order of such transitions and the evaluation of their dynamic ranges. In particular, it characterizes whether these transitions are first-order (characterized by abrupt changes) or second-order (characterized by gradual shifts). This evaluation also provides a method for determining the dynamic range of neural systems and, thus, their ability to effectively process and respond to a range of stimulus levels.

The concept of an ”order parameter” is a foundational basis for the description of phase transitions. An order parameter is a measure that determines the level of order at the boundary between two distinct phases. This parameter can be zero in one phase and non-zero in the other and therefore serves as a critical indicator of the state of the system. The order parameter quantifies the amount of order in phase transitions, such as solid to liquid (melting), liquid to gas (evaporation), or magnetic transitions in materials, and can help predict or describe the emergent properties of a system undergoing a phase change.

In the domain of critical phenomena in physics, order parameters have been crucial for characterizing transitions from one state to another. For example, in the Ising model of magnetism, the order parameter, *M*, which typically represents the net magnetization of the system and is the sum of all the individual magnetic moments (or spins) in the material, is utilized to distinguish a transition from a disordered state to an ordered magnetic state. An ordered state in a magnetic system might signify that all of the magnetic moments (spins) are aligned, whereas in a disordered state, they would be randomly oriented.[70]

In neural systems, transitions of interest often involve moving from a de-synchronized to a synchronized state of neuronal firing. This occurs despite the fact that neural systems inherently operate far from thermodynamic equilibrium. The order parameter used in this study aligns with the Kuramoto model of coupled oscillators. The Kuramoto order parameter quantifies the degree of phase synchronization within a population of oscillators, such as neurons, providing a measure of system synchronization. In more detail, the Kuramoto order parameter is a powerful measure of the degree of phase synchronization within a population of oscillators, such as neurons. This measure shows how well the oscillators are in phase with each other and provides clear indications of the level of system synchronization. The order parameter, denoted as ”$r$”, typically ranges from 0 (no synchronization) to 1 (full synchronization). Mathematically, this order parameter is calculated by averaging the exponential of each oscillator’s phase, which is then normalized by the total number of oscillators. This calculation takes into account both the amplitude and phase of the oscillators, which provides a comprehensive measure of synchro-

nization.[3,73,74,98,103,105]

In summary, critical phenomena analysis and the order parameter concept are multidisciplinary tools offering valuable insights into complex systems ranging from magnetism to neural networks. This approach offers a quantifiable set of tools to analyze the intricacies associated with neural avalanches, improving our comprehension of their involvement in neural function and information processing. Taken together, the analysis based on the physics of critical phenomena, considering neural avalanches and order parameters, may shed light on the understanding of the E/I ratio.

To this end, in 2.3 we initially measured the transition in a leaky integrate-and-fire network by introducing a Kuramoto order parameter. This parameter is based on the coupling between sequences of spikes and the phase of temporal fluctuations of the population-average voltage (PAV).

In this work, we showed that by increasing the coupling between neurons, i.e., the connection strength $K$, a second-order transition from desynchronized firing with low spike-phase coupling (SPC) to a synchronized firing state with high spike-phase coupling is observed at the critical value $K_c$. This finding is independent of the network's inhibition, as demonstrated in 2.4.

In this study (2.4), we investigated the effects of inhibition on network behavior and whether the probability of finding the network in the critical regime increases or decreases. To determine differences between inhibition levels, we utilized the order parameter (defined in 2.3) to measure the network's transition. We then conducted dynamical range analysis to identify differences between inhibition percentages (i.e., different E/I ratio).

Here, the term dynamic range refers to the range over which an order parameter changes as a function of a control parameter, such as connection strength $K$.

## 1.3 Effects of Optogenetic Stimulation on Gamma Activity in The Visual Cortex

Substantial E/I balance has been documented in various contexts, e.g., somatosensory cortex [141], auditory cortex [138,151,152], cortical up states both in vitro [119] and in vivo [49], gamma oscillations in vitro and in vivo [9], as well as spontaneous activity [92]. Studies have also shown the stability of the ratio between excitatory and inhibitory synapses on various dendritic branches of neurons. [57] For a more comprehensive understanding of the precision and presynaptic origins of this balance, exploring optogenetic techniques shows promise. Optogenetics is a method of neuromodulation that involves a combination of techniques from optics and genetics, enabling the control and monitoring of individual neural activities in living tissue with the ability to measure the effects of manipulation in real-time. [31,147,148]

In summary, the balance between excitatory and inhibitory activity is highly dynamic, sensitive to context and not static. This has been historically difficult to understand because of the lack of tools to selectively modulate neural circuits in real-time, but optogenetics enable us to overcome this issue. [4]

In more detail, this method has completely revolutionized the field by allowing researchers to selectively target either excitatory or inhibitory neurons in a specific region of the brain. This is achieved through the use of specific promoters for certain types of neurons. For instance, the CaMKIIa promoter can be employed to target excitatory neurons, while the Gad2 promoter can be used to target inhibitory neurons. Then, by genetically engineering only the specific subtype of neurons, researchers can independently modulate the activity of either the excitatory or inhibitory neurons to understand how each contributes to the overall E/I balance. [4,80,139,148]

Optogenetics also enables real-time manipulation and monitoring. Researchers can introduce a sudden imbalance, such as overexciting a particular neural circuit, and then monitor how the system compensates. Does it increase inhibitory signaling? How quickly? These were questions that were previously challenging to address. [136]

However, while optogenetics is a powerful tool, it is not without its ethical and technical challenges. The implantation of optical fibers through surgery limits its application, and the introduction of foreign genes into an organism's genome raises concerns about long-term effects. Furthermore, translating findings from animal models to humans is not always a straightforward process. Despite these challenges, optogenetics remains one of the most promising techniques for advancing our understanding of the brain. [34]

In vitro and in vivo studies have extensively documented the E/I balance in gamma oscillations. [9] On the other hand, advances in optogenetic techniques have deepened our understanding of the critical mechanisms underlying gamma oscillations, particularly for visual processing and cognition. In particular, there is a correlation between gamma band activity and the speed of visual change detection in humans, and extensive research investigating the correlation between gamma oscillations and visual stimuli, highlighting its importance in understanding cognitive processes. [54,106,115,118]

In addition, the researchers investigated the visual dependence of the power spectrum on the local field potential within the primary visual cortex (V1). The results showed a positive correlation between the amplitude of gamma oscillations and the power of a visual stimulus. In other words, as the strength of the visual stimulus increased, so did the intensity of gamma oscillations within the modeled network. This relationship highlights the potential adaptability of neural circuits in V1, where they may modulate their activity based on the robustness of the sensory input, further highlighting the complex dynamics of perceptual processing at the cortical level. [63] To understand how each neuron is involved in the individual activity, it is possible

to activate only one type of neuron and monitor the overall activity or another type of neuron in a region. The response can show how the inhibitory and excitatory neurons, which are in balance, contribute to the outcome. Optogenetics allows scientists to activate only one type of neuron.
Neural activity and behavioral studies have examined the effects of optogenetic stimulation under different stimuli. In one study, activity in the primary motor (M1) and ventral premotor (PMv) cortices of two macaque monkeys was monitored during awake resting periods and during reaching and grasping movements. The study used optogenetic manipulation to examine cortical dynamics during these states. In a separate investigation, the scientists used optogenetic methods to activate excitatory neurons in the primary visual cortex of the awake macaque, conducting experiments with and without concurrent visual stimulation.[79,91]
The visual cortex is an extremely complex, multi-layered structure composed of a diverse array of excitatory and inhibitory neurons. Optogenetic techniques enable researchers to precisely target and either activate or suppress specific layers or categories of cells within this complex structure. This precise control is essential for analyzing their individual contributions to visual information processing or for understanding the balance between excitation and inhibition. Investigations of this type are crucial, as they potentially offer deep insights into the neural underlying mechanisms of various visual functions, including object recognition, motion perception, and higher-level visual decisions such as pattern recognition. Through such targeted stimulation or inhibition, the subtle roles of different neural components in complex visual processing can be better understood.
In the last study (paper 2.5), we investigated the induction of gamma oscillations by optogenetic stimulation in different layers of the visual cortex and examined the local field potential (LFP) responses to simultaneous optogenetic and visual stimuli. Our investigation centered on gamma oscillation in the visual cortex following optogenetic stimulation.
Our experiments initially involved the stimulation of excitatory cells with opsins, which may have triggered the inhibitory cell activation. The goal is the investigation of either a decrease or minimal effect on the magnitude of the gamma oscillations. We aimed to evaluate whether optogenetic activation can induce gamma oscillations across diverse levels of the visual cortex and comprehend the correlation between these oscillations and different laser intensities.
We subsequently used modeling to identify significant parameters that influence the stimulus response. According to the Wilson-Cowan model[144], the key parameter affecting our model appears to be the variations in the injected current.

## 1.4 Objective of the Thesis

This research aims to investigate the role of synaptic plasticity in enabling neural circuits to identify and learn repetitive spatio-temporal spike patterns in their input signals. In addition, it will investigate the learning of spatio-temporal spike patterns with a focus on the balance between excitation and inhibition. Also, one important part of this study is looking into the excitation-inhibition (E/I) ratio to see how it affects the network's dynamic range.
Moreover, this thesis will investigate the effects of optogenetic stimulation on excitatory neurons within the visual cortex, specifically in regions V1 and V4. A key component of this study is to determine whether such targeted neural interactions induce observable changes in gamma power frequency. Through these varied approaches, the study aims to provide essential insights into the mechanisms of neuronal adaptability.

**The specific objectives are:**

1. Learning of Spatio-Temporal Spike Patterns:

    - Investigating whether combining types of synaptic plasticity can result in a balance between excitation and inhibition.
    - Proposing a biologically plausible mechanism for learning spatiotemporal spike patterns.
    - Exploration of strategies for addressing the stability vs. plasticity dilemma in spatiotemporal spike patterns.

2. Excitatory / Inhibitory Ratio and Dynamic Range:

    - Formulation of an order parameter for the measurement of phase transitions in neural networks.
    - Investigation of inhibitory effects on dynamic range.

3. Effects of Optogenetic Stimulation on Gamma Activity in the Visual Cortex:

    - Investigation of how stimulation of excitatory neurons in V1 and V4 affects gamma power.
    - Development of models to account for variations in gamma behavior between layers V1 and V4.

# Bibliography


[1] Larry F Abbott. Theoretical neuroscience rising. *Neuron*, 60(3):489–495, 2008.

[2] Wickliffe C Abraham and Anthony Robins. Memory retention–the synaptic stability versus plasticity dilemma. *Trends in neurosciences*, 28(2):73–78, 2005.

[3] Juan A Acebrón, Luis L Bonilla, Conrad J Pérez Vicente, Félix Ritort, and Renato Spigler. The kuramoto model: A simple paradigm for synchronization phenomena. *Reviews of modern physics*, 77(1):137, 2005.

[4] Hillel Adesnik. Layer-specific excitation/inhibition balances during neuronal synchronization in the visual cortex. *The Journal of physiology*, 596(9):1639–1657, 2018.

[5] Ramkumar Aishworiya, Tatiana Valica, Randi Hagerman, and Bibiana Restrepo. An update on psychopharmacological treatment of autism spectrum disorder. *Neurotherapeutics*, 19(1):248–262, 2022.

[6] Christian Albers, Maren Westkott, and Klaus Pawelzik. Perfect associative learning with spike-timing-dependent plasticity. *Advances in neural information processing systems*, 26, 2013.

[7] Evdokia Anagnostou. Clinical trials in autism spectrum disorder: evidence, challenges and future directions. *Current opinion in neurology*, 31(2):119–125, 2018.

[8] Alain Artola, S Bröcher, and Wolf Singer. Different voltage-dependent thresholds for inducing long-term depression and long-term potentiation in slices of rat visual cortex. *Nature*, 347(6288):69–72, 1990.

[9] Bassam V Atallah and Massimo Scanziani. Instantaneous modulation of gamma oscillation frequency by balancing excitation with inhibition. *Neuron*, 62(4):566–577, 2009.

[10] Th A Ban, W Guy, and WH Wilson. Description and distribution of the subtypes of chronic schizophrenia based on leonhard's classification. *Psychiatric developments*, 2 (3):179–199, 1984.

[11] Hiroko Bannai, Fumihiro Niwa, Mark W Sherwood, Amulya Nidhi Shrivastava, Misa Arizono, Akitoshi Miyamoto, Kotomi Sugiura, Sabine Lévi, Antoine Triller, and Katsuhiko Mikoshiba. Bidirectional control of synaptic gabaar clustering by glutamate and calcium. *Cell reports*, 13(12):2768–2780, 2015.

[12] Helen S Bateup, Caroline A Johnson, Cassandra L Denefrio, Jessica L Saulnier, Karl Kornacker, and Bernardo L Sabatini. Excitatory/inhibitory synaptic imbalance leads to hippocampal hyperexcitability in mouse models of tuberous sclerosis. *Neuron*, 78(3): 510–522, 2013.

[13] Lorenz Baumgarten and Stefan Bornholdt. Critical excitation-inhibition balance in dense neural networks. *Physical Review E*, 100(1):010301, 2019.

[14] John M Beggs and Dietmar Plenz. Neuronal avalanches in neocortical circuits. *Journal of neuroscience*, 23(35):11167–11177, 2003.

[15] Federico Bermúdez-Rattoni. Neural plasticity and memory: from genes to brain imaging. 2007.

[16] Nils Bertschinger and Thomas Natschläger. Real-time computation at the edge of chaos in recurrent neural networks. *Neural computation*, 16(7):1413–1436, 2004.

[17] Aanchal Bhatia, Sahil Moza, and Upinder Singh Bhalla. Precise excitation-inhibition balance controls gain and timing in the hippocampus. *Elife*, 8:e43415, 2019.

[18] Romain Brette. Philosophy of the spike: rate-based vs. spike-based theories of the brain. *Frontiers in systems neuroscience*, 9:151, 2015.

[19] Nicolas Brunel. Dynamics of sparsely connected networks of excitatory and inhibitory spiking neurons. *Journal of computational neuroscience*, 8:183–208, 2000.

[20] Anthony N Burkitt. A review of the integrate-and-fire neuron model: I. homogeneous synaptic input. *Biological cybernetics*, 95:1–19, 2006.

[21] Anthony N Burkitt. A review of the integrate-and-fire neuron model: Ii. inhomogeneous synaptic input and network properties. *Biological cybernetics*, 95:97–112, 2006.

[22] Roberto Canitano and Roberto Palumbi. Excitation/inhibition modulators in autism spectrum disorder: Current clinical research. *Frontiers in Neuroscience*, 15:753274, 2021.

[23] CE Carr and M Konishi. A circuit for detection of interaural time differences in the brain stem of the barn owl. *Journal of Neuroscience*, 10(10):3227–3246, 1990.

[24] Warasinee Chaisangmongkon, Sruthi K Swaminathan, David J Freedman, and Xiao-Jing Wang. Computing by robust transience: how the fronto-parietal network performs sequential, category-based decisions. *Neuron*, 93(6):1504–1517, 2017.

[25] Chia-Hsiung Cheng, Pei-Ying S Chan, David M Niddam, Shang-Yueh Tsai, Shih-Chieh Hsu, and Chia-Yih Liu. Sensory gating, inhibition control and gamma oscillations in the human somatosensory cortex. *Scientific reports*, 6(1):20437, 2016.

[26] Roshan Cools. The costs and benefits of brain dopamine for cognitive control. *Wiley Interdisciplinary Reviews: Cognitive Science*, 7(5):317–329, 2016. doi: 10.1002/wcs.1401.

[27] Jennifer A Cummings, Rosel M Mulkey, Roger A Nicoll, and Robert C Malenka. Ca2+ signaling requirements for long-term depression in the hippocampus. *Neuron*, 16(4):825–833, 1996.

[28] R Christopher Decharms and Michael M Merzenich. Primary cortical representation of sounds by the coordination of action-potential timing. *Nature*, 381(6583):610–613, 1996.

[29] Javier DeFelipe. Neocortical neuronal diversity: chemical heterogeneity revealed by colocalization studies of classic neurotransmitters, neuropeptides, calcium-binding proteins, and cell surface molecules. *Cerebral cortex*, 3(4):273–289, 1993.

[30] Nima Dehghani, Adrien Peyrache, Bartosz Telenczuk, Michel Le Van Quyen, Eric Halgren, Sydney S Cash, Nicholas G Hatsopoulos, and Alain Destexhe. Dynamic balance of excitation and inhibition in human and monkey neocortex. *Scientific reports*, 6(1): 23176, 2016.

[31] Karl Deisseroth, Guoping Feng, Ania K Majewska, Gero Miesenböck, Alice Ting, and Mark J Schnitzer. Next-generation optical technologies for illuminating genetically targeted brain circuits. *Journal of Neuroscience*, 26(41):10380–10386, 2006.

[32] Sophie Denève and Christian K Machens. Efficient codes and balanced networks. *Nature neuroscience*, 19(3):375–382, 2016.

[33] Christian W Eurich, J Michael Herrmann, and Udo A Ernst. Finite-size effects of avalanche dynamics. *Physical review E*, 66(6):066137, 2002.

[34] Gidon Felsen and Jennifer Blumenthal-Barby. 7 ethical issues raised by recent developments in neuroscience: The case of optogenetics. *Neuroscience and Philosophy*, 2022.

[35] Răzvan Florian. The chronotron: a neuron that learns to fire temporally-precise spike patterns. *Nature Precedings*, pages 1–1, 2010.

[36] Răzvan V Florian. The chronotron: A neuron that learns to fire temporally precise spike patterns. 2012.

[37] Robert M French. Catastrophic forgetting in connectionist networks. *Trends in cognitive sciences*, 3(4):128–135, 1999.

[38] Samuel Frere and Inna Slutsky. Alzheimer's disease: from firing instability to homeostasis network collapse. *Neuron*, 97(1):32–58, 2018. doi: 10.1016/j.neuron.2017.11.030.

[39] Jessica Frey and Irene A Malaty. Tourette syndrome treatment updates: a review and discussion of the current and upcoming literature. *Current Neurology and Neuroscience Reports*, 22(2):123–142, 2022.

[40] Nir Friedman, Shinya Ito, Braden AW Brinkman, Masanori Shimono, RE Lee DeVille, Karin A Dahmen, John M Beggs, and Thomas C Butler. Universal critical dynamics in high resolution neuronal avalanche data. *Physical review letters*, 108(20):208102, 2012.

[41] Robert C Froemke. Plasticity of cortical excitatory-inhibitory balance. *Annual review of neuroscience*, 38:195–219, 2015.

[42] Robert C Froemke, Michael M Merzenich, and Christoph E Schreiner. A synaptic memory trace for cortical receptive field plasticity. *Nature*, 450(7168):425–429, 2007.

[43] Corinna Giorgi and Silvia Marinelli. Roles and transcriptional responses of inhibitory neurons in learning and memory. *Frontiers in Molecular Neuroscience*, 14:689952, 2021.

[44] Elakkat D Gireesh and Dietmar Plenz. Neuronal avalanches organize as nested theta- and beta/gamma-oscillations during development of cortical layer 2/3. *Proceedings of the National Academy of Sciences*, 105(21):7576–7581, 2008.

[45] SD Greenhill and Roland SG Jones. Diverse antiepileptic drugs increase the ratio of background synaptic inhibition to excitation and decrease neuronal excitability in neurones of the rat entorhinal cortex in vitro. *Neuroscience*, 167(2):456–474, 2010.

[46] Robert Gütig. Spiking neurons can discover predictive features by aggregate-label learning. *Science*, 351(6277):aab4113, 2016.

[47] Robert Gütig and Haim Sompolinsky. The tempotron: a neuron that learns spike timing–based decisions. *Nature neuroscience*, 9(3):420–428, 2006.

[48] Gerald Hahn, Thomas Petermann, Martha N Havenith, Shan Yu, Wolf Singer, Dietmar Plenz, and Danko Nikolić. Neuronal avalanches in spontaneous activity in vivo. *Journal of neurophysiology*, 104(6):3312–3322, 2010.

[49] Bilal Haider, Alvaro Duque, Andrea R Hasenstaub, and David A McCormick. Neocortical network activity in vivo is generated through a dynamic balance of excitation and inhibition. *Journal of Neuroscience*, 26(17):4535–4545, 2006.

[50] Donald Olding Hebb. *The organization of behavior: A neuropsychological theory*. Psychology Press, 2005.

[51] Pascal Helson, Daniel Lundqvist, Per Svenningsson, Mikkel C Vinding, and Arvind Kumar. Cortex-wide topography of 1/f-exponent in parkinson's disease. *bioRxiv*, pages 2023–01, 2023.

[52] Stewart H Hendry, HD Schwark, EG Jones, and J Yan. Numbers and proportions of gaba-immunoreactive neurons in different areas of monkey cerebral cortex. *Journal of Neuroscience*, 7(5):1503–1519, 1987.

[53] John A Hertz. *Introduction to the theory of neural computation*. Crc Press, 2018.

[54] Nienke Hoogenboom, Jan-Mathijs Schoffelen, Robert Oostenveld, and Pascal Fries. Visually induced gamma-band activity predicts speed of change detection in humans. *Neuroimage*, 51(3):1162–1167, 2010.

[55] Oliver D Howes and Ekaterina Shatalina. Integrating the neurodevelopmental and dopamine hypotheses of schizophrenia and the role of cortical excitation-inhibition balance. *Biological psychiatry*, 92(6):501–513, 2022.

[56] ZJ Huang, G Di Cristo, and F Ango. Development of gaba innervation in the cerebral and cerebellar cortices. *Nature Reviews Neuroscience*, 8(9):673–686, 2007.

[57] Daniel Maxim Iascone, Yujie Li, Uygar Sümbül, Michael Doron, Hanbo Chen, Valentine Andreu, Finola Goudy, Idan Segev, Hanchuan Peng, and Franck Polleux. Whole-neuron synaptic mapping reveals local balance between excitatory and inhibitory synapse organization. *bioRxiv*, page 395384, 2018.

[58] Robin AA Ince, Stefano Panzeri, and Christoph Kayser. Neural codes formed by small and temporally precise populations in auditory cortex. *Journal of Neuroscience*, 33(46): 18277–18287, 2013.

[59] Jeffry S Isaacson and Massimo Scanziani. How inhibition shapes cortical activity. *Neuron*, 72(2):231–243, 2011.

[60] Eugene M Izhikevich. Polychronization: computation with spikes. *Neural computation*, 18(2):245–282, 2006.

[61] Georgina M Jackson, Amelia Draper, Katherine Dyke, Sophia E Pépés, and Stephen R Jackson. Inhibition, disinhibition, and the control of action in tourette syndrome. *Trends in Cognitive Sciences*, 19(11):655–665, 2015.

[62] Roland S Johansson and Ingvars Birznieks. First spikes in ensembles of human tactile afferents code complex spatial fingertip events. *Nature neuroscience*, 7(2):170–177, 2004.

[63] Kukjin Kang, Michael Shelley, James Andrew Henrie, and Robert Shapley. Lfp spectral peaks in v1 cortex: network resonance and cortico-cortical feedback. *Journal of computational neuroscience*, 29:495–507, 2010.

[64] Adam Kepecs and Gordon Fishell. Interneuron cell types are fit to function. *Nature*, 505 (7483):318–326, 2014.

[65] Paul D Kieffaber, Emily S Kappenman, Misty Bodkins, Anantha Shekhar, Brian F O'Donnell, and William P Hetrick. Switch and maintenance of task set in schizophrenia. *Schizophrenia research*, 84(2-3):345–358, 2006.

[66] Osame Kinouchi, Rosa W Diez-Garcia, Adriano J Holanda, Pedro Zambianchi, and Antonio C Roque. The non-equilibrium nature of culinary evolution. *New Journal of Physics*, 10(7):073020, 2008.

[67] James Kirkpatrick, Razvan Pascanu, Neil Rabinowitz, Joel Veness, Guillaume Desjardins, Andrei A Rusu, Kieran Milan, John Quan, Tiago Ramalho, Agnieszka Grabska-Barwinska, et al. Overcoming catastrophic forgetting in neural networks. *Proceedings of the national academy of sciences*, 114(13):3521–3526, 2017.

[68] Christian Klos and Raoul-Martin Memmesheimer. Smooth exact gradient descent learning in spiking neural networks. *arXiv preprint arXiv:2309.14523*, 2023.

[69] Leo Kozachkov, Mikael Lundqvist, Jean-Jacques Slotine, and Earl K Miller. Achieving stable dynamics in neural circuits. *PLoS computational biology*, 16(8):e1007659, 2020.

[70] Werner Krauth. *Statistical mechanics: algorithms and computations*, volume 13. OUP Oxford, 2006.

[71] Arvind Kumar, Stefano Cardanobile, Stefan Rotter, and Ad Aertsen. The role of inhibition in generating and controlling parkinson's disease oscillations in the basal ganglia. *Frontiers in systems neuroscience*, 5:86, 2011.

[72] Baldeep Kumar, Ajay Prakash, Rakesh K Sewal, Bikash Medhi, and Manish Modi. Drug therapy in autism: a present and future perspective. *Pharmacological Reports*, 64(6): 1291–1304, 2012.

[73] Yoshiki Kuramoto. International symposium on mathematical problems in theoretical physics. *Lecture notes in Physics*, 30:420, 1975.

[74] Yoshiki Kuramoto and Yoshiki Kuramoto. *Chemical turbulence*. Springer, 1984.

[75] Rodrigo Laje and Dean V Buonomano. Robust timing and motor patterns by taming chaos in recurrent neural networks. *Nature neuroscience*, 16(7):925–933, 2013.

[76] Norman H Lam, Thiago Borduqui, Jaime Hallak, Antonio Roque, Alan Anticevic, John H Krystal, Xiao-Jing Wang, and John D Murray. Effects of altered excitation-inhibition balance on decision making in a cortical circuit model. *Journal of Neuroscience*, 42(6):1035–1053, 2022.

[77] Florian Lange, Caroline Seer, and Bruno Kopp. Cognitive flexibility in neurological disorders: Cognitive components and event-related potentials. *Neuroscience & Biobehavioral Reviews*, 83:496–507, 2017. doi: 10.1016/j.neubiorev.2017.10.008.

[78] Yi Liu, Pan Ouyang, Yingjun Zheng, Lin Mi, Jingping Zhao, Yuping Ning, and Wenbin Guo. A selective review of the excitatory-inhibitory imbalance in schizophrenia: underlying biology, genetics, microcircuits, and symptoms. *Frontiers in Cell and Developmental Biology*, 9:664535, 2021.

[79] Yao Lu, Wilson Truccolo, Fabien B Wagner, Carlos E Vargas-Irwin, Ilker Ozden, Jonas B Zimmermann, Travis May, Naubahar S Agha, Jing Wang, and Arto V Nurmikko. Optogenetically induced spatiotemporal gamma oscillations and neuronal spiking activity in primate motor cortex. *Journal of neurophysiology*, 113(10):3574–3587, 2015.

[80] Yi Lu, Cheng Zhong, Lulu Wang, Pengfei Wei, Wei He, Kang Huang, Yi Zhang, Yang Zhan, Guoping Feng, and Liping Wang. Optogenetic dissection of ictal propagation in the hippocampal–entorhinal cortex structures. *Nature communications*, 7(1):10962, 2016.

[81] Gregory T Macleod and Konrad E Zinsmaier. Synaptic homeostasis on the fast track. *Neuron*, 52(4):569–571, 2006.

[82] Robert C Malenka, Nicoll, and Roger A. Long-term potentiation–a decade of progress? *Science*, 285(5435):1870–1874, 1999.

[83] Edward O Mann and Ole Paulsen. Role of gabaergic inhibition in hippocampal network oscillations. *Trends in neurosciences*, 30(7):343–349, 2007.

[84] Dara S Manoach, Kristen A Lindgren, Mariya V Cherkasova, Donald C Goff, Elkan F Halpern, James Intriligator, and Jason JS Barton. Schizophrenic subjects show deficient inhibition but intact task switching on saccadic tasks. *Biological psychiatry*, 51(10): 816–826, 2002. doi: 10.1016/S0006-3223(02)01311-1.

[85] Joseane Righes Marafiga, Mayara Vendramin Pasquetti, and Maria Elisa Calcagnotto. Gabaergic interneurons in epilepsy: More than a simple change in inhibition. *Epilepsy & Behavior*, 121:106935, 2021.

[86] Henry Markram, Maria Toledo-Rodriguez, Yun Wang, Anirudh Gupta, Gilad Silberberg, and Caizhi Wu. Interneurons of the neocortical inhibitory system. *Nature reviews neuroscience*, 5(10):793–807, 2004.

[87] SA Masino, M Kawamura Jr, DN Ruskin, JD Geiger, and D Boison. Purines and neuronal excitability: links to the ketogenic diet. *Epilepsy research*, 100(3):229–238, 2012.

[88] Raoul-Martin Memmesheimer, Ran Rubin, Bence P Ölveczky, and Haim Sompolinsky. Learning precisely timed spikes. *Neuron*, 82(4):925–938, 2014.

[89] Marvin Minsky and Seymour A Papert. *Perceptrons, reissue of the 1988 expanded edition with a new foreword by Léon Bottou: an introduction to computational geometry*. MIT press, 2017.

[90] Brendan K Murphy and Kenneth D Miller. Balanced amplification: a new mechanism of selective amplification of neural activity patterns. *Neuron*, 61(4):635–648, 2009.

[91] Jonathan J Nassi, Michael C Avery, Ali H Cetin, Anna W Roe, and John H Reynolds. Optogenetic activation of normalization in alert macaque visual cortex. *Neuron*, 86(6): 1504–1517, 2015.

[92] Michael Okun and Ilan Lampl. Instantaneous correlation of excitation and inhibition during ongoing and sensory-evoked activities. *Nature neuroscience*, 11(5):535–537, 2008.

[93] German I Parisi, Ronald Kemker, Jose L Part, Christopher Kanan, and Stefan Wermter. Continual lifelong learning with neural networks: A review. *Neural networks*, 113:54–71, 2019.

[94] Godfrey D Pearlson. Neurobiology of schizophrenia. *Annals of Neurology: Official Journal of the American Neurological Association and the Child Neurology Society*, 48 (4):556–566, 2000.

[95] William M Perlstein, Cameron S Carter, Douglas C Noll, and Jonathan D Cohen. Relation of prefrontal cortex dysfunction to working memory and symptoms in schizophrenia. *American Journal of Psychiatry*, 158(7):1105–1113, 2001.

[96] Thomas Petermann, Tara C Thiagarajan, Mikhail A Lebedev, Miguel AL Nicolelis, Dante R Chialvo, and Dietmar Plenz. Spontaneous cortical activity in awake monkeys composed of neuronal avalanches. *Proceedings of the National Academy of Sciences*, 106(37):15921–15926, 2009.

[97] Simon-Shlomo Poil, Richard Hardstone, Huibert D Mansvelder, and Klaus Linkenkaer-Hansen. Critical-state dynamics of avalanches and oscillations jointly emerge from balanced excitation/inhibition in neuronal networks. *Journal of Neuroscience*, 32(29):9817–9823, 2012.

[98] Antonio Politi and Michael Rosenblum. Equivalence of phase-oscillator and integrate-and-fire models. *Physical Review E*, 91(4):042916, 2015.

[99] Petra MJ Pollux. Advance preparation of set-switches in parkinson's disease. *Neuropsychologia*, 42(7):912–919, 2004. doi: 10.1016/j.neuropsychologia.2003.12.003.

[100] David J Posey, Kimberly A Stigler, Craig A Erickson, Christopher J McDougle, et al. Antipsychotics in the treatment of autism. *The Journal of clinical investigation*, 118(1): 6–14, 2008.

[101] Charlotte M Pretzsch and Dorothea L Floris. Balancing excitation and inhibition in the autistic brain. *Elife*, 9:e60584, 2020.

[102] Viola Priesemann, Michael Wibral, Mario Valderrama, Robert Pröpper, Michel Le Van Quyen, Theo Geisel, Jochen Triesch, Danko Nikolić, and Matthias HJ Munk. Spike avalanches in vivo suggest a driven, slightly subcritical brain state. *Frontiers in systems neuroscience*, 8:108, 2014.

[103] Luce Prignano, Oleguer Sagarra, and Albert Díaz-Guilera. Tuning synchronization of integrate-and-fire oscillators through mobility. *Physical review letters*, 110(11):114101, 2013.

[104] Maximiliano Rapanelli, Luciana Romina Frick, and Christopher Pittenger. The role of interneurons in autism and tourette syndrome. *Trends in neurosciences*, 40(7):397–407, 2017.

[105] Irmantas Ratas and Kestutis Pyragas. Noise-induced macroscopic oscillations in a network of synaptically coupled quadratic integrate-and-fire neurons. *Physical Review E*, 100(5):052211, 2019.

[106] Supratim Ray and John HR Maunsell. Differences in gamma frequencies across visual cortex restrict their possible use in computation. *Neuron*, 67(5):885–896, 2010.

[107] Daniel S Reich, Ferenc Mechler, and Jonathan D Victor. Independent and redundant information in nearby cortical neurons. *Science*, 294(5551):2566–2568, 2001.

[108] Pamela Reinagel and R Clay Reid. Temporal coding of visual information in the thalamus. *Journal of neuroscience*, 20(14):5392–5400, 2000.

[109] Fred Rieke, David Warland, Rob de Ruyter Van Steveninck, and William Bialek. *Spikes: exploring the neural code*. MIT press, 1999.

[110] JLR Rubenstein and Michael M Merzenich. Model of autism: increased ratio of excitation/inhibition in key neural systems. *Genes, Brain and Behavior*, 2(5):255–267, 2003.

[111] Maik Schünemann, Udo Ernst, and Marc Kesseböhmer. A rigorous stochastic theory for spike pattern formation in recurrent neural networks with arbitrary connection topologies. *arXiv preprint arXiv:2202.02520*, 2022.

[112] MP Schwellnus. Cause of exercise associated muscle cramps (eamc)—altered neuromuscular control, dehydration or electrolyte depletion? *British journal of sports medicine*, 43(6):401–408, 2009.

[113] Sheila MS Sears and Sandra J Hewett. Influence of glutamate and gaba transport on brain excitatory/inhibitory balance. *Experimental Biology and Medicine*, 246(9):1069–1083, 2021.

[114] Mary F Seideman and Travis A Seideman. A review of the current treatment of tourette syndrome. *The journal of pediatric pharmacology and therapeutics*, 25(5):401–412, 2020.

[115] Weixing Shen, Joshua L Plotkin, Veronica Francardo, Wai Kin D Ko, Zhong Xie, Qin Li, Tim Fieblinger, Jürgen Wess, Richard R Neubig, Craig W Lindsley, et al. M4 muscarinic receptor signaling ameliorates striatal plasticity deficits in models of l-dopa-induced dyskinesia. *Neuron*, 88(4):762–773, 2015.

[116] Woodrow L Shew, Hongdian Yang, Thomas Petermann, Rajarshi Roy, and Dietmar Plenz. Neuronal avalanches imply maximum dynamic range in cortical networks at criticality. *Journal of neuroscience*, 29(49):15595–15600, 2009.

[117] Woodrow L Shew, Hongdian Yang, Shan Yu, Rajarshi Roy, and Dietmar Plenz. Information capacity and transmission are maximized in balanced cortical networks with neuronal avalanches. *Journal of neuroscience*, 31(1):55–63, 2011.

[118] Vinay Shirhatti and Supratim Ray. Long-wavelength (reddish) hues induce unusually large gamma oscillations in the primate primary visual cortex. *Proceedings of the National Academy of Sciences*, 115(17):4489–4494, 2018.

[119] Yousheng Shu, Andrea Hasenstaub, Mathilde Badoual, Thierry Bal, and David A McCormick. Barrages of synaptic activity control the gain and sensitivity of cortical neurons. *Journal of Neuroscience*, 23(32):10388–10401, 2003.

[120] Yousheng Shu, Andrea Hasenstaub, and David A McCormick. Turning on and off recurrent balanced cortical activity. *Nature*, 423(6937):288–293, 2003.

[121] AM Sillito. The contribution of inhibitory mechanisms to the receptive field properties of neurones in the striate cortex of the cat. *The Journal of physiology*, 250(2):305–329, 1975.

[122] AM Sillito. Functional considerations of the operation of gabaergic inhibitory processes in the visual cortex. *Cerebral Cortex.*, pages 91–117, 1984.

[123] Katharine R Smith, Elizabeth C Davenport, Jing Wei, Xiangning Li, Manavendra Pathania, Victoria Vaccaro, Zhen Yan, and Josef T Kittler. Git1 and $\beta$pix are essential for gabaa receptor synaptic stability and inhibitory neurotransmission. *Cell reports*, 9(1): 298–310, 2014.

[124] Joshua ES Socolar and Stuart A Kauffman. Scaling in ordered and critical random boolean networks. *Physical review letters*, 90(6):068702, 2003.

[125] Vikaas S Sohal and John LR Rubenstein. Excitation-inhibition balance as a framework for investigating mechanisms in neuropsychiatric disorders. *Molecular psychiatry*, 24 (9):1248–1257, 2019.

[126] Peter Somogyi, Gabor Tamas, Rafael Lujan, and Eberhard H Buhl. Salient features of synaptic organisation in the cerebral cortex. *Brain research reviews*, 26(2-3):113–135, 1998.

[127] Edith V Sullivan, Daniel H Mathalon, Robert B Zipursky, Zoe Kersteen-Tucker, Robert T Knight, and Adolf Pfefferbaum. Factors of the wisconsin card sorting test as measures of frontal-lobe function in schizophrenia and in chronic alcoholism. *Psychiatry research*, 46(2):175–199, 1993. doi: 10.1016/0165-1781(93)90003-L.

[128] Aboozar Taherkhani, Ammar Belatreche, Yuhua Li, Georgina Cosma, Liam P Maguire, and T Martin McGinnity. A review of learning in biologically plausible spiking neural networks. *Neural Networks*, 122:253–272, 2020.

[129] Roberta Tatti, Melissa S Haley, Olivia K Swanson, Tenzin Tselha, and Arianna Maffei. Neurophysiology and regulation of the balance between excitation and inhibition in neocortical circuits. *Biological psychiatry*, 81(10):821–831, 2017.

[130] Rudi Tong, Thomas Edward Chater, Nigel John Emptage, and Yukiko Goda. Heterosynaptic cross-talk of pre-and postsynaptic strengths along segments of dendrites. *Cell reports*, 34(4), 2021.

[131] Gina G Turrigiano. The self-tuning neuron: synaptic scaling of excitatory synapses. *Cell*, 135(3):422–435, 2008.

[132] Genoveva Uzunova, Stefano Pallanti, and Eric Hollander. Excitatory/inhibitory imbalance in autism spectrum disorders: implications for interventions and therapeutics. *The World Journal of Biological Psychiatry*, 17(3):174–186, 2016.

[133] VJ Uzzell and EJ Chichilnisky. Precision of spike trains in primate retinal ganglion cells. *Journal of neurophysiology*, 92(2):780–789, 2004.

[134] Mark CW Van Rossum, Guo Qiang Bi, and Gina G Turrigiano. Stable hebbian learning from spike timing-dependent plasticity. *Journal of neuroscience*, 20(23):8812–8821, 2000.

[135] Carl Van Vreeswijk and Haim Sompolinsky. Chaos in neuronal networks with balanced excitatory and inhibitory activity. *Science*, 274(5293):1724–1726, 1996.

[136] Matthew C Walker and Dimitri M Kullmann. Optogenetic and chemogenetic therapies for epilepsy. *Neuropharmacology*, 168:107751, 2020.

[137] Michael Wehr and Gilles Laurent. Odour encoding by temporal sequences of firing in oscillating neural assemblies. *Nature*, 384(6605):162–166, 1996.

[138] Michael Wehr and Anthony M Zador. Balanced inhibition underlies tuning and sharpens spike timing in auditory cortex. *Nature*, 426(6965):442–446, 2003.

[139] Andrew J Weitz, Zhongnan Fang, Hyun Joo Lee, Robert S Fisher, Wesley C Smith, ManKin Choy, Jia Liu, Peter Lin, Matthew Rosenberg, and Jin Hyung Lee. Optogenetic fmri reveals distinct, frequency-dependent networks recruited by dorsal and intermediate hippocampus stimulations. *Neuroimage*, 107:229–241, 2015.

[140] Christoph Wiest, Flavie Torrecillos, Alek Pogosyan, Manuel Bange, Muthuraman Muthuraman, Sergiu Groppa, Natasha Hulse, Harutomo Hasegawa, Keyoumars Ashkan, Fahd Baig, et al. The aperiodic exponent of subthalamic field potentials reflects excitation/inhibition balance in parkinsonism. *Elife*, 12:e82467, 2023.

[141] W Bryan Wilent and Diego Contreras. Dynamics of excitation and inhibition underlying stimulus selectivity in rat somatosensory cortex. *Nature neuroscience*, 8(10):1364–1370, 2005.

[142] Bruno E Will. *Brain plasticity, learning, and memory*, volume 28. Springer Science & Business Media, 2013.

[143] Katrina Williams, Amanda Brignell, Melinda Randall, Natalie Silove, and Philip Hazell. Selective serotonin reuptake inhibitors (ssris) for autism spectrum disorders (asd). *Cochrane Database of Systematic Reviews*, (8), 2013.

[144] Hugh R Wilson and Jack D Cowan. A mathematical theory of the functional dynamics of cortical and thalamic nervous tissue. *Kybernetik*, 13(2):55–80, 1973.

[145] Craig D Workman and T Adam Thrasher. The influence of dopaminergic medication on balance automaticity in parkinson's disease. *Gait & posture*, 70:98–103, 2019.

[146] Hongdian Yang, Woodrow L Shew, Rajarshi Roy, and Dietmar Plenz. Maximal variability of phase synchrony in cortical networks with neuronal avalanches. *Journal of neuroscience*, 32(3):1061–1072, 2012.

[147] Hiromu Yawo, Hideki Kandori, and Amane Koizumi. *Optogenetics: light-sensing proteins and their applications*. Springer, 2015.

[148] Ofer Yizhar, Lief E Fenno, Thomas J Davidson, Murtaza Mogri, and Karl Deisseroth. Optogenetics in neural systems. *Neuron*, 71(1):9–34, 2011.

[149] Qiang Yu, Huajin Tang, Kay Chen Tan, and Haizhou Li. Precise-spike-driven synaptic plasticity: Learning hetero-association of spatiotemporal spike patterns. *Plos one*, 8(11): e78318, 2013.

[150] Huaguang Zhang, Zhanshan Wang, and Derong Liu. A comprehensive review of stability analysis of continuous-time recurrent neural networks. *IEEE Transactions on Neural Networks and Learning Systems*, 25(7):1229–1262, 2014.

[151] Li I Zhang, Andrew YY Tan, Christoph E Schreiner, and Michael M Merzenich. Topography and synaptic shaping of direction selectivity in primary auditory cortex. *Nature*, 424(6945):201–205, 2003.

[152] Mu Zhou, Feixue Liang, Xiaorui R Xiong, Lu Li, Haifu Li, Zhongju Xiao, Huizhong W Tao, and Li I Zhang. Scaling down of balanced excitation and inhibition by active behavioral states in auditory cortex. *Nature neuroscience*, 17(6):841–850, 2014.

[153] Shanglin Zhou and Yuguo Yu. Synaptic ei balance underlies efficient neural coding. *Frontiers in Neuroscience*, 12:46, 2018.

# Chapter 2

# Publications

## 2.1 Synaptic self-organization of spatio-temporal pattern selectivity

PLOS Computational Biology 19 (2), e1010876

**My contribution to this paper**:

Conceptualization
Formal analysis
Investigation
Methodology
Software
Visualization
Writing - original draft

PLOS COMPUTATIONAL BIOLOGY

RESEARCH ARTICLE

# Synaptic self-organization of spatio-temporal pattern selectivity

**Mohammad Dehghani-Habibabadi*, Klaus Pawelzik**

Institute for Theoretical Physics, University of Bremen, Bremen, Germany

* mohammad@neuro.uni-bremen.de



OPEN ACCESS

**Citation:** Dehghani-Habibabadi M, Pawelzik K (2023) Synaptic self-organization of spatio-temporal pattern selectivity. PLoS Comput Biol 19(2): e1010876. https://doi.org/10.1371/journal.pcbi.1010876

**Editor:** Abigail Morrison, Research Center Jülich, GERMANY

**Received:** February 22, 2022

**Accepted:** January 17, 2023

**Published:** February 13, 2023



**Data Availability Statement:** The codes to implement the model are available at https://github.com/MohammadDehghaniH/Synaptic-Self-Organization-of-Spatio-Temporal-Pattern-Selectivity.

**Funding:** This work was supported by DFG - grant (PA 569/5-1 to KP). The funders had no role in study design, data collection and analysis, decision to publish, or preparation of the manuscript.

**Competing interests:** The authors have declared that no competing interests exist.

## Abstract

Spiking model neurons can be set up to respond selectively to specific spatio-temporal spike patterns by optimization of their input weights. It is unknown, however, if existing synaptic plasticity mechanisms can achieve this temporal mode of neuronal coding and computation. Here it is shown that changes of synaptic efficacies which tend to balance excitatory and inhibitory synaptic inputs can make neurons sensitive to particular input spike patterns. Simulations demonstrate that a combination of Hebbian mechanisms, hetero-synaptic plasticity and synaptic scaling is sufficient for self-organizing sensitivity for spatio-temporal spike patterns that repeat in the input. In networks inclusion of hetero-synaptic plasticity that depends on the pre-synaptic neurons leads to specialization and faithful representation of pattern sequences by a group of target neurons. Pattern detection is robust against a range of distortions and noise. The proposed combination of Hebbian mechanisms, hetero-synaptic plasticity and synaptic scaling is found to protect the memories for specific patterns from being overwritten by ongoing learning during extended periods when the patterns are not present. This suggests a novel explanation for the long term robustness of memory traces despite ongoing activity with substantial synaptic plasticity. Taken together, our results promote the plausibility of precise temporal coding in the brain.

## Author summary

Neurons communicate using action potentials, that are pulses localized in time. There is evidence that the exact timing of these so called spikes carries information. The hypothesis, however, that computations in brains are indeed based on precise patterns of spikes is debated, particularly because this would require the existence of suitable detectors. While theoretically, individual neurons can perform spike pattern detection when their input synapses are carefully adjusted, it is not known if existing synaptic plasticity mechanisms indeed support this coding principle. Here, a combination of basic but realistic mechanisms is demonstrated to self-organize the synaptic input efficacies such that individual neurons become detectors of patterns repeating in the input. The proposed combination of learning mechanisms yields a balance of excitation and inhibition similar to observations in cortex, robustness of detection against perturbations and noise, and persistence of memory against plasticity during ongoing activity without the learned patterns. The

proposed learning mechanism enables groups of neurons to incrementally acquire sets of patterns thereby faithfully representing their 'which' and 'when' in sequences. These results suggest that computations based on spatio-temporal spike patterns might emerge without any supervision from the synaptic plasticity mechanisms present in the brain.

## Introduction

Despite decades of research, it is still debated which coding schemes are used in central nervous systems. While in early sensory areas of cortex, stimuli appear to be represented mostly by spike rates, it cannot be disputed that temporal information is faithfully processed. In fact, experimental studies on visual, auditory, olfactory, and somato-sensory cortex indicate that neurons can respond rather deterministically to inputs, underlining the possibility of precise spike codes. [1–8]

While this can in principle be achieved by modulated spike rates in large populations of neurons it is tempting to hypothesize that at least in higher areas, as, i.e., frontal cortex, temporally precise responses of individual neurons play an important role.

A range of theoretical studies attempted to elucidate mechanisms that could support precise coding of spatio-temporal patterns [9, 10]. It was found that with suitable synaptic weights, even simple integrate-and-fire neurons are sensitive to specific spatio-temporal input spike patterns. For instance, the Tempotron [9] was introduced as an extension of the Perceptron [11] to perform classification and detection of spatio-temporal patterns with a spike response to patterns only from a given set with a supervised algorithm for potentiating and depressing a neuron's afferents. The number of patterns that a neuron can learn to classify depends on their length, the time constants of the neurons and the synaptic inputs [12]. While in the Tempotron the action potential is allowed to occur anywhere during the time of the learned patterns, it was later shown that neurons can be forced to fire also at a specific time [10, 13] during a specific pattern's presence, which can be achieved by several more or less realistic synaptic mechanisms [14, 15]. Both the Tempotron and the Chronotron employ supervised learning mechanisms based on label and time, respectively.

Supervised learning of spatio-temporal patterns seems at odds with reality, where the input is not labeled, impinges on the neuron continuously, and is subject to distortions and noise. In particular, it would need to explain how synaptic plasticity mechanisms become informed which aspect of the data should be taken into account when a label comes only long after the patterns. A recent study addressed this latter problem. It showed that neurons can recognize spatio-temporal patterns embedded in a background of noise using only weak supervision where the known number of repetitions of a pattern is used for optimizing synaptic efficacy [16]. Based on the N-methyl-D-aspartate (NMDA) receptor [17–19], a learning rule was proposed [16] that yields similar results as obtained by optimization. The biological plausibility of this correlation-based rule, however, is questionable. It does not respect Dale's rule since synapses can change their sign, it is still supervised, and it requires a careful selection of potential weight changes such that only a given small percentage of potential changes become effective.

Therefore, it remains an open question if existing mechanisms of synaptic plasticity can be identified which enable neurons to specialize on statistically dominant patterns in the temporal stream of their inputs in an entirely unsupervised manner.

We use basic Hebbian mechanisms for the plasticity of both, excitatory and inhibitory neurons which for excitatory synapses resemble the NMDA-receptor. Dale's law is enforced, i.e.,

inhibitory and excitatory neurons can not change into one another throughout the learning process.

The instability of Hebbian mechanisms for excitatory synapses is contained by a combination of three known mechanisms. First, upper bounds on synaptic efficacies are imposed. Second, we implement synaptic scaling: It has been shown that neurons do not remain silent for long periods, but scale their weights to achieve a genetically intended spike rate [20]. Third, we employ (post-synaptic) hetero-synaptic plasticity which provides negative changes of efficacy (i.e. long term depression; LTD) through by a competition for resources for weight increases that are provided by the post-synaptic neuron (e.g. receptors).

When several target neurons are present, we also include pre-synaptic hetero-synaptic plasticity, which induces competition for resources provided by the pre-synaptic neuron. This mechanism serves specialization of target neurons in subsets of all patterns [21].

The combination of these realistic mechanisms turns out to be sufficient for the self-organization of pattern detection in single neurons. At times when no pattern is present excitatory and inhibitory inputs become globally balanced. During the time when a learned pattern is present we find detailed balance, where excitatory and inhibitory inputs cancel each other in temporal detail. These results parallel findings of the global and detailed balance of excitation and inhibition in cortex [22–24].

The resulting synaptic efficacies are then shown to ensure robust pattern recognition that is resistant to temporal jitter and noise. When basing learning on jittered patterns and also on Poisson rate modulations instead of precisely repeating patterns we obtain even more robust pattern detection. These results underline that the proposed mechanisms can be based on imprecise patterns and temporally modulated rate codes.

Next, we wondered if and how learned memory traces vanish during ongoing plasticity when only random patterns are presented which contain no statistically dominant structures. We find extremely long memory persistence already for a single output neuron. This leads to the question if the proposed mechanisms might contribute to solving the stability-plasticity problem [25], such that they would support incremental learning where patterns occur rarely and are intermingled with random activity and/or different patterns. We investigated this for groups of output neurons where competition for patterns is induced by pre-synaptic hetero-synaptic plasticity [26]. Thereby the output neurons specialize on different subsets of patterns such that the group as a whole self-organizes faithful representation of the 'which' and 'when' of patterns in the input. The memory persistence in this setting is finally shown to support incremental learning of sets of patterns in neuronal populations.

## Results

In all simulations, we consider simple leaky integrate and fire neurons [27, 28] with a fixed membrane time constant of 15 ms and pre-synaptic spikes originating from 500 input neurons (80% excitatory and 20% inhibitory). They provide input currents via kernels that have the shape of alpha-functions. For each synapse, the amplitudes of the input currents depend on a single parameter, the synaptic weight. The kernels have different time constants for excitatory and inhibitory synapses. The signs of the weights are not allowed to change during learning, i.e., Dale's law is enforced.

### Single post-synaptic neuron

Synaptic plasticity is based on correlations between the input-kernels and deflections of the membrane potentials with respect to a threshold. For changes of the inhibitory synapses, positive deflections increase the weights, and negative deflections lead to their decay. For changes

of the excitatory synapses, we let only positive deflections contribute, mimicking NMDA-dependent mechanisms. Without further constraints, this Hebbian mechanism is unstable for excitatory efficacies.

Runaway instabilities are avoided by a combination of three simple but biologically highly plausible mechanisms: First, unbounded growth is made impossible by clipping the weights at upper limits for excitatory synapses. Second, positive weight changes for excitatory synapses are quenched when the long time activity exceeds a pre-determined rate, which mimics synaptic scaling [20, 29]. Third, the negative weight changes for excitatory synapses are induced by hetero-synaptic plasticity. Specifically, we include post-synaptic hetero-synaptic plasticity where the weight changes of different afferents are made dependent such that the resources needed for strong increases of the post-synaptic contributions to synaptic efficacies are taken from synapses which would otherwise increase only weakly. Thereby the latter synapses' efficacies become reduced. Note, however, that this does not imply strict normalization of excitatory weights (see Materials and methods).

It turns out that these ingredients are sufficient for robust self-organization of spatio-temporal spike pattern detection in single neurons. As an example, Fig 1 shows the membrane potential (MP) of a single neuron before and after learning a random pattern of length 50 ms that has the same statistics as the random background but repeats in every training epoch of length 1000 ms.

Fig 2 captures the combined effect of the plasticity mechanisms on the inputs to a post-synaptic neuron. After convergence of the weights, we separated the excitatory and inhibitory inputs to see how their respective contributions lead to firing only during the pattern (Fig 2A). In particular, the antagonistic effect of correlations based Hebbian plasticity of excitatory and inhibitory synapses leads to global and detailed balance. Fig 2A indicates that inhibitory and excitatory inputs cancel each other outside of the embedded pattern in the mean (global balance). Averaging these inputs on epochs (Fig 2C) explicitly shows that in the mean fluctuations are removed, which corresponds to global balance. In contrast, during the time of the embedded pattern, the respective contributions to the membrane potential both increase but remain mostly balanced also across time (detailed balance). This balance is the fixed point of the weight dynamics. Fig 2B depicts the spike-triggered average of the inhibitory and excitatory inputs, respectively, underlining the detailed balance during the learned pattern. In fact, only some residual imbalance between excitatory and inhibitory afferents allow the post-synaptic neuron to fire during this period of time. The detailed balance during the embedded pattern is quantified by the anti-correlation between excitatory and inhibitory afferents which is substantial and minimal close to zero time shift (Fig 2D). Last not least, the synaptic scaling enforces the desired mean firing rate of 2Hz leading to two spikes during the pattern. Thereby, synaptic scaling limits the growth of total excitation which additionally is constrained by clipping synaptic weights at a maximal value. Note that in this model pre-synaptic hetero-synaptic plasticity is the only source of LTD for excitatory synapses.

To quantify the performance of the learning mechanism for ensembles of random patterns, we consider the average percentage $R$ of spikes that correctly detect the pattern:

$$R = \left\langle \frac{n_s^p(L)}{n_s + \zeta} \right\rangle_\mu , \tag{1}$$

where $n_s$ is the total number of spikes during a testing period and $n_s^p$ the spikes' number related to the presence of the pattern to be detected. Since patterns can induce spikes also shortly after the pattern due to the finite decay time of the excitatory synaptic kernel, the time window for testing if spikes occur inside the pattern is extended by $L$ ms after the pattern has ended.

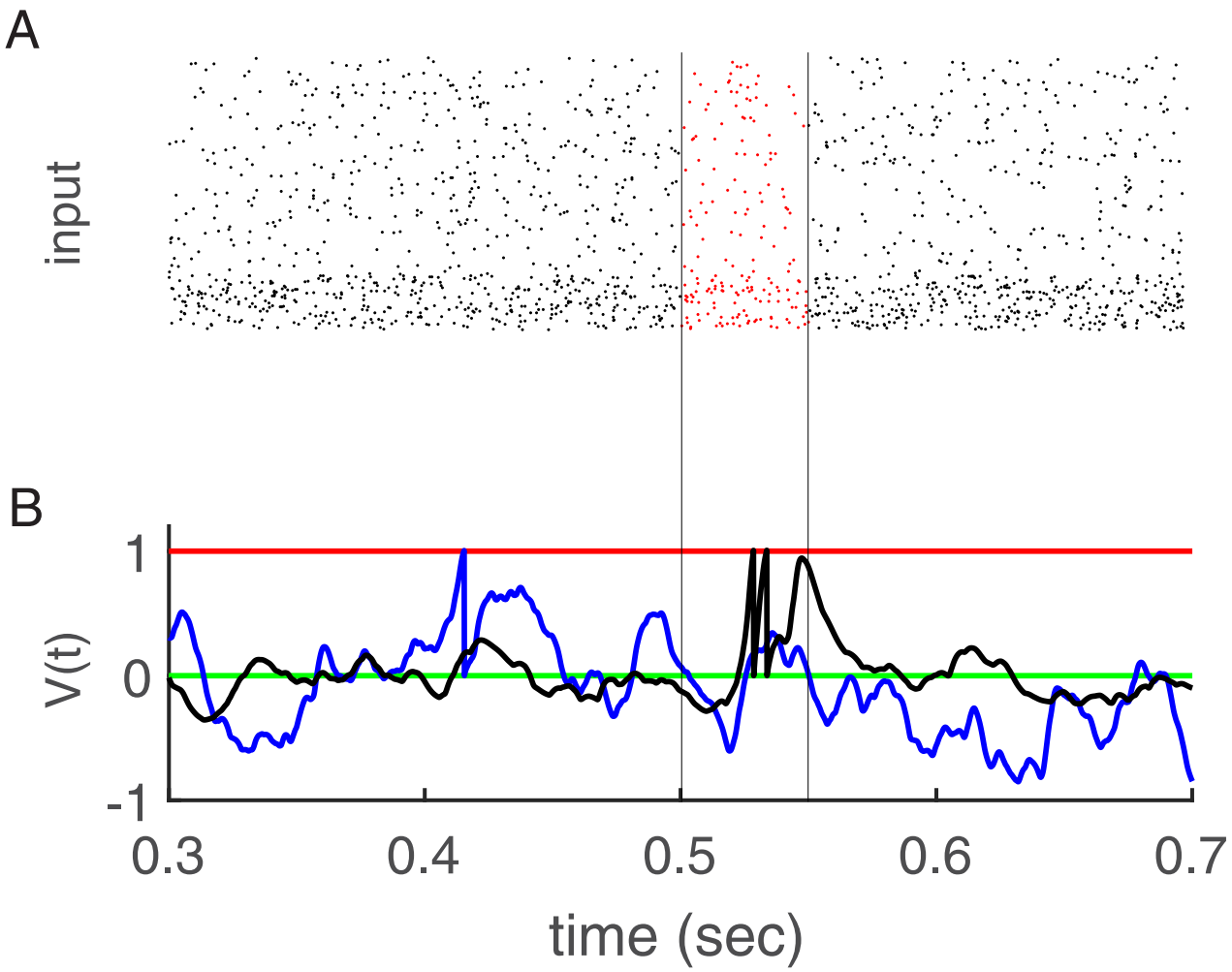


**Fig 1. Learning of one embedded pattern. (A)** Input activity in the raster plot. Five hundred afferents (80% excitatory and 20% inhibitory) send inputs to one post-synaptic neuron. The excitatory neurons' rate is 5 Hz, and the inhibitory neurons' rates are 20 Hz. There is a random embedded pattern of length 50 ms in the red area between black vertical lines. **(B)** Membrane potential versus time. The black trace shows that after learning the fluctuations outside of the embedded pattern are attenuated as compared to the case where the weights were learned from random background alone. As result two spikes occur during embedded pattern time (between the vertical black lines). The green line is for resting potential, red is for threshold, blue is membrane potential after weight initialization by learning with only random patterns, and black is for after learning.

https://doi.org/10.1371/journal.pcbi.1010876.g001

Adding an arbitrary small number $\zeta$ to the denominator ensures a definite result ($R = 0$) when no spikes occur at all. The ratio is averaged for an ensemble of independent embedded patterns $\mu$.

Occasionally, we also consider a variant of this criterion $R^*$ where the average is taken only on the epochs in which there is at least one spike occurring in post-synaptic neuron:

$$R^* = \left\langle \frac{n_s^p(L)}{n_s} \right\rangle_{\hat{\mu}}, \tag{2}$$

where $\hat{\mu}$ refers to the ensemble of independent embedded patterns for which the post-synaptic neuron elicited at least one spike during the pattern presentation.

Before embedded patterns are shown in this study's simulations, only random spike patterns are shown; thus, postsynaptic neurons have already achieved $r_0$ mainly because of

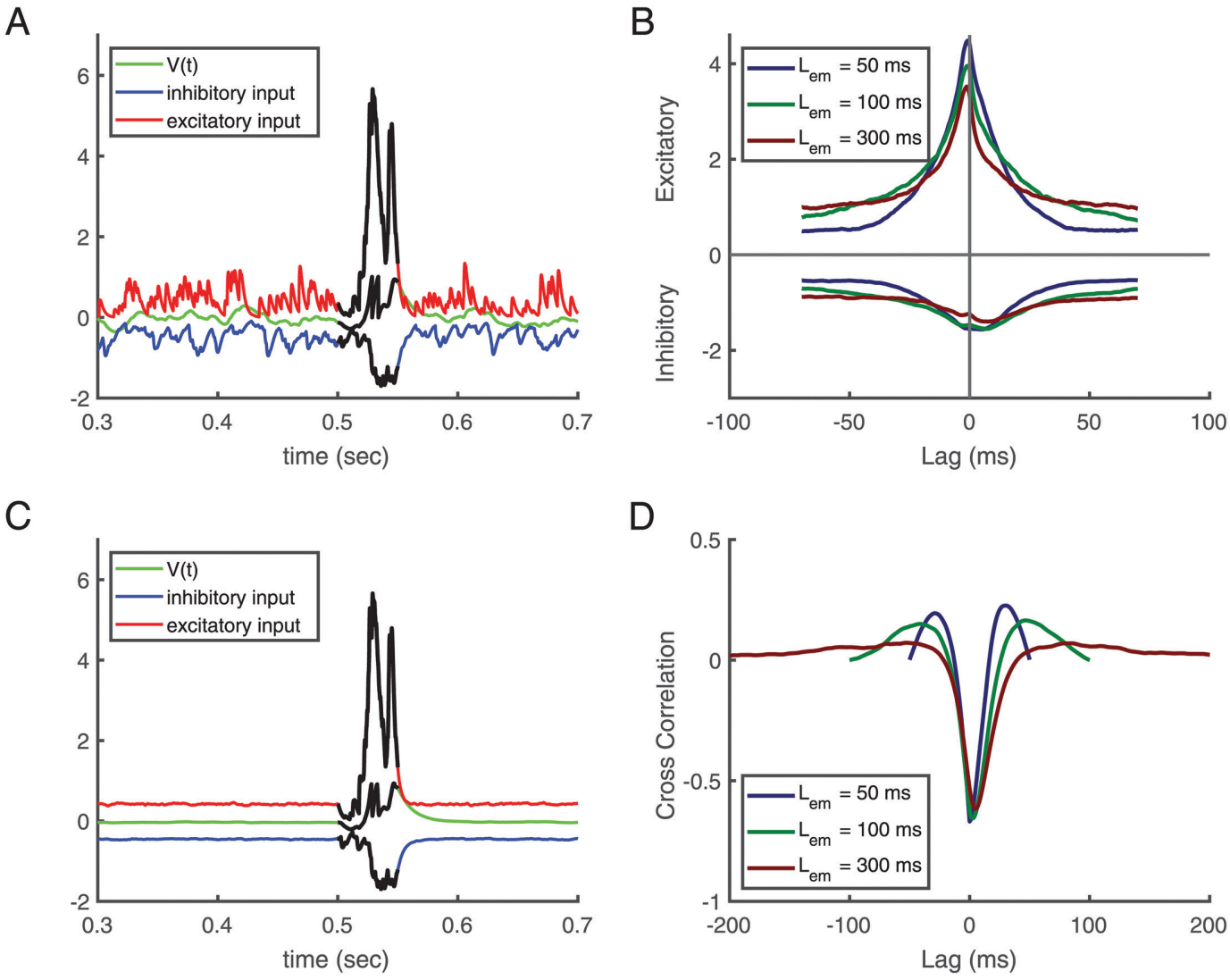


**Fig 2. Balance of excitation and inhibition.** **(A, C)** A fixed repeating pattern is embedded between 500 ms and 550 ms, i.e. duration $L_{em}$ = 50 ms. **(B, D)** Averages over different learned patterns of lengths $L_{em}$ = 50, 100, and 300 ms starting from 500 ms (using 500 epochs). **(A)** Excitatory and inhibitory inputs and the membrane potential after convergence of self-organization with this pattern. **(B)** Spike triggered average of respective inputs for different pattern lengths after convergence. In the more extended patterns the minimum of inhibitory inputs follows the maximum of excitatory inputs. **(C)** Average contribution of excitatory and inhibitory inputs from 500 epochs. **(D)** Cross-correlation between inhibitory and excitatory inputs for neurons that where exposed to learned patterns. In all figures, the length of the training epoch is 1000 ms, and the desired number of spikes is 2, i.e., the desired firing rate is $r_0$ = 2 Hz.

https://doi.org/10.1371/journal.pcbi.1010876.g002

synaptic-scaling. Fig 3A depicts the number of spikes in a single postsynaptic neuron at each learning cycle with only random input spike patterns. There are no output spikes in the first learning cycles since weight vectors are small in magnitude. However, on average, the neuron learns to fire at $r_0$ Hz after a few learning cycles. Then we show an embedded pattern in each cycle after 2000 learning cycles and calculate the cosine between the weight vector at learning cycle 2000 and the new weight vector (Fig 3B). While the neuron has achieved $r_0$ at learning cycle 2000, the weight vectors are changed when the embedded patterns start to be shown. Fig 3C shows that neurons learn to fire only in response to the embedded pattern and remain silent otherwise. Extending the testing window by $L$ = 15 ms reveals that the performance

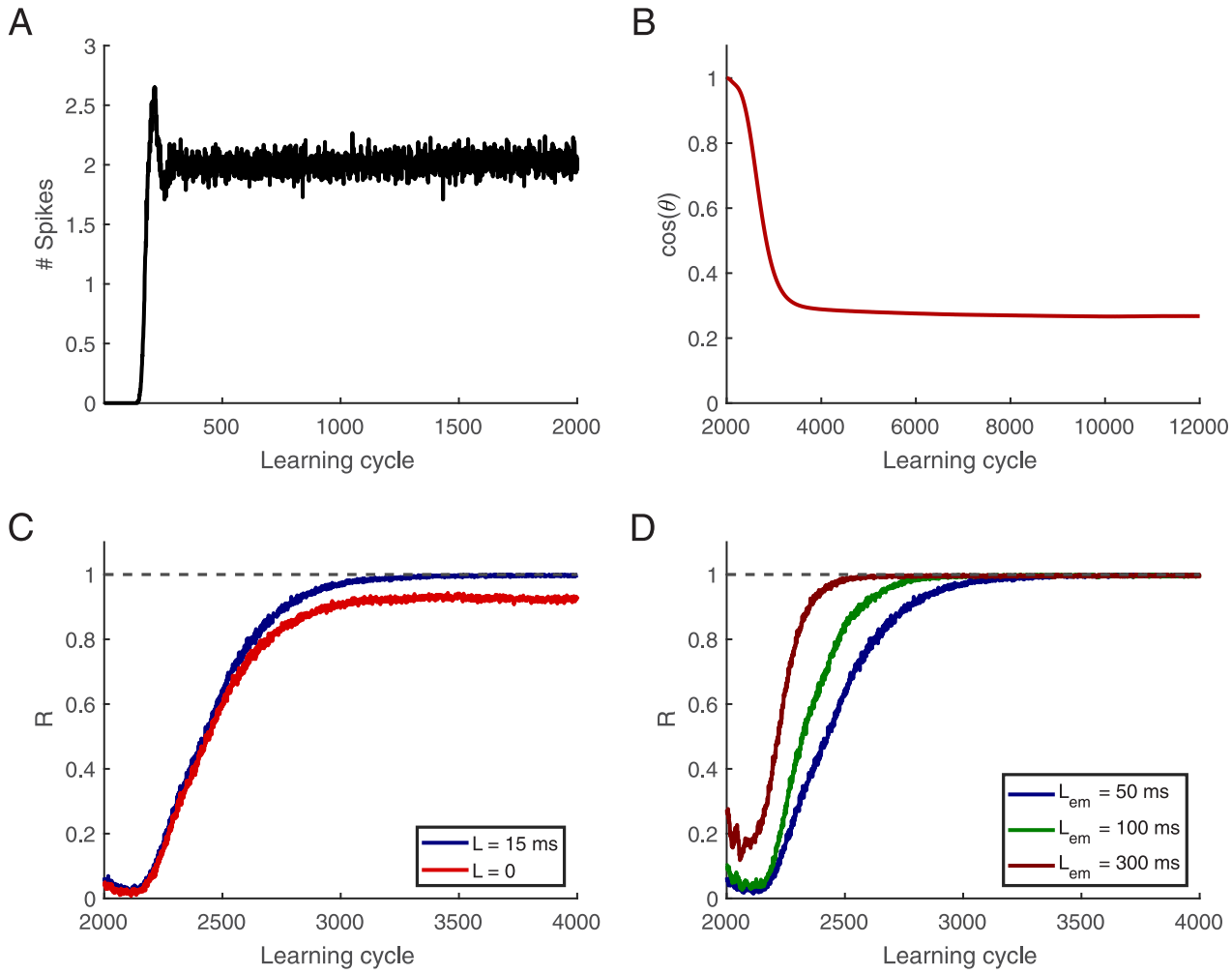


**Fig 3. Convergence of learning.** There is no embedded pattern till learning cycle 2000 in afferents, and there is a 50 ms embedded pattern in afferent from learning cycle 2001 shown in afferents beginning from 500 ms. **(A)** Number of elicited spikes versus learning cycle, on average the post-synaptic neuron fires two times in response to the noisy background. **(B)** The cosine between the current weight vector and the initial weight vector at learning cycle 2000. **(C)** Learning performance R versus learning cycle, for $L = 0$ and $L = 15$ ms. A 50 ms pattern is embedded between 500 and 550 ms. **(D)** R versus learning cycle, $L = 15$ ms. Patterns duration, $L_{em}$, are 50, 100, and 300 ms, shown in afferents from 500 ms. R is an average of 500 simulations, in which there are 500 afferents, and the length of the training epoch is 1000 ms. The desired firing rate is $r_0 = 2$ Hz.

https://doi.org/10.1371/journal.pcbi.1010876.g003

becomes perfect. Fig 3D shows that using longer embedded patterns allows neurons to learn them faster: a more extended embedded pattern leaves more room for residual excitatory-inhibitory imbalances and more contribution to the weight changes; therefore, it can find the embedded pattern more rapidly.

## Noise and memory robustness

We wondered if and how the memory for the originally learned pattern decays when synaptic plasticity is present during long periods of random inputs where an already learned pattern does not re-appear. Note that plasticity was switched off when we tested whether it remembers the originally learned pattern. Fig 4A shows that even after 60000 learning cycles, $>$ 80 percent of spikes would still occur during the embedded pattern time (chance level is 0.05). In particular, after dropping to this value $R$ remains constant for a period that would correspond to more

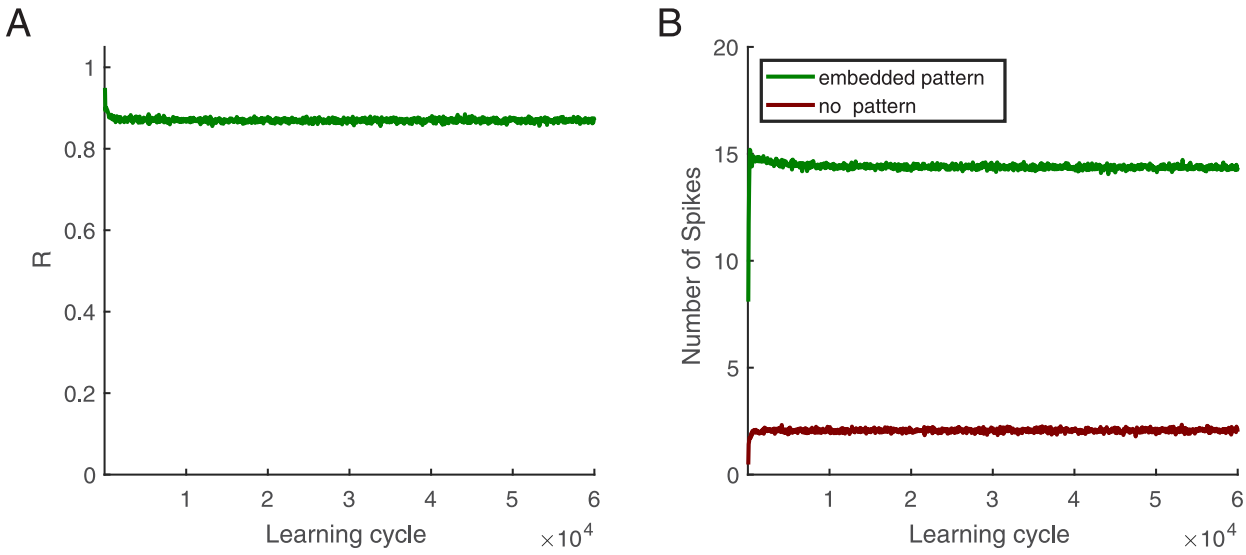


**Fig 4. Long term robustness of memory traces. (A)** *R* as memory criterion versus learning cycle: Without learned patterns in afferents, learning continues, and every 50 cycles, learning is paused, and the learned pattern is placed in the background, then R is computed as a memory criterion. **(B)** Number of spikes versus learning cycle. Neuron elicits more spikes when the embedded pattern is in the afferents (green) than the situation without the pattern (red). Patterns duration is 50 ms, shown in afferents starting from 500 ms, $L = 15$ ms, and this figure is based on an average of 500 simulations.

https://doi.org/10.1371/journal.pcbi.1010876.g004

than 16 hours, with practically no further decay and diffusing in weight vectors. This striking memory persistence can be understood by considering that due to the synaptic scaling inherent the neurons will change synapses until the pre-determined long-term firing rate is achieved also for random patterns (red in Fig 4B). Since the inputs have no structure, the weights mostly become only scaled, which per se cannot erase the selectivity for the learned pattern. When the learned pattern is then again presented to the afferents, the neuron fires additional spikes during the pattern, which leads to a much higher firing rate for the pattern (green in Fig 4B).

This firing with higher rate cannot be considered a real rate code since also with the scaled weights the system remains deterministic. That is, the spikes during the pattern will then still be at precise temporal positions, albeit we will have more spikes than when learned with regularly occurring patterns. Generally, the first spikes in these bursts occur earlier. Furthermore, in many simulations we find the spikes to occur at a similar position as after learning with regularly occurring patterns (not shown). If now the activities of many such neurons would feed again into a subsequent detector neuron it can (as we show for rate based patterns below) still learn to respond to the corresponding pattern, particularly when the pattern is short.

The changes between a new weight vector and the initial weight vector can be in amplitude and angle. In order to keep the memory, the learned weight vector should not change its direction in weight space. If the cosine of the angle remains close to one, the neuron would still remember the pattern, while the change in the number of spikes is caused by increasing the norm of a weight vector. As Fig 5A shows the norm of the weight vector indeed changes dramatically while the angle changes are rather insignificant (Fig 5B).

Taken together, we find that when learning is continued with random input the neuron achieves the desired firing rate mostly by scaling its synapses up and then randomly fires in response to the noisy input.

Taking these findings into account both learning and persistence of pattern selectivity can heuristically be understood in combination. Let's first consider the weight changes caused by

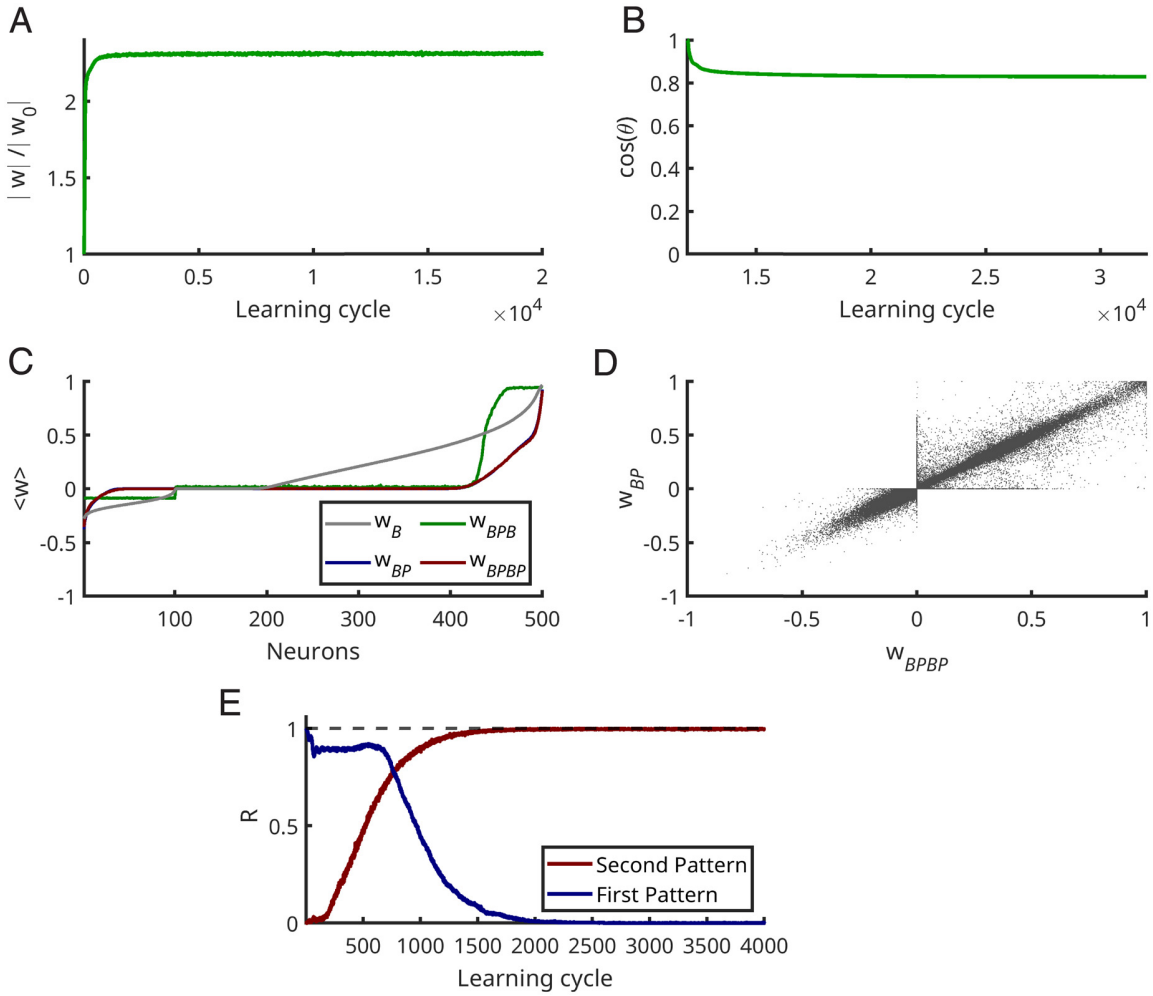


**Fig 5. Stability of memory. (A, B)** Without learned patterns in afferents, learning continues. **(A)** Average of the ratio of the norm of the current weight vector divided by the norm of the learned pattern weight vector ($w_0$). **(B)** Average of the cosine between the current weight vector and $w_0$. **(C)** Average of weight values in each stage of learning: First neurons learned to fire 2 Hz while there is no embedded pattern in afferents till the learning cycle 2000. $W_B$ (gray line in **(C)**) is the average of sorted weights for this case. Then in each simulation an embedded pattern is present in the afferents for 10000 learning cycles. $W_{BP}$ (blue line) is the mean of sorted weights obtained after neurons learned the embedded patterns. Next there is again no embedded pattern in afferents for 20000 learning cycles, and $W_{BPB}$ shows the resulting weight vector at this learning cycle, however, displayed using the ranks from $W_{BP}$. Finally, there is again the original embedded pattern in the afferents for further 20000 learning cycles; $W_{BPBP}$ shows the resulting averaged weights with the same sorting. In the mean the sorting is conserved, and the values return to the same size. **(D)** The scatter plot from all simulations demonstrates that most of the weights remain roughly the same, i.e. learning a pattern leads to a fixed point in weight space. **(E)** The neurons first learn the first embedded pattern for the 10000 learning cycles, and then there is another different embedded pattern (second pattern) in afferents for another 10000 learning cycles. This figure shows the R-value for the second 10000 learning cycles. This figure is based on an average of 500 simulations.

https://doi.org/10.1371/journal.pcbi.1010876.g005

stochastic background only. Here, the instability of Hebbian excitatory plasticity drives a subset of weights to large values until the desired number of spikes occurs in the mean (Figs 3A and 5C). Simultaneous Hebbian plasticity of inhibition ensures that global balance is achieved. Then, the neuron is in the fluctuation driven regime, with rather strong excitatory and inhibitory weights which leads to large fluctuations of the membrane potential (Fig 1, blue lines). After achieving this balance further weight changes induced by the stochastic background induce mainly some random walk confined around this fixed point (green line in Fig 5C).

This raises the question if the fixed point of the weights learned from random input alone is too stable to allow for subsequently learning a particular pattern. Fig 3 demonstrates that learning is indeed possible also with this initialization. Intuitively, when only random input is presented the weights perform a random walk around the fixed point, but when a repeating pattern is introduced an additional drift systematically shifts the weights away from this fixed point until the desired number of spikes occur only for the pattern and none in response to the background [30]. Note, that this entails that some of the weights originally acquired from the background (Fig 5C) decay. This weight dynamics continues until the spikes occur only in the period of the repeating pattern. Then the remaining weight changes cause diffusion around this new fixed point (red and blue line in Fig 5C). Hence, also with such an initialization the neuron can learn to fire in response to the embedded pattern. The learning speed, however, is reduced. Fig 3C shows that the R-value approaches one, and Fig 3B that the cosine between the new weight vector and the initial weigh vector changes.

In order to understand why the memory for the learned pattern persists when learning continues without the embedded pattern being present note that the weights for pattern detection are specific for the repeating pattern and at the same time guarantee that the background alone will not elicit spikes. When learning continues without the repeating pattern all weights are mainly scaled up by both the mechanisms of excitatory plasticity, synaptic scaling and the instability of the Hebbian term. In consequence the norm of the weight vector grows (Fig 5A) while its direction is preserved (Fig 5B). Thereby the structure of the learned weights persists.

The trained neuron (with weight vector $W_{BP}$) has been responding to noisy input for a long time; therefore, weight vectors will be changed to $W_{BPB}$ (Fig 5C). To show that the embedded pattern is stored in particular synapses, we subsequently present again the embedded pattern and continue learning to determine whether weight vectors ($W_{BPBP}$) are oriented toward $W_{BP}$. Fig 5D shows that the most components of weight vectors persist. This illustrates how the memory is protected from being overwritten by noise. It will, however, become overwritten if the trained neuron receives another embedded pattern (Fig 5E).

The plausibility of spike pattern coding depends on its robustness against noise and pattern distortions. For neurons that have learned a particular pattern without noise we examined the dependency of detection performance on three types of perturbations:

**First**: we removed spikes inside the embedded patterns and examined if neurons can still recognize the embedded pattern. Fig 6A shows the robustness against removing spikes inside the embedded pattern.

**Second**: during learning, the neuron receives inhibitory input at a frequency of 20 Hz and excitatory input at a frequency of 5 Hz (ratio 4 to 1). For testing we added $S$ random spikes per second to excitatory input neurons and $a \times S$ spikes per second to inhibitory neurons. The new rates becomes $r_E^{new} = r_E + S$ and $r_I^{new} = r_I + 4S$. Fig 6B shows that the performance R decays when $r_E^{new} > 10$ Hz. Here we define $r^* = \frac{r_{new}}{r}$.

**Third**: in this part, we examine the robustness of detection against jitter noise. For this purpose, we shuffle the times of the spikes in the afferents using a Gaussian distribution with zero mean and $\sigma$ standard deviation. Fig 6C shows that the algorithm is robust until $\sigma = 5$ ms, and after that, performance starts to decay.

Next, we wondered if precise patterns are required for self-organizing pattern selectivity. First, we perturbed the training patterns by jittering the spikes according to a Gaussian distribution with mean zero and a standard deviation of 20 ms. We found that this does not hamper learning. Fig 7A shows the R-value in each learning cycle; the blue line is for testing with the original pattern, the green line with the jittered patterns. The red line represents $R^*$, i.e. we dropped contributions to R from the epochs where no spikes at all occur. Then, we converted

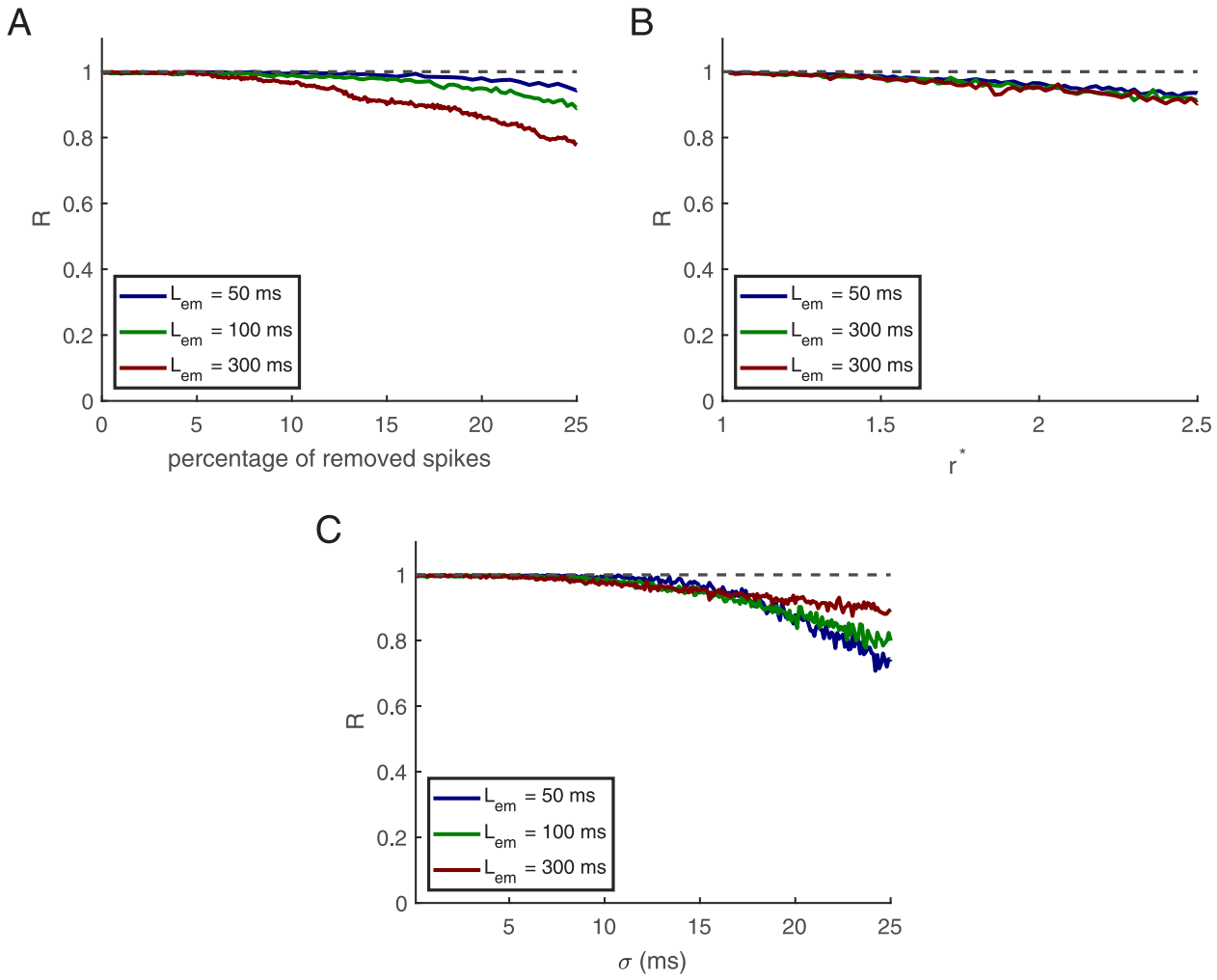


**Fig 6. Testing noise robustness. (A)** Removing spikes. **(B)** Increasing firing rates. **(C)** Jitter noise. Patterns durations are 50, 100, and 300 ms, shown in afferents starting from 500 milliseconds. This figure is based on an average of 500 simulations, in which there are 500 afferents, the length of the training epoch is 1000 ms, and $r_0 = 2$ Hz.

https://doi.org/10.1371/journal.pcbi.1010876.g006

each afferent's time code input to rate code input (i.e. Poisson spike rates). For this purpose we first convolved each spike with a Gaussian distribution with a zero mean and a standard deviation of 20 ms. The resulting function is then used as modulated firing rate of a Poisson point process. This results in an ensemble of spatio-temporal patterns based on the original pattern that has the statistics of Poisson processes, including failures and a Fano factor of 1. These distorted patterns are then used for learning and testing. This transformation is leading to a similar result (Fig 7B, the blue line is for testing with the original pattern, the green line for testing with Poisson spike rates including no spikes, the red when epochs with no spikes are dropped).

It turns out that with the corresponding weights pattern detection becomes more robust with respect to jitter noise (Fig 7C, the black and gray lines are for testing with different $\sigma$ for jittered and Poisson spike rates, respectively). These results demonstrate that codes based on temporal rate modulations and spatio-temporal pattern detection by individual neurons are compatible.

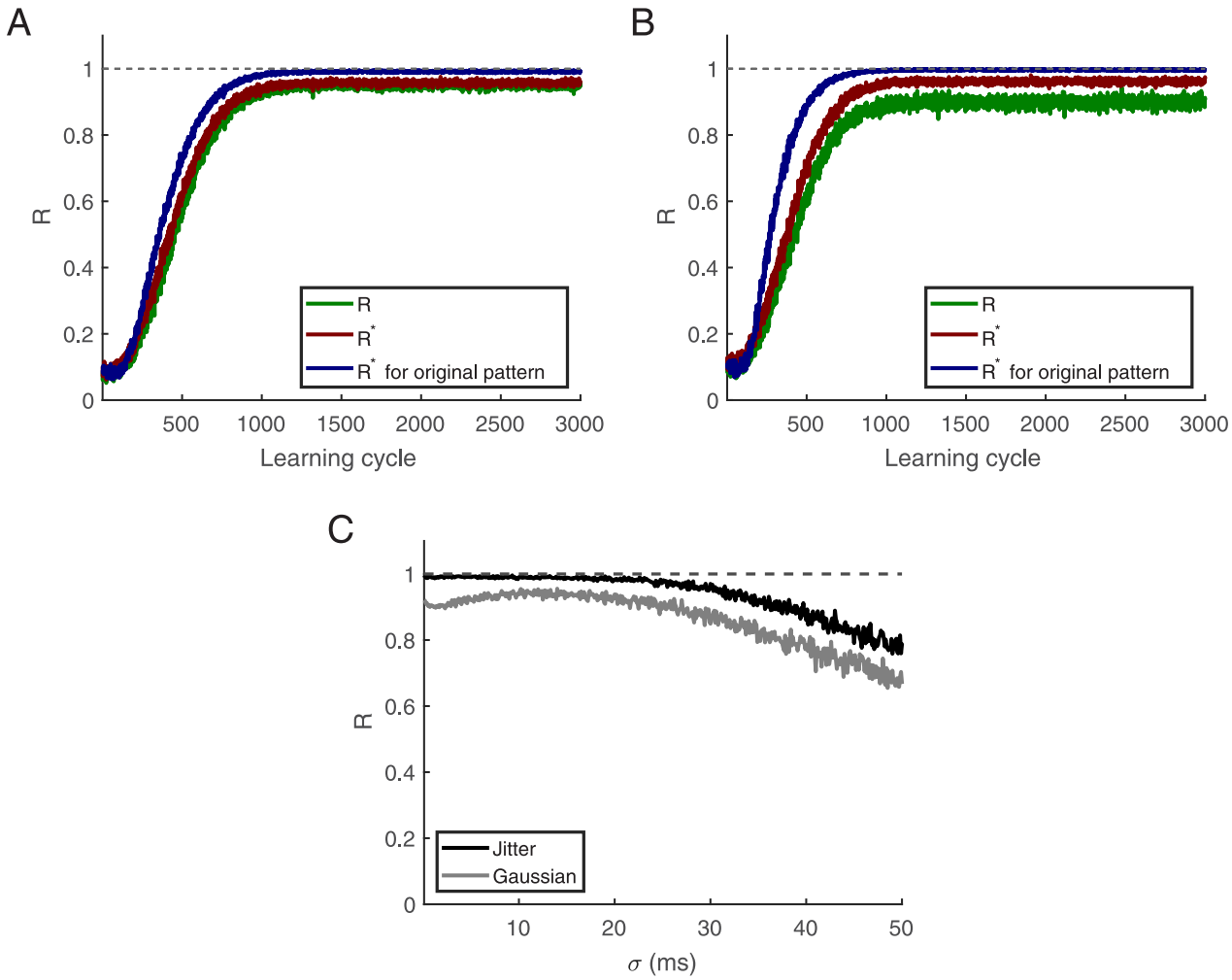


**Fig 7. Learning and testing with jittered patterns and Poisson spike rates. (A)** The training patterns are perturbed by jittering the spikes with a Gaussian distribution with a standard deviation of $\sigma = 20$ ms and a zero mean. Blue represents testing with the original pattern ($R$), the green line represents testing with jittered data including simulations with no spikes (i.e. $R$), and the red line represents the performanc when testing with jittered data but dropping episodes with no spikes (i.e. $R^*$). **(B)** Learning from Poisson spike rates: the blue line represents $R$ when testing with the original pattern, the green line represents testing with Poisson spike rates, including those with no MP spikes ($R$), and the red line shows $R^*$ where episodes with no spikes are ignored. **(C)** The black and gray lines represent tests of jittered and Poisson spike rates where the weights were trained with $\sigma = 20$ ms, respectively. This figure is based on an average of 500 simulations with 500 afferents. The training epoch is 1000 ms, $L_{em} = 50$ ms, $L = 15$ ms, and $r_0 = 2$ Hz.

https://doi.org/10.1371/journal.pcbi.1010876.g007

## Diversification by pre-synaptic hetero-synaptic plasticity

In the approach presented so far a single neuron can become a detector for more than only one pattern, along the lines of the Tempotron [9] (Fig 8A, 8B and 8C). Its activity would then, however, obscure which individual pattern was present at which time. The number of patterns a single neuron can learn depends on the desired firing rate. As shown in Fig 8C, 60 percent of the ensemble learns two patterns when $r_0$ is two, but when it is nine, almost 50 percent of the ensemble learns at least three patterns (Note there are for independent embedded patterns.). Here the memory for the case of two embedded patterns and a single post-synaptic neuron is tested too. When synaptic plasticity is active throughout extended periods of random inputs when previously learned patterns do not reappear, memory for them decays. We turned off

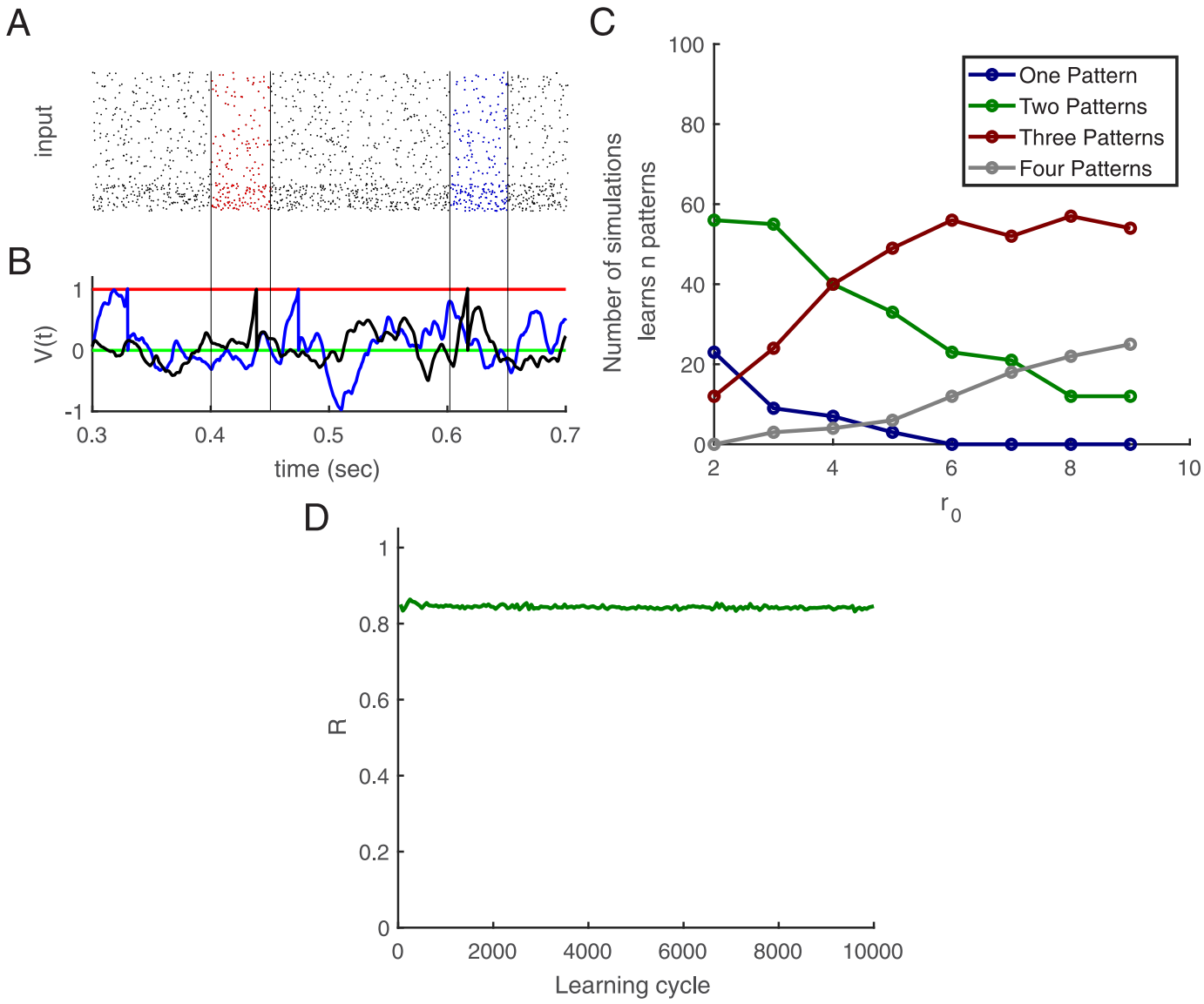


**Fig 8. Learning more than one embedded pattern. (A)** Input activity in the raster plot, five hundred afferents (80% excitatory and 20% inhibitory) send inputs to one post-synaptic neuron. The excitatory neurons' rate is 5 Hz, and the inhibitory neurons' rates are 20 Hz. There are two random embedded patterns of length 50 ms in the red and blue areas (between black vertical lines), $r_0 = 4$ Hz, and the length of the training epoch is 1000 ms. **(B)** Membrane potential versus time. The black trace shows that after learning the neuron responds to both embedded patterns. The green line is for resting potential, red is for threshold, blue is for before learning, and black is for after learning. **(C)** During learning, all embedded patterns are in the epoch, and we compute the percentages of neurons that can detect only one of the patterns (blue), two (green), three (red), and four of them depending on the target rate $r_0$. This figure is based on an average of 100 simulations with 500 afferents. The training epoch is 1000 ms, $L_{em} = 50$ ms, $L = 15$ ms. **(D)** First, the neuron learns two embedded patterns, and then $R$ as a memory criterion vs. learning cycle is computed: Learning continues without learned patterns in afferents, and every 50 cycles, learning is paused, and the learned patterns are placed in the background, then R is computed as a memory criterion. There are two 50 ms embedded patterns, shown in afferents starting from 400 ms and 800 ms, $L = 15$ ms, and this figure is based on an average of 500 simulations. $r_0 = 4$ Hz.

https://doi.org/10.1371/journal.pcbi.1010876.g008

plasticity when we investigated whether it recalls the first learned patterns. Fig 8D indicates that even after 10000 learning cycles, more than 80% of spikes would still occur within the embedded pattern duration (chance level is 0.1). Here, we consider R as the summation of the R-values for patterns one, $R_1$, and two, $R_2$. Therefore $R = R_1 + R2$.

For a faithful representation of a sequence of patterns, as e.g. the phonemes in spoken human language, it is therefore desirable that different neurons in a network become specialized for different subsets of patterns such that as a whole a network represents precisely the which and when of patterns in a sequence. If successful, such a system could, e.g., be used for unsupervised speech recognition [16].

As a first step into this direction we wondered which realistic synaptic mechanism might enforce the specialization of different neurons in a network for different pattern sets. As a simple example we consider several target neurons that receive input from the same set of input neurons. We found that already synaptic competition induced by pre-synaptic hetero-synaptic plasticity [26] yields sufficient selectivity for different patterns in such an ensemble of target neurons such that identity and order of patterns are represented faithfully (for details of the computational implementation see Materials and methods).

To quantify the performance, we use the rank of a matrix where each row represents one of the neurons, and each column one of the patterns. The matrix element in each row is set to 1 if the corresponding neuron is active for that pattern, and to 0 otherwise. The rank of this matrix provides the number of linearly independent row vectors. When it meets the number of the different patterns in a given stimulus the population of neurons faithfully represents the presence and the order of the patterns. Therefore, we introduce the ratio of the rank of this matrix to the number of patterns as performance measure $\Omega$.

As an example, we trained networks of different sizes with four patterns where always all patterns were present in each training epoch. We found that the pre-synaptic competition leads to selectivity for all four patterns as soon as 7 post-synaptic neurons were present. In contrast, without this pre-synaptic competition, separation does not become complete (Fig 9A).

We then tested the persistence of learned selectivities (with 7 neurons) when learning is continued with random input. We tested performance (with plasticity switched off) and found practically no decay of $\Omega$ even when learning was continued 10X longer than it takes for learning all 4 patterns.

This result motivated us to test if learning a set of patterns is possible from learning epochs that contain only subsets of all patterns. First results indicate that such incremental learning is indeed possible. As an example, we considered 4 embedded patterns and 7 post-synaptic neurons. Each embedded pattern has a 0.2 probability of being present in each learning cycle in the epoch. Note that thereby some learning cycles have no embedded pattern in the epoch. Also, we randomly chose locations from ([85, 85 + $L_{em}$), [175, 175 + $L_{em}$), . . .[895, 895 + $L_{em}$] ms) to put the embedded patterns in them. As Fig 9B shows the relative rank $\Omega$ goes to one, indicating that patterns can be learned also incrementally and the R value goes to one for all post-synaptic neurons Fig 9C.

We then tested how many post-synaptic neurons are required to separate different numbers of embedded patterns. Fig 9D shows a linear increase in the number of post-synaptic neurons necessary for selecting different numbers of embedded patterns (where $\Omega \geqslant 0.96$). However, most of the post-synaptic neurons respond to only two of the embedded patterns. Here we look at which post-synaptic neuron fires for which patterns and count them. As shown in Fig 10, most neurons respond to a few embedded patterns; on average, 8 respond to only one, 19 to two, and 3 to three embedded patterns.

## Discussion

Neurons respond faithfully to input sequences [31]. That is, they are rather deterministic devices and with suitable synaptic efficacies, individual neurons can, in principle, serve as detectors for specific spatio-temporal input spike patterns. This opens the possibility that

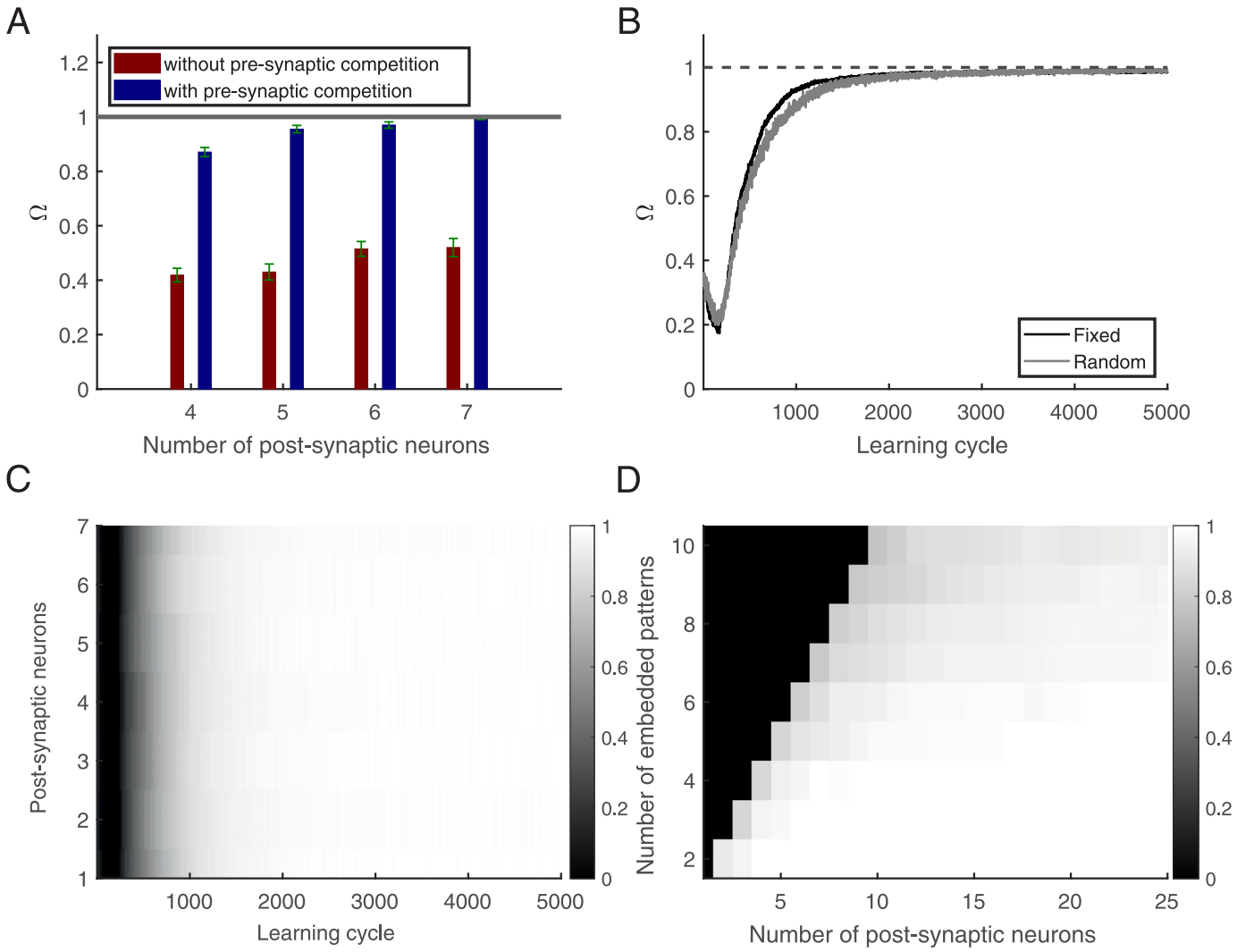


**Fig 9. Self-supervised neural networks. (A)** The system's Ω (rank/4) versus the number of post-synaptic neurons after learning. **(B)** Ω versus learning cycle (There are 7 post-synaptic neurons). Black line: Each pattern is shown in each learning cycle in a fixed position. Gray line: Each pattern is shown in the epoch with the probability of 0.2 at a random place. **(C)** Each row shows the mean R values for the case of 7 post-synaptic neurons. **(D)** Ω: number of post-synaptic neurons to separate different numbers of embedded patterns (Ω is computed when the number of post-synaptic neurons equals or exceeds the number of embedded patterns.) **(A)**, and **(D)** are based on an average of 50 simulations. **(B)** and **(C)** are based on an average of 500 simulations. In all simulations, the epoch length is 1000 ms, the embedded patterns' duration is 50 ms, $L = 15$ ms, and $r_0 = 2$ Hz. In **(A)**, **(B)**, and **(C)**, there are 4 different independent embedded patterns in each simulation.

https://doi.org/10.1371/journal.pcbi.1010876.g009

coding and computation in brains are at least in part based on temporally precise action potentials.

In the past, this hypothesis has been investigated in simple integrate and fire models. Supervised learning rules were proposed that enable neurons to signal the presence of a pattern [9] and to fire at predefined time points during a specific pattern [10, 13, 32]. It was further demonstrated that relatively weak supervision can be sufficient for learning the synaptic weights for pattern detection [16]. Here, only knowledge about the number of pattern occurrences is needed for the specialization of a neuron. While a learning rule for this 'aggregate label learning' was rigorously derived, the proposed biological realization suffers from several rather unrealistic assumptions. In particular, excitatory and inhibitory plasticity are not treated

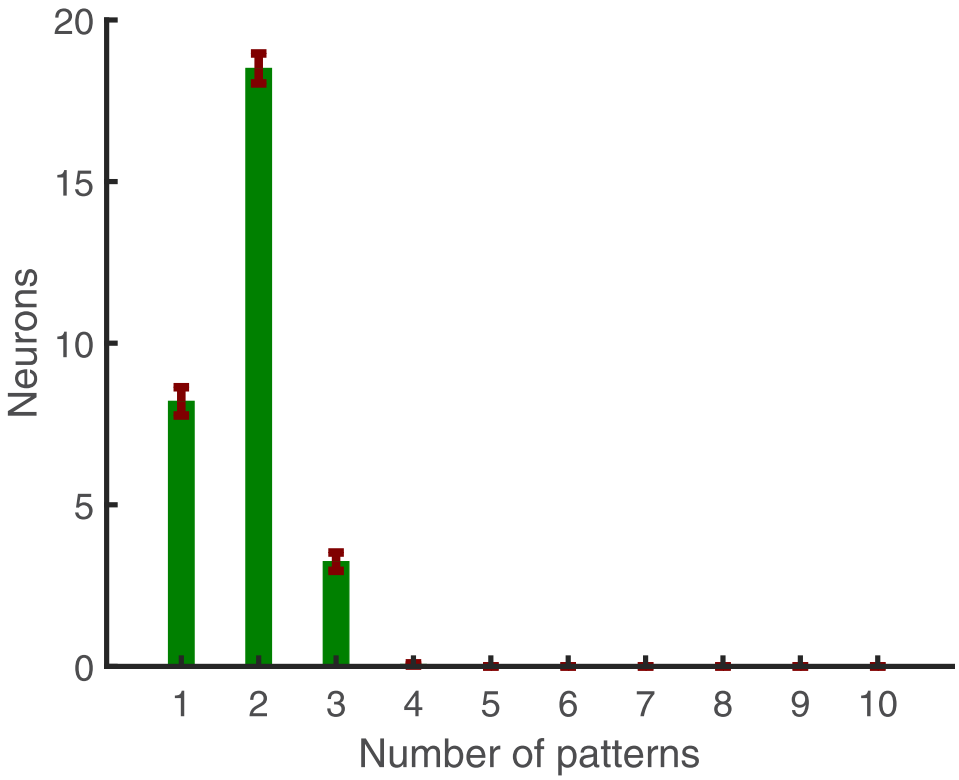


**Fig 10. Contingent of neurons responding to multiple embedded patterns.** Average count of post-synaptic neurons versus the number of embedded patterns detected. This figure is based on an average of 50 simulations with epoch length 1000 ms, 30 post-synaptic neurons, and 10 independent embedded patterns, having a duration of 50 ms each, ($L$ = 15 ms, and $r_0$ = 2 Hz.)

https://doi.org/10.1371/journal.pcbi.1010876.g010

separately, and Dale's law was not observed. When the signs of synapses may change, this has also a negative impact on the excitatory and inhibitory balance. For some patterns, there may be only few inhibitory neurons remaining in the system after learning. When there is a lack of inhibition, however, the potential can take a value close to the threshold, increasing the chance of getting random spikes outside the embedded patterns. Also, a selection criterion was used, by which independently of their sign, only the largest 10% of changes were taken into account, for which no realistic interpretation was provided.

Unsupervised learning of spatio-temporal input spike patterns has been investigated mostly in the context of spike-timing dependent plasticity (STDP) [33–35]. The model in Masquelier 2018 [36] discusses the ability of STDP of excitatory synapses to make neurons become spike pattern detectors. It requires quite careful tuning of parameters. A model closer in spirit to the present one can be found in a rather brief technical report [37]. It combines some (calcium based additive) homeostatic plasticity with a caricature of correlation based learning solely for excitatory synapses. It is demonstrated to mimic STDP and admittedly also requires careful choice of parameters. Most importantly, because of the lack of inhibition both previous models cannot exhibit balance of excitation and inhibition and therefore can neither be expected to be robust against perturbations nor to be stable with respect to continuous learning without patterns.

Therefore, it remains an open question if the synaptic plasticity mechanisms present in real neuronal networks support a robust coding scheme that is based on spatio-temporal patterns of spikes.

We found that a combination of membrane potential dependent Hebbian mechanisms, hetero-synaptic competition, and synaptic scaling indeed makes individual neurons sensitive for statistically dominant spatio-temporal patterns in their afferents without any supervision. The hetero-synaptic competition implies a threshold for long-term depression (LTD) depending on the ensemble of plasticity signals, which could be related to the Bienenstock-Cooper-Munroe (BCM) rule [38]. Along the same line the synaptic scaling regulates weight changes such that with too high post-synaptic firing rates the synapses decay. In contrast, the set of mechanisms considered here can not reproduce STDP, since mono-synaptic LTD-mechanisms are not taken into account.

Performance is shown to be robust to temporal jitter, missing spikes, and additional noise. In particular, also spatio-temporal patterns consisting of Poisson spike rate modulations are captured surprisingly well by the proposed plasticity mechanisms and lead to robust detection (Fig 7B and 7C).

The proposed combination of learning mechanisms yields a detailed balance of excitation and inhibition where this is possible: during the learned pattern. This fits nicely to experimental observations [22] revealing a negative correlation between excitatory and inhibitory inputs. Outside the pattern, global balance is achieved [24].

Balance is a natural consequence of Hebbian mechanisms when they are simultaneously present in both excitatory and inhibitory synapses, and the otherwise unstable growth of excitatory efficacies is constrained. While this has been noted before [39], we here show that Hebbian plasticity can select synaptic efficacies that make neurons detectors for spatio-temporal patterns when realistic constraints are taken into account. In particular, we found that a subtle interplay of the instability of Hebbian mechanisms for excitatory synapses and synaptic scaling enforces a local imbalance during the learned patterns which leads to specific and temporally precise spike responses.

The excitatory-inhibitory balance protects memory for rate patterns in neural networks [39, 40]. Our simulations now demonstrate that also the memory for spike patterns is protected from being overwritten by noise (Figs 4, 5D and 5E).

After successful learning of patterns, the random background input does not lead to spikes in individual neurons. When then plasticity is continuously present for a long time during which only random inputs are present, the input weights mainly become scaled up until the desired number of spikes is reached, i.e., the plasticity mechanisms considered here are consistent with synaptic scaling [20]. Obviously, scaling alone preserves the memory for the learned patterns, which will then induce far more spikes than the background. In other words, the plasticity mechanisms discussed here lead to a very long memory persistence already in a single neuron such that selectivity is preserved and sensitivity becomes even enhanced. We tested the memory persistence also in groups of neurons that specialized for subsets of the input patterns via pre-synaptic hetero-synaptic plasticity. Also here, we observed practically no decay.

This finding suggests that in groups of neurons incremental learning of sets of patterns should be possible, wherein each successive training epoch only a subset or even none of all patterns is present. We could confirm this hypothesis for simple cases; however, the question if the combination of plasticity mechanisms discussed here indeed provides a solution for the notorious stability-plasticity dilemma [25] in spatio-temporal pattern learning will require more systematic investigations which go beyond the scope of this paper.

The fact that biologically realistic plasticity mechanisms can support the self-organization of spatio-temporal pattern detection by individual neurons underlines the possibility that such temporal codes are indeed present in nervous systems. Particularly the ability to learn patterns underlying Poisson spike rates demonstrates that such a temporal coding scheme can be consistent with rate codes. We speculate that this transformation of temporally modulated rates to

spike pattern codes could explain the increase in sparsity observed in the early visual cortex when natural contexts are included [41] as well as the extreme sparsity of activations in higher cortical areas.

## Materials and methods

### Neuron model

In this work, we employ the leaky integrate and fire (LIF) model. The dynamic of the membrane potential of a single neuron $V(t)$ which is receiving current from $N$ afferents is:

$$\tau_m \frac{d}{dt} V(t) = -V(t) + R_m I_{ext}(t) \tag{3}$$

where $\tau_m$ and $R_m$ are time constant and resistance of the membrane, respectively. Whenever the neuron arrives at or passes the threshold it evokes spike output and resets to resting potential. Resting potential is zero in this study, and $I_{ext}$ is the external current from excitatory (E) and inhibitory (I) afferents:

$$I_j(t) = \sum_{i=1}^{N_E} w_{ji}^E \sum_{t_i^l < t} K^E(t - t_i^l) - \sum_{i=1}^{N_I} w_{ji}^I \sum_{t_i^l < t} K^I(t - t_i^l) \tag{4}$$

where $w_{ji}^{E,I}$ represent the respective $i'th$ afferent's excitatory and inhibitory synaptic strength to output neuron $j$. $N_E$ and $N_I$ are the numbers of excitatory and inhibitory afferents, respectively ($N = N_E + N_I$). Note that at time $t_i^l$, there is a spike in afferent $i$, and at this time, afferent $i$ starts to send input to the post-synaptic neuron $j$ amounting to $w_{ji} \times K$. The shape of the kernel is an alpha-function with the following equation:

$$K(t - t_i^l) = I_{norm} \left[ \exp\left( -\frac{t - t_i^l}{\tau_r} \right) - \exp\left( -\frac{t - t_i^l}{\tau_d} \right) \right] \theta(t - t_i^l) \tag{5}$$

where $\theta$ is the Heaviside step function. $\tau_r$ and $\tau_d$ are time constants of synaptic current, which are different for excitatory and inhibitory synapses. $I_{norm} = \frac{\eta^{\eta/\eta-1}}{\eta-1}$ normalises $K$ to unit amplitute, where $\eta = \frac{\tau_d}{\tau_r}$.

### Learning algorithm

We assume that a synapse's efficacy is the product of pre- and post-synaptic components.

$$w_{ji} = a_{ij} b_{ij} \tag{6}$$

where $a_{ij}$ is provided from the pre-synaptic neuron $i$, and $b_{ij}$ is provided by the post-synaptic neuron $j$ (Fig 11). If we have $N$ pre-synaptic neurons ($i = 1, \ldots, N$) and $M$ post-synaptic neurons ($j = 1, \ldots, M$)

$$\frac{dw_{ji}}{dt} = a_{ij} \frac{db_{ij}}{dt} + \frac{da_{ij}}{dt} b_{ij}. \tag{7}$$

Here, Dale's law is imposed: when $\delta a$ and $\delta b$ would change the sign of $a$ and $b$, respectively, we set them to zero. We assume that correlations between pre-synaptic input and post-synaptic membrane potential drive weight changes. By considering only the spike at time $t_i^l$ the correlation between $i'th$ afferent and the $j'th$ post-synaptic neuron's potential $V_j(t)$ is:

$$\vartheta_{ij}^{*l}(t) = K(t - t_i^l)\{[V_j(t) - V_0]_+ + q[V_j(t) - V_0]_-\} \tag{8}$$

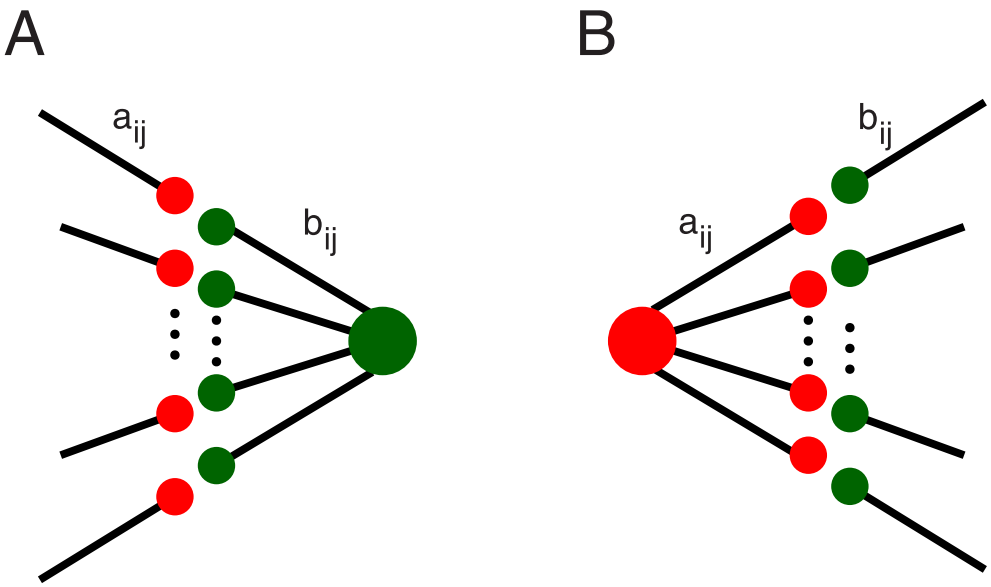


**Fig 11. Illustration of synaptic competition induced by hetero-synaptic plasticity. (A)** Competition induced by post-synaptic hetero-synaptic plasticity. Excitatory pre-synaptic neurons i target a post-synaptic neuron j. We assume that the resources required for increasing the post-synaptic components $b_{ij}$ of the weights $w_{ji} = a_{ij}b_{ij}$ are limited and therefore distributed in a competitive manner. That is, we assume hetero-synaptic plasticity where afferent synapses that receive large eligibility signals $\varepsilon_{ij}$ increase their efficacy while synapses that receive weaker (but for excitatory synapses always positive) signals will instead weaken. **(B)** Pre-synaptically induced competition is assumed to follow the same principle. The signals for the changes of the pre-synaptic components $a_{ij}$, however, are assumed to depend on the realized amount of potentiation at the post-synaptic side, i.e., to take the post-synaptic hetero-synaptic competition into account. We found that this choice is more parameter tolerant and yields more robust memory than a symmetric version where pre- and post-synaptic hetero-synaptic plasticity are based on the same eligibility signal which, however, can also realize self-organized spike pattern detection (not shown).

https://doi.org/10.1371/journal.pcbi.1010876.g011

where $V_0$ is the modification threshold [42] that is set to zero in all simulations of this study. $q$ is zero for excitatory afferents and 1 for inhibitory ones. In every time step, all $n_i$ spikes in the $i'th$ afferent are used for updating the weights.

$$\vartheta_{ij}(t) = \sum_{l=1}^{n_i} \vartheta_{ij}^{*l}(t). \tag{9}$$

As a result, we compute the correlations for all spikes $l$ and integrate them to determine the eligibility $\varepsilon$ [16] via

$$\tau_\varepsilon \frac{d\varepsilon_{ij}(t)}{dt} = -\varepsilon_{ij}(t) + \vartheta_{ij} \tag{10}$$

which is the basic signal for weight changes at synapse $(i, j)$.

For inhibitory synapses weight changes are set to be simply proportional to $\varepsilon$. For excitatory synapses changes are assumed to depend only on the positive part $[\varepsilon_{ij}]_+$ which mimics the characteristics of the NMDA receptor [17–19]. Also for excitatory weights we take synaptic scaling into account. That is, neurons tend to fire and to implement a specific firing rate $r_0$ that is genetically determined [20, 29]. That is, if a post-synaptic neuron's long-term firing rate $r_j^*$ is less than the desired $r_0$, it scales its afferent excitatory weights up, and if it is more than the desired $r_0$, it scales its afferent excitatory weights down. The long-term firing rate $r_j^*$ is

determined by

$$\tau_{r^*}\frac{dr_j^*}{dt} = -r_j^* + \sum_{t_i^I}\delta(t - t_i^I) \tag{11}$$

where $\tau_{r^*}$ is the time constant for the long-term firing rate. Changes of synapses are subject to limitations of the material provided by the respective pre and post-synaptic neurons (e.g., release sites, vesicles, receptor densities). Plausibly, this leads to competition for changes of different synapses, which affects the respective pre- and post-synaptic components a and b differently. In the current approach we include pre- and post-synaptic competition only for the changes of excitatory weights thereby modeling pre- and post-synaptic versions of hetero-synaptic plasticity [21, 26, 43, 44].

**Single post-synaptic neuron.** To compute weight change (Eq (7)) when there is only a single post-synaptic neuron ($j = 1$), we have $b_{i1} =: b_i$, $\varepsilon_{i1} =: \varepsilon_i$, and $a_{i1} =: a_i$. For simplicity we here set $a_i = 1$ and $\delta a_{ij} = 0$ (for the full version see next section).

Here inhibitory synapses are changed by

$$\tau_I\frac{db_i^I}{dt} = -b_i^I + c^I\varepsilon_i \tag{12}$$

where $\tau_I$ is the time constant for inhibitory synapses and $c^I$ the learning rate.

For excitatory synapses we subtract the mean of the plasticity signals $[\varepsilon_i]_+$, to mimick post-synaptic hetero-synaptic plasticity:

$$\tilde{\varepsilon}_i = \varepsilon_i - \frac{1}{N}\sum_{i=1}^{N}\varepsilon_i. \tag{13}$$

Note that this does not imply strict normalization since Dale's law prevents negative changes that otherwise would turn excitatory synapses to inhibitory synapses. The excitatory afferents' weights then change according to the following equation:

$$\tau_E\frac{db_i^E}{dt} = -b_i^E + c^E\tilde{\varepsilon}_i + \alpha b_i^E(r_0 - r) \tag{14}$$

where $\tau_E$ is the time constant for excitatory synapses and $c^E$ the learning rate. We consider $c^E$ less than $c^I$; therefore, inhibitory neurons adapt faster to ensure balance wherever possible (globally and detailed), and excitation can not conflict with the relatively slow limiting mechanism of synaptic scaling.

**More than one post-synaptic neuron.** When there is more than one post-synaptic neuron each afferent has different eligibility for each post-synaptic neuron (Eq (9)). Therefore $a_{ij}$ needs to be taken into account (Eq (7)).

For inhibitory synapses we use:

$$\begin{aligned}\tau_I\frac{db_{ij}^I}{dt} &= -b_{ij}^I + c^I\varepsilon_{ij}\\ \tau_I\frac{da_{ij}^I}{dt} &= -a_{ij}^I + c^I\varepsilon_{ij}\end{aligned} \tag{15}$$

As for single target neurons $j$ the changes of excitatory synapses are subject to post-synaptic hetero-synaptic plasticity that we realize by subtracting the mean of eligibilities:

$$\tilde{\varepsilon}_{ij} = \varepsilon_{ij} - \frac{1}{N}\sum_{i=1}^{N}\varepsilon_{ij}. \tag{16}$$

With this the post-synaptic components change by

$$\tau_E \frac{db_{ij}^E}{dt} = -b_{ij}^E + c^E\tilde{\varepsilon}_{ij} + \alpha b_{ij}^E(r_0 - r). \tag{17}$$

We assume that also pre-synaptic neurons have finite resources for increasing their contributions to synaptic efficacies ($a_{ij}$), as e.g., release sites or vesicle densities. Fig 11 illustrates this pre- and post-synaptic competition. We restrict the competition to excitatory neurons that up-regulate synapses because this requires resources, whereas decreases of efficacies may even release resources. To apply the competition, we first identify the signals that would scale up excitatory synapses. The pre-synaptic competition then is implemented by subtraction of the mean

$$B_{ij} = [\tilde{\varepsilon}_{ij}]_+ - \frac{\theta(\sum_j \theta([\tilde{\varepsilon}_{ij}]_+) - 1)}{\sum_j \theta([\tilde{\varepsilon}_{ij}]_+) + \zeta}\sum_{j=1}^{M}[\tilde{\varepsilon}_{ij}]_+ \tag{18}$$

where $\theta$ is a Heaviside function, $\zeta$ is a small number ($\zeta << 1$), and M is the number of post-synaptic neurons. Therefore

$$\tau_E \frac{da_{ij}^E}{dt} = -a_{ij}^E + B_{ij} + \alpha a_{ij}^E(r_0 - r). \tag{19}$$

**Simulation details.** For simplification and efficiency of simulations, we consider changes over epochs $e$ with duration $T$ ms instead of applying weight changes in each integration time step. Thereby Eq (8) is replaced by:

$$\vartheta_{ij}^l = \int_0^T dt K(t - t_i^l)\{[V_j(t) - V_0]_+ + q[V_j(t) - V_0]_-\} \tag{20}$$

and the differential equations of the form

$$\tau\frac{dy}{dt} = -y + x \tag{21}$$

change to a moving average

$$y(e+1) = \quad \gamma y(e) + (1-\gamma)\hat{x}(e). \tag{22}$$

where $\hat{x}(e)$ is the sum of contributions of $x$ in each epoch $e$ and $\gamma \simeq 1 - T/\tau$.

In all simulations, there are 500 afferents (80% excitatory and 20% inhibitory), and the learning epoch length is 1000 ms. Afferent and embedded pattern spikes are generated randomly with Poisson point processes in which the excitatory rate ($r_E$) is 5 Hz, and the inhibitory rate ($r_I$) is 20 Hz. Except for Fig 9B (gray line), all embedded patterns are in each epoch in every learning cycle.

In the network model, the initial synaptic efficacies of $a_{ij}$ and $b_{ij}$ are chosen from a Gaussian distribution with a mean of 0.1 and standard deviations of $10^{-2}$ (negative numbers are set to

zero). In the single post-synaptic neuron model, they are chosen from a Gaussian distribution with a mean of $10^{-2}$ and standard deviations of $10^{-3}$ (negative numbers are set to zero).

Synaptic scaling depends on firing rates averaged over long times. Since we perform on-line learning we use a low pass filter such that the rate estimation $r_j(c+1)$ of post-synaptic neuron $j$ used for learning in epoch $e+1$ is a running average of the actual rates $\hat{r}$ in previous epochs:

$$r_j(e+1) = \gamma^* r_j(e) + (1-\gamma^*)\hat{r}_j(e) \tag{23}$$

The parameter $\gamma^*$ is 0.9 for all figures which corresponds to a time constant of 10s. While much smaller values of this parameter do not change the asymptotic results this value was found to yield more rapid convergence.

Note that plasticity is not instantaneous but depends on an accumulation of signals for weight changes over some time which here is termed 'eligibility'. We implement also this by a

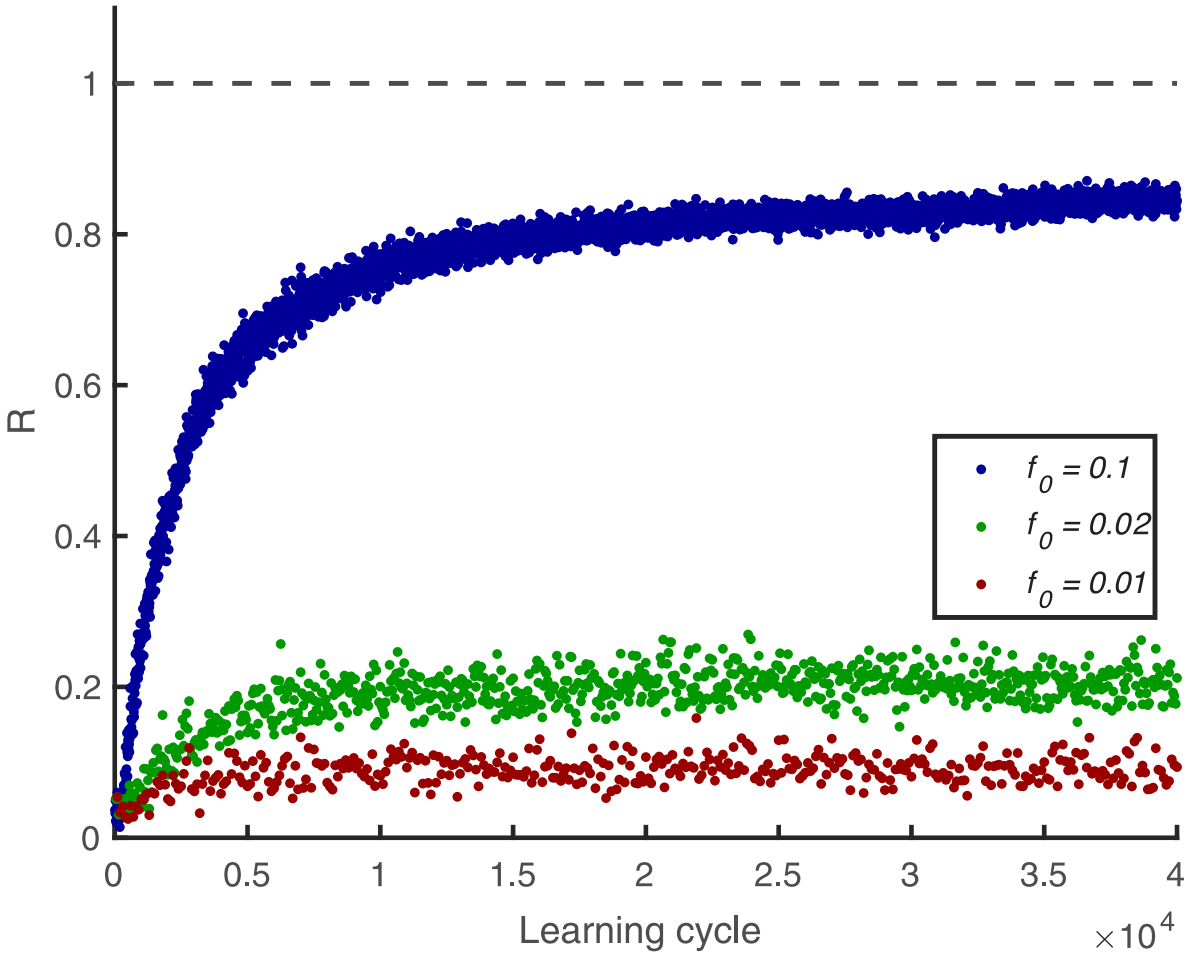


**Fig 12. Learning performance for embedded patterns presented at different rates.** Learning performance R versus learning cycle, for $L = 15$ ms. A 50 ms pattern is embedded between 500 and 550 ms and shown each 10 cycles ($f_0 = 0.1$), 50 cycles ($f_0 = 0.02$), and 100 cycles ($f_0 = 0.01$). R is an average of 100 simulations, in which there are 500 afferents, and the length of the training epoch is 1000 ms. The desired firing rate is $r_0 = 2$ Hz.

https://doi.org/10.1371/journal.pcbi.1010876.g012

**Table 1. List of parameters.**

| Symbol | Description | Value |
|---|---|---|
| $\tau_m$ | membrane time constant | 15 ms |
| $R_m$ | membrane resistance | 1 |
| $\tau_r^e$ | Rise time of excitatory currents | 0.5 ms |
| $\tau_r^i$ | Rise time of inhibitory currents | 1 ms |
| $\tau_d^e$ | Decay time of excitatory currents | 3 ms |
| $\tau_d^i$ | Decay time of inhibitory currents | 5 ms |
| $r_E$ | Rate of excitatory neurons | 5 Hz |
| $r_I$ | Rate of inhibitory neurons | 20 Hz |
| N | Number of pre-synaptic neurons | 500 |
| $N_E$ | Number of pre-synaptic excitatory neurons | 400 |
| $N_I$ | Number of pre-synaptic inhibitory neurons | 100 |
| $c^I$ | Inhibitory learning rate | $10^{-3}$ |
| $c^E$ | Excitatory learning rate | $0.9 \times 10^{-3}$ |
| $\Delta t$ | time step | 0.1 ms |
| $\alpha$ | scaling factor | 0.01 |
| $\beta$ | scaling coefficient | $0.9 \times 10^{-4}$ |

https://doi.org/10.1371/journal.pcbi.1010876.t001

low pass filter:

$$\boldsymbol{\varepsilon}_{ij}(e+1) = \quad \gamma \boldsymbol{\varepsilon}_{ij}(e) + (1-\gamma)\hat{\vartheta}_{ij}(e). \tag{24}$$

Initial conditions are $r_j(0) = 0$ and $\boldsymbol{\varepsilon}_{ij}(0) = 0$. The parameter $\gamma$ is 0.99 for all figures corresponding to a time constant of $\simeq$ 100s. This parameter limits learn-ability of patterns that are presented only rarely. E.g. for the value used in this paper learning becomes difficult when a pattern is shown only every hundredths epoch of 1000ms length (Fig 12).

Because synaptic strength cannot become arbitrarily large due to the synapses' structure and other constraints, we cut weights changes that would carry excitatory synapses out of the bounds which are set to plus one.

Besides, Dale's rule dictates that excitatory and inhibitory synapses cannot turn into each other; therefore, we assume synaptic weights to become zero if weight changes would turn their kind during the learning. As a result, subtracting the mean value in equations Eqs (13) and (18) will not change a synapse's type (Eq (7)). To numerically integrate Eq (3), we use Euler method with $\Delta t = 0.1$ ms. The parameters are found in Table 1.

Note that in the epoch approach, we implement the following equations, and the continuous version can be obtained by linearization. Therefore:

$$\delta w_{ij} = a_{ij}\delta b_{ij} + \delta a_{ij} b_{ij} + \delta a_{ij}\delta b_{ij} \tag{25}$$

**Single post-synaptic neuron**:

Inhibitory synapses:

$$\delta b_i^I = c^I \boldsymbol{\varepsilon}_i \tag{26}$$

Excitatory synapses:

$$\delta b_i^E = (1-\beta) b_i^E exp(\alpha(r_0 - r)) + c^E \tilde{\boldsymbol{\varepsilon}}_i - b_i^E \tag{27}$$

**More than one post-synaptic neuron**

Inhibitory synapses:

$$\begin{aligned} \delta b_{ij}^{I} &= c^{I}\varepsilon_{ij} \\ \delta a_{ij}^{I} &= c^{I}\varepsilon_{ij} \end{aligned} \tag{28}$$

Excitatory synapses:

$$\begin{aligned} \delta b_{ij}^{E} &= (1-\beta)b_{ij}^{E}exp(\alpha(r_0 - r)) + c^{E}\tilde{\varepsilon}_{ij} - b_{ij}^{E} \\ \delta a_{ij}^{E} &= (1-\beta)a_{ij}^{E}exp(\alpha(r_0 - r)) + c^{E}B_{ij} - a_{ij}^{E} \end{aligned} \tag{29}$$

where $\beta$ is scaling coefficient.

## Acknowledgments

We would like to thank Udo Ernst and David Rotermund for fruitful discussions and comments.

## Author Contributions

**Conceptualization:** Mohammad Dehghani-Habibabadi, Klaus Pawelzik.

**Formal analysis:** Mohammad Dehghani-Habibabadi, Klaus Pawelzik.

**Funding acquisition:** Klaus Pawelzik.

**Investigation:** Mohammad Dehghani-Habibabadi.

**Methodology:** Mohammad Dehghani-Habibabadi, Klaus Pawelzik.

**Project administration:** Klaus Pawelzik.

**Software:** Mohammad Dehghani-Habibabadi.

**Supervision:** Klaus Pawelzik.

**Validation:** Klaus Pawelzik.

**Visualization:** Mohammad Dehghani-Habibabadi, Klaus Pawelzik.

**Writing – original draft:** Mohammad Dehghani-Habibabadi, Klaus Pawelzik.

**Writing – review & editing:** Mohammad Dehghani-Habibabadi, Klaus Pawelzik.

## References

1. Johansson RS, Birznieks I. First spikes in ensembles of human tactile afferents code complex spatial fingertip events. Nature neuroscience. 2004; 7(2):170–177. https://doi.org/10.1038/nn1177 PMID: 14730306
2. Reich DS, Mechler F, Victor JD. Independent and redundant information in nearby cortical neurons. Science. 2001; 294(5551):2566–2568. https://doi.org/10.1126/science.1065839 PMID: 11752580
3. Reinagel P, Reid RC. Temporal coding of visual information in the thalamus. Journal of neuroscience. 2000; 20(14):5392–5400. https://doi.org/10.1523/JNEUROSCI.20-14-05392.2000 PMID: 10884324
4. Uzzell V, Chichilnisky E. Precision of spike trains in primate retinal ganglion cells. Journal of neurophysiology. 2004; 92(2):780–789. https://doi.org/10.1152/jn.01171.2003 PMID: 15277596
5. Ince RA, Panzeri S, Kayser C. Neural codes formed by small and temporally precise populations in auditory cortex. Journal of Neuroscience. 2013; 33(46):18277–18287. https://doi.org/10.1523/JNEUROSCI.2631-13.2013 PMID: 24227737
6. Wehr M, Laurent G. Odour encoding by temporal sequences of firing in oscillating neural assemblies. Nature. 1996; 384(6605):162–166. https://doi.org/10.1038/384162a0 PMID: 8906790

7. Carr C, Konishi M. A circuit for detection of interaural time differences in the brain stem of the barn owl. Journal of Neuroscience. 1990; 10(10):3227–3246. https://doi.org/10.1523/JNEUROSCI.10-10-03227.1990 PMID: 2213141
8. Decharms RC, Merzenich MM. Primary cortical representation of sounds by the coordination of action-potential timing. Nature. 1996; 381(6583):610–613. https://doi.org/10.1038/381610a0 PMID: 8637597
9. Gütig R, Sompolinsky H. The tempotron: a neuron that learns spike timing–based decisions. Nature neuroscience. 2006; 9(3):420–428. https://doi.org/10.1038/nn1643 PMID: 16474393
10. Florian R. The chronotron: a neuron that learns to fire temporally-precise spike patterns. Nature Precedings. 2010; p. 1–1.
11. Minsky M, Papert SA. Perceptrons, Reissue of the 1988 Expanded Edition with a new foreword by Léon Bottou: An Introduction to Computational Geometry. MIT press; 2017.
12. Rubin R, Monasson R, Sompolinsky H. Theory of spike timing-based neural classifiers. Physical review letters. 2010; 105(21):218102. https://doi.org/10.1103/PhysRevLett.105.218102 PMID: 21231357
13. Memmesheimer RM, Rubin R, Ölveczky BP, Sompolinsky H. Learning precisely timed spikes. Neuron. 2014; 82(4):925–938. https://doi.org/10.1016/j.neuron.2014.03.026 PMID: 24768299
14. Yu Q, Tang H, Tan KC, Li H. Precise-spike-driven synaptic plasticity: Learning hetero-association of spatiotemporal spike patterns. Plos one. 2013; 8(11):e78318. https://doi.org/10.1371/journal.pone.0078318 PMID: 24223789
15. Albers C, Westkott M, Pawelzik K. Perfect associative learning with spike-timing-dependent plasticity. Advances in neural information processing systems. 2013; 26.
16. Gütig R. Spiking neurons can discover predictive features by aggregate-label learning. Science. 2016; 351(6277):aab4113. https://doi.org/10.1126/science.aab4113 PMID: 26941324
17. Artola A, Bröcher S, Singer W. Different voltage-dependent thresholds for inducing long-term depression and long-term potentiation in slices of rat visual cortex. Nature. 1990; 347(6288):69–72. https://doi.org/10.1038/347069a0 PMID: 1975639
18. Cummings JA, Mulkey RM, Nicoll RA, Malenka RC. Ca2+ signaling requirements for long-term depression in the hippocampus. Neuron. 1996; 16(4):825–833. https://doi.org/10.1016/S0896-6273(00)80102-6 PMID: 8608000
19. Malenka RC,Nicoll A R. Long-term potentiation–a decade of progress? Science. 1999; 285(5435):1870–1874. https://doi.org/10.1126/science.285.5435.1870 PMID: 10489359
20. Turrigiano GG. The self-tuning neuron: synaptic scaling of excitatory synapses. Cell. 2008; 135(3):422–435. https://doi.org/10.1016/j.cell.2008.10.008 PMID: 18984155
21. Chistiakova M, Bannon NM, Chen JY, Bazhenov M, Volgushev M. Homeostatic role of heterosynaptic plasticity: models and experiments. Frontiers in computational neuroscience. 2015; 9:89. https://doi.org/10.3389/fncom.2015.00089 PMID: 26217218
22. Okun M, Lampl I. Instantaneous correlation of excitation and inhibition during ongoing and sensory-evoked activities. Nature neuroscience. 2008; 11(5):535–537. https://doi.org/10.1038/nn.2105 PMID: 18376400
23. Isaacson JS, Scanziani M. How inhibition shapes cortical activity. Neuron. 2011; 72(2):231–243. https://doi.org/10.1016/j.neuron.2011.09.027 PMID: 22017986
24. Denève S, Machens CK. Efficient codes and balanced networks. Nature neuroscience. 2016; 19(3):375–382. https://doi.org/10.1038/nn.4243 PMID: 26906504
25. Parisi GI, Kemker R, Part JL, Kanan C, Wermter S. Continual lifelong learning with neural networks: A review. Neural networks. 2019; 113:54–71. https://doi.org/10.1016/j.neunet.2019.01.012 PMID: 30780045
26. Tong R, Chater TE, Emptage NJ, Goda Y. Heterosynaptic cross-talk of pre-and postsynaptic strengths along segments of dendrites. Cell reports. 2021; 34(4):108693. https://doi.org/10.1016/j.celrep.2021.108693 PMID: 33503435
27. Burkitt AN. A review of the integrate-and-fire neuron model: I. Homogeneous synaptic input. Biological cybernetics. 2006; 95:1–19. https://doi.org/10.1007/s00422-006-0068-6 PMID: 16622699
28. Burkitt AN. A review of the integrate-and-fire neuron model: II. Inhomogeneous synaptic input and network properties. Biological cybernetics. 2006; 95:97–112. https://doi.org/10.1007/s00422-006-0082-8 PMID: 16821035
29. Van Rossum MC, Bi GQ, Turrigiano GG. Stable Hebbian learning from spike timing-dependent plasticity. Journal of neuroscience. 2000; 20(23):8812–8821. https://doi.org/10.1523/JNEUROSCI.20-23-08812.2000 PMID: 11102489
30. Yger P, Stimberg M, Brette R. Fast learning with weak synaptic plasticity. Journal of Neuroscience. 2015; 35(39):13351–13362. https://doi.org/10.1523/JNEUROSCI.0607-15.2015 PMID: 26424883

31. Mainen ZF, Sejnowski TJ. Reliability of spike timing in neocortical neurons. Science. 1995; 268 (5216):1503–1506. https://doi.org/10.1126/science.7770778 PMID: 7770778

32. Albers C, Westkott M, Pawelzik K. Learning of precise spike times with homeostatic membrane potential dependent synaptic plasticity. PloS one. 2016; 11(2):e0148948. https://doi.org/10.1371/journal.pone.0148948 PMID: 26900845

33. Bi Gq, Poo Mm. Synaptic modifications in cultured hippocampal neurons: dependence on spike timing, synaptic strength, and postsynaptic cell type. Journal of neuroscience. 1998; 18(24):10464–10472. https://doi.org/10.1523/JNEUROSCI.18-24-10464.1998 PMID: 9852584

34. Nessler B, Pfeiffer M, Buesing L, Maass W. Bayesian computation emerges in generic cortical microcircuits through spike-timing-dependent plasticity. PLoS computational biology. 2013; 9(4):e1003037. https://doi.org/10.1371/journal.pcbi.1003037 PMID: 23633941

35. Markram H, Lübke J, Frotscher M, Sakmann B. Regulation of synaptic efficacy by coincidence of postsynaptic APs and EPSPs. Science. 1997; 275(5297):213–215. https://doi.org/10.1126/science.275.5297.213 PMID: 8985014

36. Masquelier T. STDP allows close-to-optimal spatiotemporal spike pattern detection by single coincidence detector neurons. Neuroscience. 2018; 389:133–140. https://doi.org/10.1016/j.neuroscience.2017.06.032 PMID: 28668487

37. Sheik S, Paul S, Augustine C, Cauwenberghs G. Membrane-dependent neuromorphic learning rule for unsupervised spike pattern detection. In: 2016 IEEE Biomedical Circuits and Systems Conference (BioCAS). IEEE; 2016. p. 164–167.

38. Bienenstock EL, Cooper LN, Munro PW. Theory for the development of neuron selectivity: orientation specificity and binocular interaction in visual cortex. Journal of Neuroscience. 1982; 2(1):32–48. https://doi.org/10.1523/JNEUROSCI.02-01-00032.1982 PMID: 7054394

39. Vogels TP, Sprekeler H, Zenke F, Clopath C, Gerstner W. Inhibitory plasticity balances excitation and inhibition in sensory pathways and memory networks. Science. 2011; 334(6062):1569–1573. https://doi.org/10.1126/science.1211095 PMID: 22075724

40. Litwin-Kumar A, Doiron B. Formation and maintenance of neuronal assemblies through synaptic plasticity. Nature communications. 2014; 5(1):5319. https://doi.org/10.1038/ncomms6319 PMID: 25395015

41. Haider B, Duque A, Hasenstaub AR, McCormick DA. Neocortical network activity in vivo is generated through a dynamic balance of excitation and inhibition. Journal of Neuroscience. 2006; 26(17):4535–4545. https://doi.org/10.1523/JNEUROSCI.5297-05.2006 PMID: 16641233

42. Sjöström PJ, Turrigiano GG, Nelson SB. Rate, timing, and cooperativity jointly determine cortical synaptic plasticity. Neuron. 2001; 32(6):1149–1164. https://doi.org/10.1016/S0896-6273(01)00542-6 PMID: 11754844

43. Rasmussen CE, Willshaw DJ. Presynaptic and postsynaptic competition in models for the development of neuromuscular connections. Biological cybernetics. 1993; 68(5):409–419. https://doi.org/10.1007/BF00198773 PMID: 8476981

44. Wang H, Wagner JJ. Priming-induced shift in synaptic plasticity in the rat hippocampus. Journal of neurophysiology. 1999; 82(4):2024–2028. https://doi.org/10.1152/jn.1999.82.4.2024 PMID: 10515995

## 2.2 Incremental Self-Organization of Spatio-Temporal Spike Pattern Detection

MS ID: BIORXIV/2023/551088

**My contribution to this paper**:

Conceptualization
Formal analysis
Investigation
Methodology
Software
Visualization
Writing - original draft

# Incremental Self-Organization of Spatio-Temporal Spike Pattern Detection

**Mohammad Dehghani-Habibabadi**[1,*] **and Klaus Pawelzik**[1]

[1]Institute for Theoretical Physics, University of Bremen, 28359 Bremen, Germany
[*]mohammad@neuro.uni-bremen.de

## ABSTRACT

Brains learn new information while retaining previously acquired information. It is not known by what mechanisms synapses preserve previously stored memories while they are plastic and absorb new content. To understand how this stability-plasticity dilemma might be resolved, we investigate a one layer self-supervised neural network that incrementally learns to recognize new spatio-temporal spike patterns without overwriting existing memories. A plausible combination of Hebbian mechanisms, hetero-synaptic plasticity, and synaptic scaling enables unsupervised learning of spatio-temporal input patterns by single neurons. Acquisition of different patterns is achieved in networks where differentiation of selectivities is enforced by pre-synaptic hetero-synaptic plasticity. But only when the training spikes are both, jittered and stochastic past memories are found to persist despite ongoing learning. This input variability selects a subset of weights and drives them into a regime where synaptic scaling induces self-stabilization. Thereby our model provides a novel explanation for the stability of synapses related to preexisting contents despite ongoing plasticity, and suggests how nervous systems could incrementally learn and exploit temporally precise Poisson rate codes.

## Significance statement

Activity-dependent changes in synaptic efficacy are thought to underlie learning. While ongoing synaptic plasticity is necessary for learning new content, it is detrimental to the traces of previously acquired memories. Here, we show how memories for spatiotemporal patterns can be protected from overwriting. A combination of biologically plausible synaptic plasticity mechanisms turns single neurons into detectors of statistically dominant input patterns. For networks, we find that memory stability is achieved when the patterns to be learned are temporally sloppy and noisy, as opposed to being frozen. This variability drives the relevant synaptic weights to large efficacies, where they become self-reinforcing and continue to support the initially learned patterns. As a result, such a network can incrementally learn one pattern after another.

## Introduction

Memory persistence depends on the stability of synaptic weight patterns in the neuronal networks that encode memories[1]. In order to learn from and adapt to new experiences, however, a brain is required to be plastic as well. In fact, plasticity is a permanent mechanism, and neurons constantly modify their synapses also to fire at the desired biological firing rate[2,3]. Thus, it is essential to investigate how neural networks maintain stability in the face of ongoing plasticity to understand learning, memory consolidation and retrieval.

Moreover, deeper insights into the balance between stability and plasticity in biological neural networks has the potential to lead to the development of more robust and efficient artificial neural networks. In particular, stable networks may fail to learn new information, while hyperplastic networks may suffer from forgetting, which occurs if previously learned information is "forgotten" when new information is learned.[4–6] Therefore, it is a matter of question what mechanisms are required for a neural network to be both stable and plastic, the notorious so-called stability-plasticity dilemma (SPD)[7].

In the past biologically more or less plausible algorithms were proposed for learning spatio-temporal spike patterns. A basic Tempotron can distinguish between patterns based on their duration and synaptic time constants[8], however, utilizes a supervisory signal. While the Tempotron provides no spike timing information, the supervised learning algorithms for Chronotrons can train neurons to fire at specific times during a pattern[9–11]. Toward a biological learning algorithm, as a network always receives input, it is required to be quiescent when receiving random input and to fire when a specific embedded pattern is present. This can be achieved through aggregate label learning based on the N-methyl-D-Aspartate (NMDA) receptors[12–14] by selecting synapses with a sufficiently significant correlation between input and membrane potential[15]. Also aggregate label learning requires some information about the presence of patterns. The selection of synapses can be done completely unsupervised based on pre- and post-synaptic hetero-synaptic plasticity[16]. In fact, a combination of fundamental but realistic mechanisms,

including synaptic scaling, Hebbian mechanisms, and hetero-synaptic plasticity, was demonstrated to allow individual neurons to become detectors of repetitive patterns in the input without any supervision. It was found that the memory for the learned pattern is retained if the pattern is not shown again and only noise is presented afterwards which allow for learning also rarely presented consistent patterns. In fact, if the learned embedded patterns are not presented to the neuron and the scaling term is large enough, all weights are scaled up and some synaptic efficacies will reach their maximal values, until the neuron fires at the desired rate. This explains why memory is maintained when learning continues with random input patterns[16]. In stark contrast, however, if a different embedded pattern is presented after learning a first pattern, this model encounters catastrophic forgetting: the memory for the original pattern becomes lost, and the new pattern is learned. This raises the question which mechanisms might alleviate the stability-plasticity dilemma (SPD) for neuronal networks that serve spike pattern detection.
In this study, we address the SPD in the context of spatio-temporal spike patterns. First, we identify realistic mechanisms enabling neurons to learn spatio-temporal spike patterns. Then, we investigate the conditions for which a learned weight distribution remains stable during ongoing plasticity without the learned patterns in the input. Finally, we find that with these conditions new patterns are indeed learnable while the weight vectors of previously learned patterns are maintained, which allows for incremental learning.

## Results

Neurons receive input from a large number of excitatory and inhibitory neurons. For simplicity, we in the following demonstrate our results with the simple example of 400 excitatory and 100 inhibitory neurons which all spike with Poisson statistics and fixed rates (5Hz and 20Hz, respectively). Embedded patterns are short epochs with the same statistics, however contain consistent patterns which either have fixed spike positions or are noisy versions of a fixed pattern. We wondered if existing plasticity mechanisms are able to make target neurons selective for these patterns (see Materials and Methods).
The learning algorithm employs two types of synaptic plasticity for which the signs of the weights remain unchanged throughout the learning process, i.e., Dale's law is enforced. First, we consider homeostatic plasticity that is applied to excitatory synapses and works to regulate the firing rate to match the biological firing rate[2,3]. This means that when the long-term firing rate exceeds the desired rate, all synapses undergo a process of down-scaling, and they are scaled up when the firing rate is lower than desired. This synaptic scaling is crucial for the maintenance of system stability. However, because it is universally applied to all synapses, regardless of their efficacy, it is not sufficient to identify embedded patterns, that is, spike timing is not specific under synaptic scaling.
To determine whether a neuron has learned or memorized a particular pattern, we look at the timing of the spikes in the post-synaptic neurons. If all output spike occur during the embedded pattern presented in the input, we can conclude that the neuron has learned and remembered that pattern. To evaluate how well the learning mechanism and the memory recall work in the recognition of random patterns in groups, we examine the average percentage of spikes that correctly identify the patterns, which is denoted by $R$.

$$R = \left\langle \frac{n_s^p(L)}{n_s + \zeta} \right\rangle_\mu , \tag{1}$$

where $n_s$ is the total number of spikes observed during a test period and $n_s^p$ is the number of spikes related to the presence of the pattern to be detected. To account also for spikes that may occur shortly after the pattern due to the finite decay time of the excitatory synaptic kernel, the test window is extended by $L$ ms after the pattern ends. To ensure a definitive result ($R = 0$) when no spikes are observed, a small arbitrary positive value $\zeta << 1$ is added to the denominator. The ratio is then averaged over an ensemble of inputs denoted by $\mu$, where each input contains the embedded patterns and independent random background spikes.
Furthermore we consider Hebbian mechanisms of synaptic plasticity and their potential role in the self-organization of spike pattern selectivity. Hebbian mechanisms affect both excitatory and inhibitory synapses and depend on correlations between input kernels and deviations of the membrane potential from a given threshold. For changes in inhibitory synapses, weight enhancement is driven by positive deflections, while negative deflections contribute to their attenuation. For excitatory synapses, we allow only positive deflections to contribute, mimicking NMDA-dependent processes. It is well understood that without any further constraints, this approach would lead to an instability of excitatory synaptic efficacy. This is avoided by a combination of two simple but biologically plausible mechanisms.
**First:** By initially capping excitatory synaptic weights at their upper limits, unbounded growth is effectively prevented.
**Second:** Decreases in excitatory synaptic weights are induced by hetero-synaptic plasticity where pre- and post-synaptic components of each synapse are modified differently. Hetero-synaptic plasticity couples the weight changes of different synapses in such a way that the resources required for significant increases in efficacy are drawn from components with otherwise small increases. In pre-synaptic hetero-synaptic plasticity a large increase of a pre-synaptic component constrains or

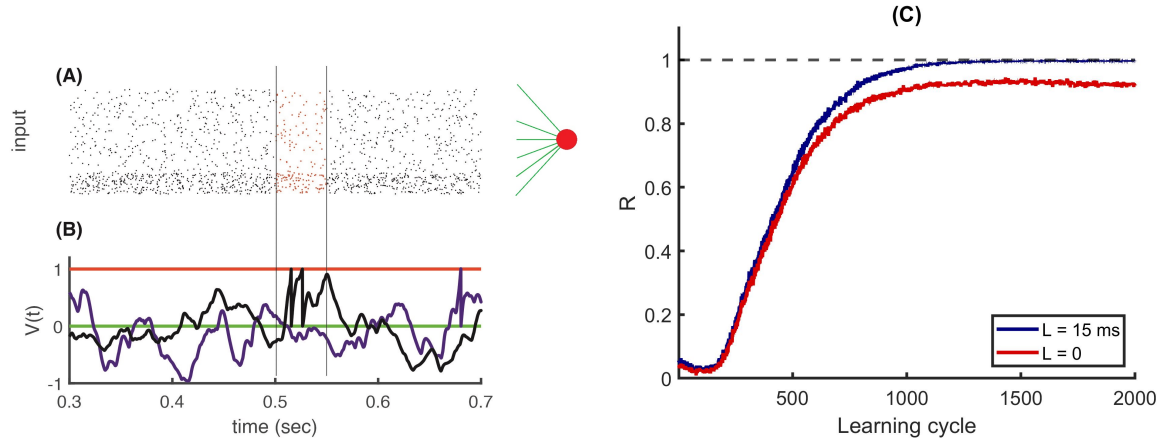


**Figure 1.** Learning of one embedded pattern. A: the input activity and B: membrane potential of a neuron in response to input from 500 afferents, with 80% excitatory and 20% inhibitory neurons. The excitatory neurons fired at a rate of 5 Hz, while the inhibitory neurons fired at 20 Hz. A 50 ms random pattern is embedded in the red area between two black vertical lines. The membrane potential of the neuron is in black trace showing that learning reduced fluctuations in the membrane potential outside the embedded pattern, compared to the case where the weights were learned from the random background alone. As a result, two spikes occurred during the embedded pattern time, between the vertical black lines. The green line represents the resting potential, the red line represents the threshold, the blue line represents the membrane potential after weight initialization by learning with random patterns only, and the black line represents the membrane potential after learning. C: Learning performance R versus learning cycle, for $L = 0$ and $L = 15$ ms (based on an average of 500 simulations).

even inverts a potential increase of all synaptic components originating from the pre-synaptic neuron to which these components belong. In post-synaptic hetero-synaptic plasticity it is the post-synaptic neuron that provides the limited resources for efficacy increases such that a substantial increase in one post-synaptic component comes at expense of the other post-synaptic components that target the same neuron. Note that these implementations of hetero-synaptic plasticity do not imply strict normalization of excitatory weights (see Materials and Methods).

## 1 Single post-synaptic neuron, excluding pre-synaptic hetero-synaptic plasticity

With the mechanisms mentioned above (for details see Material and Methods), we first determine whether a single post-synaptic neuron has the ability to learn embedded patterns based on post-synaptic hetero-synaptic plasticity. We then investigate the stability and plasticity of the system.

Figure 1A shows the membrane potential of the neuron before and after learning a random fixed pattern of length 50 ms that has the same statistics as the random background. Note that spikes are elicited already before learning the pattern because we always initialize the weights by applying the plasticity mechanisms with random spike patterns with the same statistics (Poisson process with fixed firing rates: 5Hz for the 400 excitatory input neurons, and 20 Hz for the 100 inhibitory input neurons). Thus, the post-synaptic neurons already fire with average rate $r_0$, mainly due to synaptic scaling before the training patterns are presented. The embedded patterns used for the subsequent learning are taken from the same processes for inhibitory and excitatory neurons, but are fixed and repeated in every stimulation. Figure 1C shows that the R-value, used as a measure of convergence, is approaching one. This shows that the neurons learn to fire only when presented with the embedded pattern and remain inactive otherwise. When the test window is extended by $L = 15$ ms, the performance becomes perfect. To evaluate the robustness and stability of the memory trace over time, the embedded pattern used for training is not presented to the neuron, and learning continues (figure 2).

Figure 2A shows that after 20,000 learning cycles with only random input spikes and without the learned embedded pattern, still over 80% of the spikes would occur during the embedded pattern, exceeding the chance level of 0.05 by far. With realistic parameters the memory in this simulation would persists for over 5 hours without any decay or diffusion of the weight vector. This striking stability is explained by synaptic scaling that scales the excitatory synaptic efficacies up until a predetermined long-term firing rate is reached also for the random patterns (as shown by the red line in figure 2B). Weights are only scaled because the random inputs lack structure and therefore do not lose their selectivity for the learned pattern. That is, the weight vector mainly becomes larger and when the learned pattern is presented (only for testing) the neurons fire far more spikes, resulting in a much higher firing rate (as shown by the green line in figure 2B). To further evaluate this result, we consider

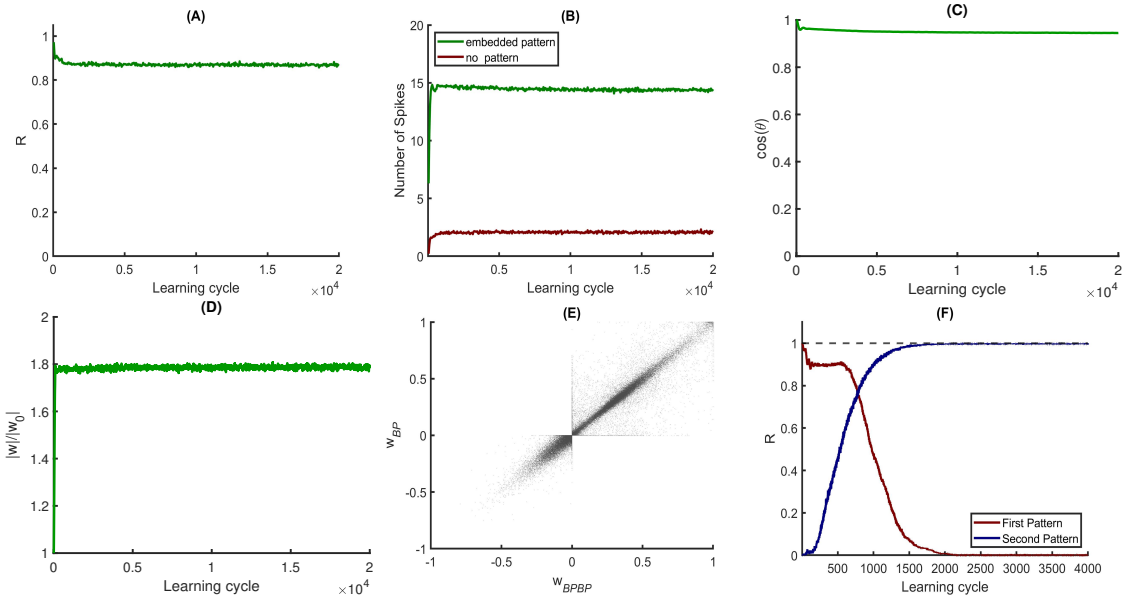


**Figure 2.** A: R as a memory criterion versus the learning cycle without learned patterns in afferents, learning continues, and every 50 cycles, learning is paused, and the learned pattern is placed in the background. Then R is computed as a memory criterion. B: Number of spikes versus learning cycle; the post-synaptic neuron elicits more spikes when the embedded pattern is in the afferents (green) than in the absence of the pattern (red). (C and D) Without learned patterns in afferents, learning continues. C: Average of the ratio of the norm of the current weight vector divided by the norm of the learned pattern weight vector ($w_0$). D: Average of the cosine between the current weight vector and $w_0$ E: First, neurons learned to fire at 2 Hz, while there was no embedded pattern in afferents until the learning cycle 5000 ($W_B$). Then, in each simulation, an embedded pattern is present in the afferents for 10,000 learning cycles ($W_{BP}$). Next, there is again no embedded pattern in afferents for 20000 learning cycles ($W_{BPB}$). Finally, there is again the original embedded pattern in the afferents for another 20000 learning cycles($W_{BPBP}$). The scatter plot from all simulations demonstrates that most of the weights remain roughly the same, i.e., learning a pattern leads to a fixed point in weight space. F: The neurons first learn the first embedded pattern for the 10000 learning cycles, and then there is another different embedded pattern (the second pattern) in afferents for another 10000 learning cycles. This figure shows the R-value for the second 10000 in learning cycles. This figure is based on an average of 500 simulations.

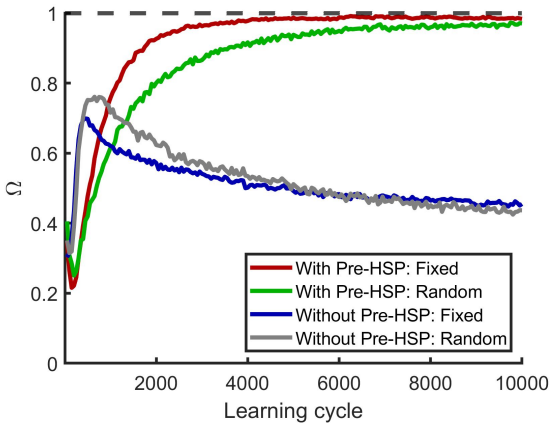


**Figure 3.** Representation of four embedded patterns by seven post-synaptic neurons. Ω versus learning cycle (There are 7 post-synaptic neurons). Red and Blue lines: Each pattern is shown in each learning cycle in a fixed position. Green and Gray lines: Each pattern is shown in the epoch with the probability of $1/4$ at a random position. Note that in this case some learning cycles have no embedded pattern in the epoch. Also, we randomly chose locations from $([85\ 85+L_{em}), [175\ 175+L_{em}), ...[895\ 895+L_{em}]$ ms) to position the embedded patterns. (The data are from every 50'th learning cycles. This figure is based on the average of 500 simulations.)

the cosine of the weight vector from last learning cycle with patterns embedded in the input and each further learning cycle with random spikes alone (i.e. without the learned pattern in the input, figure 2C). The simulation results show that the cosine remains constantly high, which demonstrates the stability of the memory. The same procedure is used to calculate the norm of the weight vector, showing that the unstructured data leads to a gain in synaptic strength (figure 2D). However, the memory is stored in the same synapses because when we subsequently use the embedded pattern again for relearning, the weights return to their fixed point (figure 2E). However, this system is not able to preserve the memory for the first pattern if another different embedded pattern is repeatedly presented (figure 2F).

## 2 Neural network, including Pre-synaptic hetero-synaptic plasticity

In principle, a single neuron is capable of learning many embedded patterns along the lines of the Tempotron[8]. However, a system with only one post-synaptic neuron cannot identify when and which patterns are in the input. This would require and ensemble of output neurons which acquire different selectivities. It was already shown that for this purpose pre-synaptic hetero-synaptic plasticity is essential[16].

For investigation of the conditions under which plasticity and stability meet, we consider a simple network with several post-synaptic neurons and include also pre-synaptic hetero-synaptic plasticity.

We find that synaptic competition induced by pre-synaptic hetero-synaptic plasticity is sufficient to faithfully represent pattern identity and order in an ensemble of target neurons with shared input from a set of input neurons if during learning all patterns are presented in each epoch.

To quantify this, we use a matrix-based approach to evaluate the performance of the population of neurons. The matrix has rows representing neurons and columns representing patterns, with matrix elements set to 1 if a neuron is active for a particular pattern and 0 otherwise. The rank of this matrix reflects the number of linearly independent row vectors. We propose a performance measure, denoted Ω, which is the ratio of the matrix rank to the number of patterns. When the rank of the matrix is equal to the number of patterns, it indicates that the population of neurons accurately represents the presence and order of the patterns in a stimulus. In this study, Ω is utilized as a criterion for evaluating learning, plasticity, and stability.

As a simple example, we trained a network with seven post-synaptic neurons using four embedded patterns in each training epoch. We found that when the pre-synaptic competition was present, all four patterns were selectively represented by the neurons, regardless of their consistent presentation (figure 3). In the absence of pre-synaptic competition, the patterns were not effectively distributed among the neurons[16]. Therefore, hetero-synaptic plasticity promotes the functional specialization of output neurons to different subsets of patterns, facilitating the self-organization of a precise representation of the "which" and "when" aspects of input patterns by the neuronal ensemble.

The fact that specialization ($\Omega \to 1$) takes place also when each pattern is shown intermittently (i.e., not in each epoch, the green line in figure 3) indicates the robustness of memories not only against the absence of patterns but also against the presence

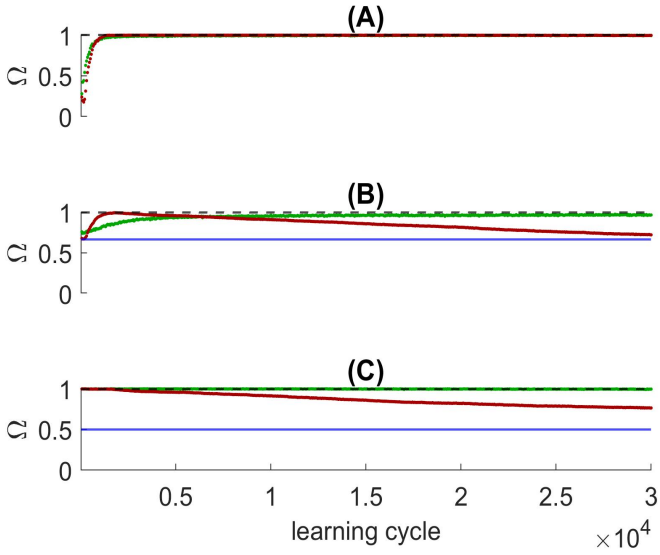


**Figure 4.** Learning, Plasticity and Stability. Green: Poisson spike rate. Red: Initial fixed pattern. A, B, and C represent learning (0 to 2), plasticity (2 to 3), and stability (2 to 1), respectively. Blue lines show baselines. Green and red lines show the performance of learning with Poisson rate patterns and the original noiseless and temporally precise patterns, respectively. A: After learning noise, the network continues learning with two different embedded patterns for 30,000 learning cycles. B: The network continues learning with the third embedded pattern, while the first two are no longer shown. C: The network continues learning with only one of the embedded patterns, with initial conditions from the last learning cycles of A. Every 50 learning cycles, learning is stopped and Ω is computed for all two embedded patterns in A and C, and for all three embedded patterns in B. There are 7 post-synaptic neurons and the results are averages over 500 simulations.

of different patterns. This raises the question under which conditions true incremental learning is possible without overwriting previous memories. We find that this is indeed the case, however only when the patterns are given as Poisson rate modulations, as opposed to precise pattern repetitions.

To generate a temporally modulated Poisson spike pattern, a given fixed time-coded spike input of each afferent was converted into rate-coded input by first convolving of each spike with a Gaussian distribution characterized by a mean of zero and a standard deviation of 2 ms. The resulting function then served as a modulated firing rate for a Poisson point process. This procedure generates for each given fixed pattern an ensemble of spatio-temporal patterns with the statistics of a Poisson point process including failures and a Fano factor equal to 1. These modified patterns were then used for learning, plasticity and stability purposes.

In figure 4A, the initial learning phase involves 7 target neurons learning two embedded patterns. Subsequently, in figure 4B, learning continues with a third embedded pattern, without presenting the previously learned patterns again. The system's ability to recognize all patterns is tested every 50 cycles to assess memory retention. In figure 4C, we start with the initial conditions from the last learning cycle in figure 4A, but with only one of the two embedded pattern for ongoing learning. Every 50 learning cycles, the learning process is paused and the system's ability to recognize both initial patterns is tested.

To understand the superior stability of memories for patterns when learned from temporally modulated Poisson rate patterns we investigated the weight matrix $w = ab$ and its components $a$ and $b$. In particular, we tested the hypothesis that stability relates to the orthogonality of the weight vectors. As a graded measure $O$ of 'orthogonality' we consider the volume spanned by the $M$ weight vectors in the $N$-dimensional input space. We normalized the weight vectors leading to a matrix $Y$. The volume is then given by the product of the square roots of the $M$ largest eigenvalues $\lambda_i$ of $X = YY^T$:

$$O = \prod_{i=1}^{M} |\lambda_i(X)|^{\frac{1}{2}} \tag{2}$$

If the $M$ normalized vectors are all mutually orthogonal this volume is $O = 1$, if one or more weight vectors are linearly dependent on the others this volume collapses to zero ($O = 0$). Figure 5 A, B and C shows that without patterns in the input the weights are close to zero which is expected for random positive vectors. However, when then two rigid patterns are learned the weight vectors become more orthogonal while the orthogonality is close to one for jittered noisy (Poisson rate) patterns

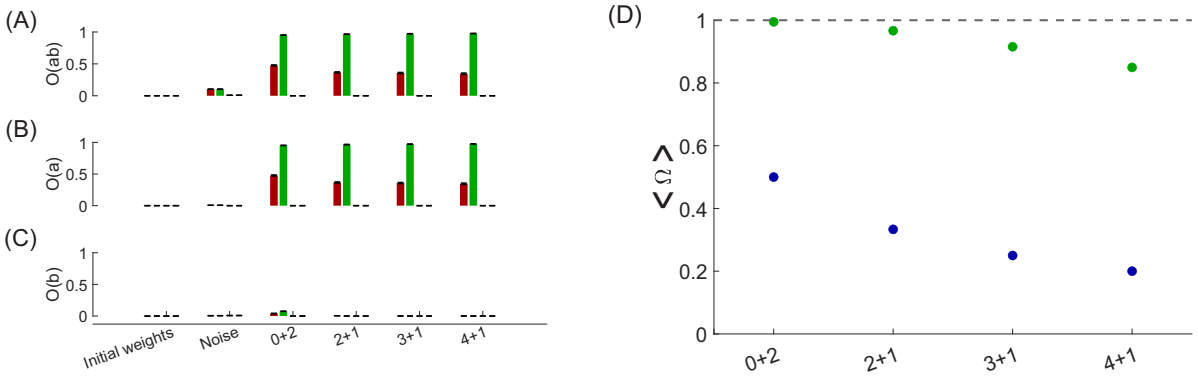


**Figure 5.** Orthogonality with and without pre-synaptic hetero-synaptic plasticity for original fixed patterns and Poisson spike rates. Red: with pre-synaptic hetero-synaptic plasticity and original patterns. Green: with pre-synaptic hetero-synaptic plasticity and Poisson spike rates. Blue: without pre-synaptic hetero-synaptic plasticity and original patterns. Gray: without pre-synaptic hetero-synaptic plasticity and Poisson spike rates. (A) The orthogonality measure is applied to the overall synaptic efficacy (i.e. $w = ab$), (B) to the pre-synaptic part (i.e. $a$), and (C) to the post-synaptic part (i.e. $b$). Initial weights: Random weight vectors in the first learning cycle. Noise: inputs are random spikes for 2000 learning cycles. 0+2: After learning noise, the network continues learning with two distinct embedded patterns for 30,000 learning cycles. 2+1: The network continues learning with the third embedded pattern, while the first two are no longer shown (30,000 learning cycles) and so on. D: Averaged Ω with pre-synaptic hetero-synaptic plasticity and Poisson spike rates (green dots) and the corresponding baseline line in blue dots. There are 7 post-synaptic neurons and the results are averages over 500 independent simulations.

and increases even further when subsequently a third pattern is incrementally learned. Also, we see that without pre-synaptic hetero-synaptic plasticity the weights stay practically linearly dependent for both cases. Figure 5D shows averaged Ω far from baseline at each incremental learning step evaluating learning, plasticity, and stability.

To better understand why the system maintains stability and plasticity simultaneously, we show the weight distribution of a target neuron at (0+2, 2+1, and 3+1 stages) using weight sorting when the system has learned two patterns (Figure 6: the red line is (0+2). The averaged sorted weight vectors, $w = ab$, for the (0+2) stage are represented by the red line. The green and blue lines, respectively, represent the averaged weight vector for the (2+1) and (3+1) stages (using the same sorting as the red line).As shown in figure 6, the decrease in the weight vector amount is much smaller in the learning with rate code than in the original patterns. However, some intermediate weight vectors are amplified in noise learning. The study shows that pre-synaptic hetero-synaptic plasticity is essential but insufficient for memory retention. The advantage of introducing noise is that some important spikes in certain learning cycles are missed, resulting in an identical input-output correlation across all synapses on average. As a result, the effects of synaptic scaling overshadow hetero-synaptic plasticity. As a result, large weight vectors scale up more than when the network learns the original pattern; therefore, post-synaptic neurons search for the new embedded pattern within smaller and zero-weight vectors.

## Discussion

Selectivity for spatio-temporal patterns can self-organize in simple one-layer networks of integrate and fire neurons through a combination of Hebbian plasticity mechanisms, synaptic scaling for excitatory synapses and hetero-synaptic plasticity[16]. We found that the competition for weight increases of the pre-synaptic components of excitatory synapses that are controlled by the pre-synaptic neuron (termed 'pre-synaptic hetero-synaptic plasticity') have a tendency to orthogonalize the weight vectors of the receiving neurons in input space (figure 5, 0+2). When the patterns, however, are to be learned one after the other, our simulations demonstrate that the weights of the output neurons of a network stay fully orthogonal only if the patterns are stochastic variants of the original pattern. We showed this by generating the training patterns from a Poisson process with temporally modulated firing rates obtained from convolving the originally fixed pattern with a Gaussian function. In this case, the orthogonality of the weights is preserved also when the patterns are learned incrementally. The orthogonality then supports minimal interference with previously learned weight vectors[17,18]. This novel mechanism realizes the balance of stability and plasticity, in particular, the robustness of already present memories against ongoing learning together with the ability to absorb new contents (4).

Take together, we proposed a biologically realistic solution to the stability-plasticity dilemma for networks that learn to

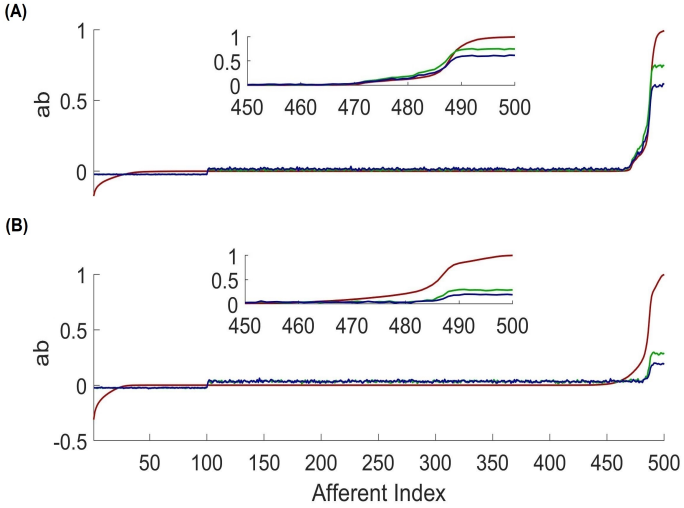


**Figure 6.** Weight vector distributions for the Poisson rate (A) and for the original pattern (B). First, there is no embedded pattern in the afferents for 2000 learning cycles. Then, there are two embedded patterns in the afferent for 30,000 learning cycles (0+2). The red line shows the average sorted weights for this case ($w = ab$). Then, in each simulation, there is another distinct embedded pattern in the afferents for 30,000 learning cycles, and the first two learned patterns are not shown, and the average of the sorted weights is obtained in this learning cycle ( 2+1, the green line, and using the ranks from the red line). Finally, there is again another distinct embedded pattern in the afferents for 30,000 learning cycles, and the blue line shows the resulting weight vector at this learning cycle (using the ranks from the red line). There are seven post-synaptic neurons, and this figure is averaged over 500 simulations.

detect spatio-temporal spike patterns without any supervision. This approach relies on the balance between excitatory and inhibitory inputs that naturally emerges during learning[16] and is believed to be necessary for maintaining memory[19]. However, the dependence of the balance between stability and plasticity on the balance between excitation and inhibition remains to be investigated. In particular, inhibitory neurons try to inhibit excitatory activity, and memory is maintained until the excitatory/inhibitory balance is entirely destroyed and neurons burst; however, investigating this question is beyond the scope of this paper.

To our knowledge this is the first approach towards a biologically realistic model for incremental self-supervised learning of spatio-temporal spike patterns. Previous approaches were proposed for recurrent networks[20,21] and rate-based models[17] which relied also on systematic orthogonalization of weight vectors, however by different mechanisms. Furthermore, our approach relies heavily on mechanisms for synaptic scaling mechanism which has been also proposed before as a mechanisms for stabilizing long term memories, however in rate based models and with a $w^2$ dependence of scaling[21] which in our case is detrimental (not shown) for performance of learning.

Last but not least, our results align with previous research[22] emphasizing the critical role of noise in the input for incremental learning by driving weights to become orthogonal, and it serves to minimize their overlap for different output neurons. In summary, we have shown that accounting for noise and hetero-synaptic plasticity is sufficient for incremental learning.

## Materials and Methods

Signal transmission is more effective when pre-synaptic neurons release more neurotransmitters and fire more frequently, and also when post-synaptic neurons have more receptors and sensitivity. Therefore, the efficacy of a synapse,$w_{ji}$ (pre-synaptic neuron $i$ targeting a post-synaptic neuron $j$), can be expressed in terms of the combination of pre-synaptic and post-synaptic components.

$$w_{ji} = a_{ij} b_{ij}. \tag{3}$$

where the resources for $a_{ij}$ are provided by the pre-synaptic neuron $i$ and $b_{ij}$ is supported by the post-synaptic neuron $j$. In the following we assume $N$ pre-synaptic neurons ($i = 1, ..., N$) and $M$ post-synaptic neurons ($j = 1, ..., M$).

The efficacy of a synapse can be modified separately in the pre- and the post-synaptic components through synaptic plasticity, resulting in changes in the total efficacy of the synapse in transmitting signals between neurons.

$$\frac{dw_{ji}}{dt} = a_{ij}\frac{db_{ij}}{dt} + \frac{da_{ij}}{dt}b_{ij}. \tag{4}$$

Here, we first consider the homeostatic plasticity of synaptic strength to maintain the overall stability of neuronal activity, referred to as synaptic scaling, in order to modify the synapse. It has been shown that neurons regulate their excitatory synaptic weights to achieve the biologically desired firing rate, $r_0$[3,23]. It allows the neuron to decrease or increase synaptic effectiveness when the long-term firing rate, $r_j$, is greater or less than $r_0$.

$$\tau_E\frac{da^E_{ij}}{dt} = -a^E_{ij} + \alpha a^E_{ij} tanh(r_0 - r_j). \tag{5}$$

$$\tau_E\frac{db^E_{ij}}{dt} = -b^E_{ij} + \alpha b^E_{ij} tanh(r_0 - r_j). \tag{6}$$

where $\alpha$ and $\tau_E$ are the scaling factor and time constant, respectively. Note that the sub- and superscript $E$ indicate excitatory synapses. The long-term firing rate $r_j$ is determined by

$$\tau_r\frac{dr_j}{dt} = -r_j + \sum_{t^l_i}\delta(t - t^l_i). \tag{7}$$

where $\tau_r$ is the time constant for the long-term firing rate. At the time $t^l_i$ there is a spike in the afferent $i$, and at that time the afferent $i$ begins to send input to the post-synaptic neuron $j$ equal to $w_{ji} \times K$.
The kernel shape, $K$, is an alpha function with the equation:

$$K(t - t^l_i) = I_{norm}\left[\exp\left(-\frac{t - t^l_i}{\tau_d}\right) - \exp\left(-\frac{t - t^l_i}{\tau_r}\right)\right]\theta(t - t^l_i). \tag{8}$$

In this equation, $\theta$ represents the Heaviside step function. $\tau_r$ and $\tau_d$ denote the time constants for rise and decay respectively associated with the synaptic current, with different values for excitatory ($\tau^E_d, \tau^E_r$) and inhibitory synapses ($\tau^I_d, \tau^I_r$). The term $I_{norm} = \frac{\eta^{\eta/\eta-1}}{\eta-1}$ normalizes the amplitude of $K$ to unity, where $\eta = \frac{\tau_d}{\tau_r}$. Note that the parameters are chosen to be as close to the biologically plausible range as possible.
While synaptic scaling is effective in stabilizing the firing activity of a network, it is insufficient for learning the information encoded in the input. Therefore, a correlation-based learning rule inspired by the N-Methyl-D-Aspartate (NMDA) receptor[12–14] has been proposed in previous works[15,16]. In the weakly supervised learning rule[15] neurons are able to learn embedded patterns, and in [16] an unsupervised version following Dale's rules and operate in an unsupervised manner[16].
In more detail, the correlation between the input from pre-synaptic neuron $i$ and output membrane potential of post-synaptic neuron $j$, denoted as $V_j(t)$, provides the signal for modifying the synaptic strength, denoted as $\varepsilon_{ij}(t)$ which is referred to as eligibility[15]:

$$\tau_\varepsilon\frac{d\varepsilon_{ij}(t)}{dt} = -\varepsilon_{ij}(t) + \vartheta_{ij}. \tag{9}$$

In this context, $\vartheta_{ij}(t)$ represents the correlation between the input from the afferent $i$ and the output neuron $j$, reflected by the membrane potential $V_j$.

$$\vartheta_{ij}(t) = \sum_{l=1}^{n_i} K(t - t^l_i)\{[V_j(t) - V_0]_+ + q[V_j(t) - V_0]_-\}. \tag{10}$$

In the simulations discussed in this paper, $V_0$ represents the modification threshold[24] and is consistently set to zero. The parameter $q$ takes a value of zero for excitatory afferents and a value of 1 for inhibitory afferents[16]. During each time step, all spikes $n_i$ in the $i$-th afferent (eliciting before time $t$) are employed to update the synapses. Note, $V_j(t)$ is described by the simple leaky integrate and fire neurons differential equation[25,26]:

$$\tau_m\frac{d}{dt}V_j(t) = -V_j(t) + R_m I^{ext}_j(t). \tag{11}$$

where $\tau_m$ and $R_m$ are the membrane time constant and resistance, respectively. The external current, $I_j^{ext}$, is determined by the synaptic strength of the excitatory and inhibitory afferents, denoted by $w_{ji}^E$ and $w_{ji}^I$, respectively:

$$I_j^{ext}(t) = \sum_{i=1}^{N^E} w_{ji}^E \sum_{t_i^l<t} K^E(t-t_i^l) - \sum_{i=1}^{N^I} w_{ji}^I \sum_{t_i^l<t} K^I(t-t_i^l). \tag{12}$$

where $N^E$ and $N^I$ represent the number of excitatory and inhibitory afferents, respectively, and $N = N^E + N^I$. The external current is determined by the convolutions of the input spike trains with their respective synaptic kernels (Eq. 8), $K^E(t)$ and $K^I(t)$.

Despite the continuous positive signal in excitatory synapses, hetero-synaptic plasticity provides selectivity and specificity in this context. Here, we consider that the resources required to enhance the pre-and post-synaptic components $a_{ij}$ and $b_{ij}$ of the weights $w_{ji} = a_{ij}b_{ij}$ are inherently limited. As a result, we propose that these resources are distributed competitively, reflecting the limited availability and competitive nature of their allocation. The hetero-synaptic plasticity of both pre- and post-synaptic regions is a function of the induced eligibility signal. The post-synaptic hetero-synaptic plasticity, obtained by subtracting the mean of the eligibilities, affects changes in the post-synaptic components $b_{ij}$.

$$\tilde{\varepsilon}_{ij} = \varepsilon_{ij} - \frac{1}{N}\sum_{i=1}^{N} \varepsilon_{ij}. \tag{13}$$

Nevertheless, it is hypothesized that the signals governing the changes in the pre-synaptic components $a_{ij}$ depend on the magnitude of the potentiation observed on the post-synaptic side[16]. The signal for pre-synaptic competition then is implemented by subtraction of the mean.

$$B_{ij} = [\tilde{\varepsilon}_{ij}]_+ - \frac{\theta(\sum_j \theta([\tilde{\varepsilon}_{ij}]_+) - 1 - \zeta)}{\sum_j \theta([\tilde{\varepsilon}_{ij}]_+) + \zeta} \sum_{j=1}^{M} [\tilde{\varepsilon}_{ij}]_+. \tag{14}$$

where $\theta$ is a Heaviside function, $\zeta$ is a small positive number ($\zeta << 1$), and M is the number of post-synaptic neurons. Therefore

$$\tau_E \frac{da_{ij}^E}{dt} = -a_{ij}^E + \alpha a_{ij}^E tanh(r_0 - r_j) + c^E B_{ij}. \tag{15}$$

$$\tau_E \frac{db_{ij}^E}{dt} = -b_{ij}^E + \alpha b_{ij}^E tanh(r_0 - r_j) + c^E \tilde{\varepsilon}_{ij}. \tag{16}$$

where $\tau_E$ is the time constant for excitatory synapses and $c^E$ the learning rate. For inhibitory neurons:

$$\tau_I \frac{da_{ij}^I}{dt} = -a_{ij}^I + c^I \varepsilon_{ij}. \tag{17}$$

$$\tau_I \frac{db_{ij}^I}{dt} = -b_{ij}^I + c^I \varepsilon_{ij}. \tag{18}$$

where $\tau_I$ is the time constant for inhibitory synapses and $c^I$ is the learning rate. Note that the sub and superscript $I$ indicate inhibitory synapses. We consider $c^E$ to be smaller than $c^I$; therefore, inhibitory neurons can adapt more quickly to maintain balance at both global and detailed levels, and excitation cannot conflict with the relatively slow limiting mechanism of synaptic scaling[16].

Here, the Hebbian plasticity of inhibition is essential for maintaining a global balance within neural systems. The neuron is placed in a fluctuating regime by this balance, where the excitatory and inhibitory weights exhibit significant strength. Once this balance is achieved, further weight adjustments driven by the stochastic background restrict the weights to a fixed point balance via a random walk process. Furthermore, the integration of a frequent pattern induces an additional drift that systematically shifts the weights away from the fixed point until the target number of spikes is induced by the pattern alone, independent of the response of the background activity [16,27].

## Simulation Details

In all simulations, 80% of the afferents are excitatory and 20% inhibitory (400 excitatory and 100 inhibitory neurons). Afferent and embedded pattern spikes are generated randomly with Poisson point processes in which the excitatory rate ($r_E$) is 5 Hz, and the inhibitory rate ($r_I$) is 20 Hz. In each learning cycle, the learning epoch length is 1000 ms. To optimize the simulations, changes over epochs $e$ with a duration of $T$ ms are considered instead of implementing weight changes at each integration step. Consequently, equation (10) is replaced by

$$\vartheta_{ij}^{l} = \int_0^T dt K(t - t_i^l)[V_j(t) - V_0]_+ + q[V\,j(t) - V_0]_-. \tag{19}$$

Differential equations of this form:

$$\tau \frac{dy}{dt} = -y + x. \tag{20}$$

Transition to a moving average:

$$y(e+1) = \gamma y(e) + (1-\gamma)\hat{x}(e). \tag{21}$$

where $\hat{x}(e)$ is the sum of contributions of $x$ in each epoch $e$ and $\gamma \simeq 1 - T/\tau$.
Synaptic scaling relies on firing rates averaged over long periods of time. In online learning, a low-pass filter is used to ensure that the rate estimate $r_j(c+1)$ of the post-synaptic neuron $j$ for learning in epoch $e+1$ is based on the running average of the actual rates $\hat{r}$ from previous epochs:

$$r_j(e+1) = \gamma^* r_j(e) + (1-\gamma^*)\hat{r}_j(e). \tag{22}$$

The parameter $\gamma^*$ is set to 0.9 for all numbers, which corresponds to a time constant of 10s. Although smaller values do not change the asymptotic results, this value allows for faster convergence.
Plasticity is not immediate; it depends on the accumulation of signals for weight changes over time, called 'eligibility'[15]. A low-pass filter is used to implement this:

$$\varepsilon_{ij}(e+1) = \gamma \varepsilon_{ij}(e) + (1-\gamma)\hat{\vartheta}_{ij}(e). \tag{23}$$

The initial conditions are $r_j(0) = 0$ and $\varepsilon_{ij}(0) = 0$. The parameter $\gamma$ is 0.99 for all figures, which corresponds to a time constant of about 100s. This parameter limits the learnability of infrequently presented patterns patterns[16].
Due to structural limitations and other factors, synaptic strength cannot increase indefinitely. As a result, we restrict weight changes to prevent excitatory synapses from exceeding the upper limit of one.
Dale's rule states that excitatory and inhibitory synapses cannot convert into each other. Therefore, we consider synaptic weights to be zero if weight changes during learning would change their type. This ensures that subtracting the mean in Eq (13) and Eq (14) does not affect the type of a synapse. We use the Euler method with a time step of $\Delta t$ for the numerical integration of Eq (12), and the associated parameters are available in table 1.
Note, for the network model, the initial synaptic efficacies $a_{ij}$ and $b_{ij}$ are drawn from a Gaussian distribution with a mean of 0.1 and $10^{-2}$ standard deviations, while negative values are set to zero. In the single post-synaptic neuron model, they are drawn from a Gaussian distribution with a mean of $10^{-2}$ and standard deviations of $10^{-3}$, with negative values set to zero. In cases where there is only a single post-synaptic neuron, all values of $a_{ij}$ are initially set to 1. Since there is no pre-synaptic hetero-synaptic plasticity, these $a_{ij}$ values will remain at their initial value of 1, regardless of the number of learning cycles.
In the epoch-based approach, we use the following equations, which can be linearized to obtain the continuous version:

$$\delta w_{ij} = a_{ij}\delta b_{ij} + \delta a_{ij} b_{ij} + \delta a_{ij}\delta b_{ij}. \tag{24}$$

### *Inhibitory synapses*

$$\delta a_{ij}^I = c^I \varepsilon_{ij}. \tag{25}$$
$$\delta b_{ij}^I = c^I \varepsilon_{ij}. \tag{26}$$

**Table 1.** List of parameters.

| Symbol | Description | Value |
|---|---|---|
| $\tau_m$ | Membrane time constant | 15 ms |
| $R_m$ | Membrane resistance | 1 |
| $\tau_r^E$ | Rise time of excitatory currents | 0.5 ms |
| $\tau_r^I$ | Rise time of inhibitory currents | 1 ms |
| $\tau_d^E$ | Decay time of excitatory currents | 3 ms |
| $\tau_d^I$ | Decay time of inhibitory currents | 5 ms |
| $r^E$ | Rate of excitatory neurons | 5 Hz |
| $r^I$ | Rate of inhibitory neurons | 20 Hz |
| $N$ | Number of pre-synaptic neurons | 500 |
| $N^E$ | Number of pre-synaptic excitatory neurons | 400 |
| $N^I$ | Number of pre-synaptic inhibitory neurons | 100 |
| $c^I$ | Inhibitory learning rate | $10^{-3}$ |
| $c^E$ | Excitatory learning rate | $0.9 \times 10^{-3}$ |
| $\Delta t$ | Time step | 0.1 ms |
| $\alpha$ | Scaling factor | 0.01 |
| $T$ | Epoch duration | 1000 ms |
| $\chi$ | Decay term | $10^{-4}$ |

#### *Excitatory synapses*

$$\delta a_{ij}^E = -\chi a_{ij}^E + \alpha a_{ij}^E tanh(r_0 - r_j) + c^E B_{ij}. \tag{27}$$

$$\delta b_{ij}^E = -\chi b_{ij}^E + \alpha b_{ij}^E tanh(r_0 - r_j) + c^E \tilde{\varepsilon}_{ij}. \tag{28}$$

where $\chi$ is a decay term.

## Acknowledgements

We acknowledge support by the following grants: DFG - grant (PA 569/5-1 to KP)

## References

1. Hebb, D. O. *The organization of behavior: A neuropsychological theory* (Psychology Press, 2005).
2. Turrigiano, G. G. The self-tuning neuron: synaptic scaling of excitatory synapses. *Cell* **135**, 422–435 (2008).
3. Van Rossum, M. C., Bi, G. Q. & Turrigiano, G. G. Stable hebbian learning from spike timing-dependent plasticity. *J. neuroscience* **20**, 8812–8821 (2000).
4. Abraham, W. C. & Robins, A. Memory retention–the synaptic stability versus plasticity dilemma. *Trends neurosciences* **28**, 73–78 (2005).
5. French, R. M. Catastrophic forgetting in connectionist networks. *Trends cognitive sciences* **3**, 128–135 (1999).
6. Kirkpatrick, J. *et al.* Overcoming catastrophic forgetting in neural networks. *Proc. national academy sciences* **114**, 3521–3526 (2017).
7. Parisi, G. I., Kemker, R., Part, J. L., Kanan, C. & Wermter, S. Continual lifelong learning with neural networks: A review. *Neural Networks* **113**, 54–71 (2019).
8. Gütig, R. & Sompolinsky, H. The tempotron: a neuron that learns spike timing–based decisions. *Nat. neuroscience* **9**, 420–428 (2006).
9. Florian, R. V. The chronotron: A neuron that learns to fire temporally precise spike patterns. (2012).
10. Memmesheimer, R.-M., Rubin, R., Ölveczky, B. P. & Sompolinsky, H. Learning precisely timed spikes. *Neuron* **82**, 925–938 (2014).

**11.** Albers, C., Westkott, M. & Pawelzik, K. Learning of precise spike times with homeostatic membrane potential dependent synaptic plasticity. *PloS one* **11**, e0148948 (2016).

**12.** Artola, A., Bröcher, S. & Singer, W. Different voltage-dependent thresholds for inducing long-term depression and long-term potentiation in slices of rat visual cortex. *Nature* **347**, 69–72 (1990).

**13.** Cummings, J. A., Mulkey, R. M., Nicoll, R. A. & Malenka, R. C. Ca2+ signaling requirements for long-term depression in the hippocampus. *Neuron* **16**, 825–833 (1996).

**14.** Malenka, R. C., Nicoll & A, R. Long-term potentiation–a decade of progress? *Science* **285**, 1870–1874 (1999).

**15.** Gütig, R. Spiking neurons can discover predictive features by aggregate-label learning. *Science* **351**, aab4113 (2016).

**16.** Dehghani-Habibabadi, M. & Pawelzik, K. Synaptic self-organization of spatio-temporal pattern selectivity. *PLOS Comput. Biol.* **19**, e1010876 (2023).

**17.** Leibold, C. Neural kernels for recursive support vector regression as a model for episodic memory. *Biol. Cybern.* **116**, 377–386 (2022).

**18.** Chenani, A. *et al.* Hippocampal ca1 replay becomes less prominent but more rigid without inputs from medial entorhinal cortex. *Nat. communications* **10**, 1341 (2019).

**19.** Koolschijn, R. S. *et al.* Memory recall involves a transient break in excitatory-inhibitory balance. *Elife* **10**, e70071 (2021).

**20.** White, O. L., Lee, D. D. & Sompolinsky, H. Short-term memory in orthogonal neural networks. *Phys. review letters* **92**, 148102 (2004).

**21.** Tetzlaff, C., Kolodziejski, C., Timme, M., Tsodyks, M. & Wörgötter, F. Synaptic scaling enables dynamically distinct short-and long-term memory formation. *PLoS Comput. Biol.* **9**, e1003307 (2013).

**22.** Schug, S., Benzing, F. & Steger, A. Presynaptic stochasticity improves energy efficiency and helps alleviate the stability-plasticity dilemma. *Elife* **10**, e69884 (2021).

**23.** Bi, G.-q. & Poo, M.-m. Synaptic modifications in cultured hippocampal neurons: dependence on spike timing, synaptic strength, and postsynaptic cell type. *J. neuroscience* **18**, 10464–10472 (1998).

**24.** Sjöström, P. J., Turrigiano, G. G. & Nelson, S. B. Rate, timing, and cooperativity jointly determine cortical synaptic plasticity. *Neuron* **32**, 1149–1164 (2001).

**25.** Burkitt, A. N. A review of the integrate-and-fire neuron model: I. homogeneous synaptic input. *Biol. cybernetics* **95**, 1–19 (2006).

**26.** Burkitt, A. N. A review of the integrate-and-fire neuron model: Ii. inhomogeneous synaptic input and network properties. *Biol. cybernetics* **95**, 97–112 (2006).

**27.** Yger, P., Stimberg, M. & Brette, R. Fast learning with weak synaptic plasticity. *J. Neurosci.* **35**, 13351–13362 (2015).

## 2.3 Spike-phase coupling as an order parameter in a leaky integrate-and-fire model

**Title**: ”Spike-phase coupling as an order parameter in a leaky integrate-and-fire model”

**Journal**: Physical Review E, Volume 102, Pages 052202, Published 2 November 2020

**DOI**: https://doi.org/10.1103/PhysRevE.102.052202

**Authors**: Nahid Safari, Farhad Shahbazi, Mohammad Dehghani-Habibabadi, Moein Esghaei, Marzieh Zare

**My contribution to this paper**:

Proposing the idea
Assisting with computational analyses

## 2.4 Impact of the Excitatory-Inhibitory Neurons Ratio on Scale-Free Dynamics in a Leaky Integrate-and-Fire Model

MS ID: BIORXIV/2023/569071

**My contribution to this paper**:

Conceptualization
Formal analysis
Funding acquisition
Investigation
Methodology
Software
Visualization
Writing - original draft

# Impact of the Excitatory-Inhibitory Neurons Ratio on Scale-Free Dynamics in a Leaky Integrate-and-Fire Model

**Mohammad Dehghani-Habibabadi[1,*], Nahid Safari[2], Farhad Shahbazi[3], and Marzieh Zare[4,*]**

[1]Institute for Theoretical Physics, University of Bremen, 28359 Bremen, Germany
[2]Department for Neuro- & Sensory Physiology, University Medical Center Göttingen, 37073 Göttingen, Germany
[3]Department of Physics, Isfahan University of Technology, 84156-83111 Isfahan, Iran
[4]Dreeven Technologies, Montreal, QC, Canada J4P 2A2
[*]mohammad@neuro.uni-bremen.de
[*]marzieh.z.zare@gmail.com

## ABSTRACT

The relationship between ratios of excitatory to inhibitory neurons and the brain's dynamic range of cortical activity is crucial. However, its full understanding within the context of cortical scale-free dynamics remains an ongoing investigation. To provide insightful observations that can improve the current understanding of this impact, and based on studies indicating that a fully excitatory neural network can induce critical behavior under the influence of noise, it is essential to investigate the effects of varying inhibition within this network. Here, the impact of varying inhibitory-excitatory neuron ratios on neural avalanches and phase transition diagrams, considering a range of synaptic efficacies in a leaky integrate-and-fire model network, is examined. Our computational results show that the network exhibits critical, sub-critical, and super-critical behavior across different synaptic efficacies. In particular, a certain excitatory/inhibitory (E/I) ratio leads to a significantly extended dynamic range compared to higher or lower levels of inhibition and increases the probability of the system being in the critical regime. In this study, we used the Kuramoto order parameter and implemented a finite-size scaling analysis to determine the critical exponents associated with this transition. To characterize the criticality, we studied the distribution of neuronal avalanches at the critical point and found a scaling behavior characterized by specific exponents.

## Introduction

The balance between excitatory and inhibitory neuronal activity, commonly referred to as the E/I balance, is a fundamental feature of neural network operation that has a significant impact on network dynamic stability, modulation of neural responses, and facilitating information processing[1–3]. The balance of these synaptic membrane currents is widely recognized as essential for the spontaneous activity of neurons and their responses to sensory stimuli[4–10]. On the other hand, disturbances of the cortical E/I balance in the brain emerged as a contributor to neurological diseases, such as epilepsy[11], Parkinson's disease (PD)[12], Tourtette's syndrome[13], autism[14], and schizophrenia[15–17].

Although synaptic plasticity can balance a neuron's input after a synaptic connection[18,19], hyper-excitation could theoretically occur if the neural network has a significantly higher proportion of excitatory neurons than inhibitory neurons. On the other hand, an excess of inhibitory neurons can inhibit normal brain activity, resulting in reduced responsiveness or diminished functionality of neural circuits.[1,20,21] Therefore, maintaining an optimal ratio of excitatory and inhibitory neurons is critical to ensuring a balanced interplay of excitation and inhibition in the brain. In addition, experimental studies have shown that approximately 20% of neurons are inhibitory GABAergic neurons in the cortex[22–28].

The activities of inhibitory neurons have been identified as the source of various oscillatory rhythms[29], and pharmacologically blocking them causes an epileptic seizure in cortical activity[30]. Moreover, it has been shown that excitation and inhibition are balanced in detail and globally[1,2,4,5,18,31], providing a basis for neuronal oscillations and avalanches[32–34]. A neural avalanche refers to a sequential propagation of neuronal firing activity within a network in a correlated manner, initiated by the firing of a single neuron or a small group of neurons. The neural avalanche dynamic may critically depend on the E/I balance, as shown in experiments in cortical cultures, anesthetized rats, and awake monkeys[35–37].

Neuronal oscillations and neural avalanches exhibiting global behavior embedded in neuronal activity patterns were observed *in vitro*[32,36,38] and *in vivo*[39]. Numerous studies show that optimal operations including phase synchrony[36], information storage[40], communication, and information transition[32], optimal communication[32,34,41–44], transition capability[34], computational power[42], and dynamic range[34,45] are found when the brain works near criticality. A critical point sets a boundary between an ordered

and a less ordered state with different scaling behaviors[38]. At criticality, neural networks display power law distribution in a statistical collective behavior of the system, for instance, neural avalanche.

Studies show that avalanche size, and lifetime distributions are indicators of long-range correlation[32]. The widely varying profile of neural avalanche distribution in size is described by a single universal scaling exponent, $\beta$ in size, $P(S) \sim S^{\beta}$, and a single universal exponent in duration, $\tau$, $P(T) \sim T^{\tau}$, where $S$ and $T$ denote the size, and the duration of avalanches, respectively. Power-law distributions in neuronal avalanches appeared in cortex slice cultures of rats in vitro[35,36], rat cortical layer 2/3 at the beginning and end of the second week postnatal[46], Local Field Potentials (LFPs) of anesthetized cats[47,48], newborn rats[36], and monkeys[39,48].

Despite numerous experiments and modeling studies aimed at establishing the plausibility of the critical brain state and exploring the E/I ratio as a fundamental mechanism in brain dynamics, the impact of inhibition on both dynamics remains to be further investigated.

In this study, we address this problem by quantitatively analyzing the properties of a phase transition, including the order of the transition and its dynamic range, by varying the inhibition percentages systematically.

The order parameter is crucial in describing the transition between states in both critical equilibrium phenomena, e.g. Ising magnetic, which is a disordered-ordered transition[49], and systems out of equilibrium phase, e.g. neural systems, which is a desynchronized-synchronized transition[50–52] defined based on the Kuramoto order parameter[53–55].

In particular, we recently introduced the Kuramoto-based order parameter spike-phase coupling (*SPC*), which can detect the different levels of network-level synchrony in a purely excitatory leaky integrate-and-fire network[56]. Here, the *SPC* refers to the coupling between spike sequences[57,58] and the phase of temporal fluctuations of a macroscopic observable of the network, namely the population average voltage (*PAV*)[59]. The study showed that an estimation of the strength of *SPC*, represented as '$m$', is equal to the average of the instantaneous phases of *PAV* for all spikes in the firing time series throughout the entire neuronal network[56]. The m-value is zero when synaptic efficacy, $K$, is minimal and reaches one when it is substantial, resulting in complete synchronization of the network[56].

In this study, we take into account the inhibition in the network and show a significant level of inhibition can prevent the network from being synchronized. In particular, when there is a dominance of excitation in a network with few or no inhibitions, the changes in $m$ with respect to $K$ are usually the same. This means that a significant value for $K$ can result in full synchronization ($m \approx 1$) in the network. In contrast, when inhibition is the dominant factor, complete synchronization is impossible, and $m$ saturates at values below one, regardless of increasing $K$. As inhibition increases, $m$ remains the same at a small value for all levels of synaptic efficacy.

Moreover, in line with results from previous studies suggesting that a balance of excitation and inhibition in cortical networks promotes criticality, thereby maximizing dynamic range and improving input processing[35] we investigate the effects of varying the ratio of excitatory to inhibitory neurons, focusing on the dynamic range. It is shown that certain inhibition ratios increase the probability of the system operating in the critical regime, thereby extending its dynamic range.

## Results

In the studied network, both excitatory and inhibitory neurons receive a Gaussian input characterized by an identical mean and standard deviation. The input's mean value effectively maintains the membrane potential below the threshold, yet the non-zero standard deviation or noise can stochastically drive the neurons to the threshold. Once a neuron reaches or exceeds a specific threshold, it fires and then returns to its resting state. This behavior suggests that neurons oscillate between their resting state and activation threshold. In this research, the activation threshold and resting state are represented by numerical values one and zero, respectively. When excitatory neurons fire, they increase the potential of their neighboring connections by an amount $K$, while inhibitory neurons decrease it by the same amount. To investigate balance and criticality, we use two key variables: coupling strength ($K$) and inhibitory percentage ($I$). Specifically, the network displays critical behavior when the coupling strength ($K$) is equal to the critical value ($K_c$). The neurons are distributed on a lattice with periodic boundary conditions and simulations are performed on lattices with $N = 1600$, 2500, and 3600 neurons where $N = L \times L$ for $T = 2 \times 10^7$ time steps (see Methods section).

Here we first, compare the spike and *PAV* time series generated by the model for different $K$ values. The *PAV* is defined as follows:

$$PAV(t) = \frac{1}{N} \sum_{i=1}^{N} x_i(t) \tag{1}$$

where $N$ denotes the total number of neurons within the network, while $x_i(t)$ refers to the membrane voltage of the $i'th$ neuron at time $t$ . Fig. 1 shows spikes and the associated *PAV* for three different synaptic efficacies when 20 percent of the neurons in the network are inhibitory ($I = 20$). This illustration shows that the branching pattern becomes apparent when the system

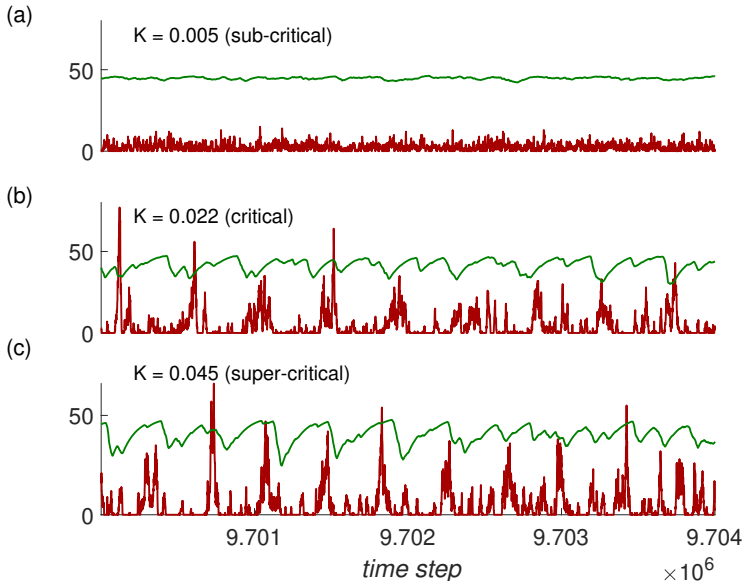


**Fig. 1.** The time series data is presented for spike number (in red) and the product of *PAV* and *L* (*PAV* multiplied by *L*, denoted in green): (a) in the sub-critical state with $K = 0.005$, (b) at the critical point with $K = 0.022$, and (c) within the super-critical domain at $K = 0.045$. The network's size ($L$) is 50, which corresponds to a total of 2500 neurons, of which 20 percent are inhibitory.

operates in the critical and super-critical regimes. In contrast, within the sub-critical regime, all *PAV* fluctuations are suppressed close to the threshold of the neuron. This behavior is a result of the irregularities observed in the spike patterns. The following sections provide detailed explanations on how to determine critical, sub-critical, and super-critical regimes. Additionally, the sections shed light on the contributions of excitatory and inhibitory neurons to the overall network dynamics, with a focus on the order parameter and the analysis of neural avalanches. The first step involves determining the transition type based on varying percentages of inhibition. Next, neural avalanche analysis is conducted to investigate the impact of inhibitory neurons on the observed behaviors.

## Order parameter and dynamical range

This section will begin by reviewing the definition of the order parameter for a pure excitatory neural network[56]. The mentioned definition has a crucial role in quantifying the synchronization within the network. Moreover, by employing the order parameter, we can characterize the critical points where the network transitions between various states of synchronization. The systematic comparison of different states within the network is possible by employing this parameter, particularly when considering various inhibition levels. Such comparative analysis enhances our understanding of how the percentage of inhibitory neurons affects the overall dynamics and helps develop a comprehensive understanding of the network's behavior. Here, *SPC* measures the connection between the *PAV* and the timing of neuronal spikes. To calculate the *SPC*, three steps will be performed:

1. The instantaneous phase of *PAV* is calculated for each spike in the spike train of every neuron in the network. This is performed using the Hilbert transform, and the results are then averaged to obtain a mean instantaneous phase value for $j'th$ neuron in the network ($M_j$).

$$M_j = \frac{1}{n_s^j} \sum_{l=1}^{n_s^j} exp(i\phi_l^j(t)) \tag{2}$$

where $n_s^j$ shows the number of spikes for neuron $j$ and $i = \sqrt{-1}$. Here, $\phi_l^j(t)$ is the instantaneous phase of *PAV* corresponding to the $l'th$ spike of the $j'th$ neuron and is extracted from the Hilbert transform of the *PAV* time series.
2. The phase-locking value (*PLV*) is calculated by averaging over all $M_j$ values[60].

$$PLV(N) = \frac{1}{N} \sum_{j=1}^{N} M_j \tag{3}$$

where $N$ is the number of neurons in the network ($N = L \times L$). The $PLV$ functions as a synchronization metric. A $PLV$ value of zero indicates either a lack of spikes or complete desynchronization (when $n_s \to \infty$), while a value of one (in absolute terms) indicates perfect phase locking and synchronization between the spikes. This step assists in evaluating the alignment of the phases of different spikes, which provides a measure of coherence within the system.
3. The absolute value of $PLV$ is used to estimate the $SPC$. This absolute value is used as the order parameter ($m$) to describe the synchronized behavior of the network.

$$m(N) = |PLV(N)| \tag{4}$$

Fig. 2a shows variations of order parameter, $m$, with respect to the control parameter, $K$ for a particular lattice size, $L = 40$. It shows that including inhibitory neurons has a dual effect. First, it widens the transitional region between de-synchronized and synchronized states, effectively increasing the range of conditions under which these transitions occur (the horizontal length between the stochastic and synchronized parts of the transition region expands). Second, it leads to a reduction in the value of the parameter $m$, especially for stronger coupling strength at high levels of inhibition. To further investigate, we evaluate this expansion by the dynamic range, providing insight into how the varying ratio of excitatory and inhibitory neurons affects the system's behavior. While the transition between states remains continuous across all examined ratios, a distinct pattern emerges, specifically at an inhibitory ratio of 20%. To quantify these transitions for different inhibition percentages, we employ the dynamical range, denoted by $\Delta_h$:

$$\Delta_h = 10\log_{10}\left(\frac{K(0.9)}{K(0.1)}\right) \tag{5}$$

Here, $K(x)$ is the value of $K$ for which the order parameter curve attains a value that is $x$ times the maximum of $m$, or more specifically:

$$m(K(x)) := x \cdot max(m) \tag{6}$$

The calculation of the dynamic range for different inhibitory percentages and lattice sizes requires determining the order parameter at higher $K$, where it becomes saturated and independent of $K$, as shown in Fig 2b. The black dashed lines in the figure assist in identifying the key parameters $K(0.9)$ and $K(0.1)$, which are then used to compute the dynamical range, as given in Equation (5). Additionally, Fig 2c shows the dynamic range as a function of different inhibition ratios. The figure shows that the dynamic range reaches its maximum value for $I = 20\%$, a result that is consistent for all lattice sizes examined. The results of the study show that while inhibitory neurons in the system may initially prevent or postpone synchronization, the introduction of an optimal level of inhibition can actually expand the dynamic range of the system. This is particularly noticeable when the control parameter is significantly larger than that of networks with other inhibitory percentages and the system is still not in synchronized phase. Therefore, inhibition performs a subtle function, both restricting and perhaps enhancing the operational flexibility of the system. The depicted transition between different states of synchronization is continuous, highlighting the gradual shift in behavior as the parameters vary. We prove that this system undergoes a continuous transition and critical behavior by using the finite-size scaling theory. This approach provides a better and more detailed comprehension of the system's behavior. In this context, we examine the interplay between the order parameter, coupling strength, and lattice size, considering the network's composition of 20 percent inhibitory neurons. Here, the relationship between the order parameter, coupling strength, and lattice size is assumed as follows:

$$m(L,K) = L^{-\beta/\nu}\mathscr{M}(|K - K_c|L^{1/\nu}) \tag{7}$$

$\beta$ and $\nu$ are the critical exponents corresponding to order parameter and correlation length, respectively. $\mathscr{M}(x)$ is the scaling function. For systems of large sizes, the behavior of $\mathscr{M}(x)$ is expected to be as follows:

$$\mathscr{M}(x) \sim x^{\beta} \quad \text{as} \quad x \to \infty \tag{8}$$

In the infinite size limit when $K > K_c$, the following relation is necessary for a continuous phase transition.

$$m \sim (K - K_c)^{\beta} \tag{9}$$

Fig. 3a shows the order parameter as a function of the control parameter parameter $K$ for inhibition level of 20% at lattice sizes $L = 40, 50$, and 60. Fig. 3b illustrates the collapsing of the data over a range of lattice sizes for 20% inhibition percentages.

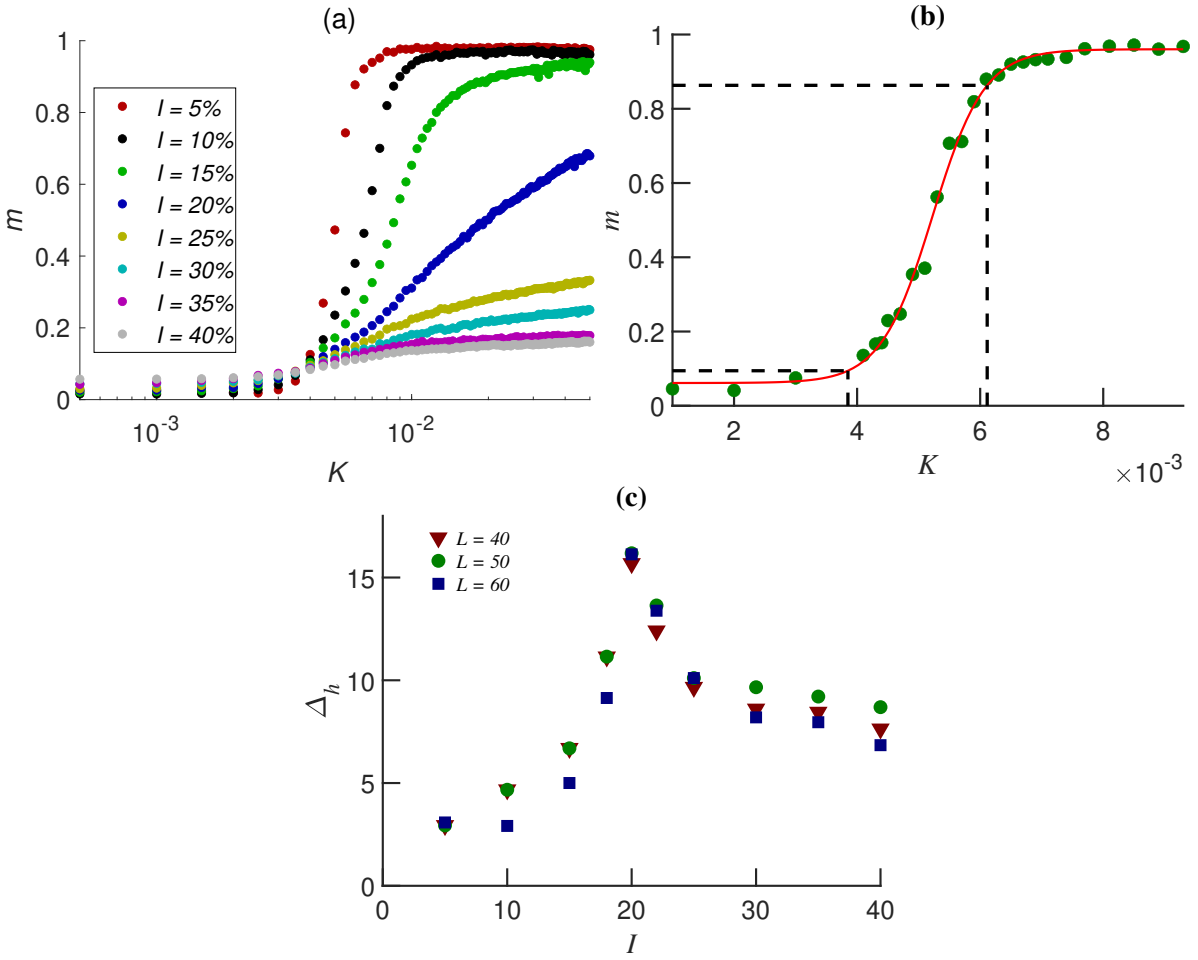


**Fig. 2.** (a) The dependence of the order parameter $m$ on the parameter $K$ is shown for lattices of linear size $L = 40$ and different inhibition percentages: 5%, 10%, 15%, 20%, 25%, 30%, 35%, and 40%. (b) The plot of $m$ as a function of $K$, with vertical lines indicating the values of $K(0.9)$ and $K(0.1)$ for $L = 60$ and an inhibition percentage of 5%. (c) Analysis of the dynamic range $\Delta_h$ over different lattice sizes and inhibition percentages.

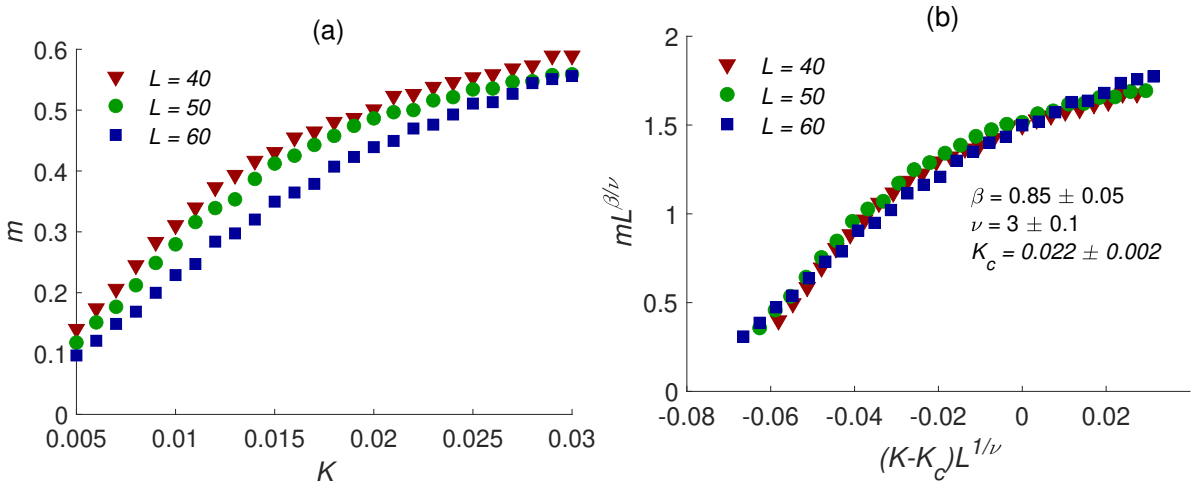


**Fig. 3.** (a) Variation of the magnitude of the order parameter ($m$) with parameter $K$, plotted for lattices of linear sizes $L = 40$, 50, 60 and inhibition ratio 20% around the critical point. (b) Rescaled $m - K$ curves showing collapse for different lattice sizes and inhibition ratio 20%.

The observed behavior shows a distinct class of universality, differing from both mean-field directed percolation with $\beta = 1$ and $\nu = 0.5$, and directed percolation with $\beta = 0.580(4)$ and $\nu = 0.729(1)$ in 2+1 dimention[61]. In more detail, the result suggests that synchronization within the system is suppressed by the inhibitory neurons' attenuating effect on excitatory activity. The underlying mechanisms of this effect can be understood in terms of the synchronized activity between excitation and inhibition. Here, inhibitory inputs can balance the excitatory input received by an excitatory neuron when both types of neurons are active simultaneously. As a result, while synchronization between excitatory and inhibitory neurons may initially prevent the synchronized phase within the system, which is measured by the m-value, the implementation of an optimal level of inhibition can indeed expand the dynamic range. This effect is especially noticeable when the control parameter is significantly large and the system has not yet been synchronized. Therefore, it might be a result of a different phase between excitatory and inhibitory activity.

### Inhibition effects on neuronal avalanches

In the current study, the introduction of inhibition into the network resulted in the same type of transition from desynchronized to synchronized behavior in a pure LIFM[56]. However, this led us to question how inhibition operates within the coupling domains, leading to the emergence of criticality, a region we specifically call the critical domain. Our recent studies investigated the emergence of criticality using temporal complexity and avalanche analysis[62–64] in a leaky integrate-and-fire model following finite-size scaling[56].

In this study, we perform neural avalanche analysis to determine the possibility of criticality emergence by considering different percentages of inhibition in the system. In more detail, an avalanche is characterized by two main features: its size, represented by $S$, and its lifetime, commonly known as duration, represented by $T$ (see the Methods section). Neural systems exhibit diverse sizes and durations, where their probability distributions follow a power-law pattern[32]. This behavior is characterized by a single universal scaling exponent: $\tau$ for size, represented by $p(S) = S^{-\tau}$, and $\alpha$ for duration, represented by $p(T) = T^{-\alpha}$ which follwos a shape collapse in cultured slices of cortical tissue[38].

Despite the power-law behavior of avalanche size and duration, demonstrating criticality behavior in avalanche data requires universal scaling[65]. Therefore, we perform a scaling analysis over different network sizes and different inhibition percentages. According to the single scaling theory, in the case of a network with a size of $L$, the probabilities are expressed as follows[65]:

$$\begin{aligned} p(S) &= L^{-\mu\tau}\mathscr{S}(SL^{-\mu}), \\ p(T) &= L^{-z\mu\alpha}\mathscr{T}(TL^{-z\mu}), \\ \langle S\rangle(T) &= L^{\mu}\mathscr{F}(TL^{-z\mu}), \end{aligned} \tag{10}$$

where $\mu$ is the scaling exponent of the size of avalanches versus the linear size of the lattice and $z$ is the dynamical exponent which determines the scaling relations of the duration and size of the avalanches. Here $\langle S\rangle(T)$ is the average of avalanche size conditioned on a given duration[65]. Here $\mathscr{S}(x)$, $\mathscr{T}(x)$, and $\mathscr{F}(x)$ represent universal functions. Their behavior in the large $x$ limit ($x \to \infty$, corresponding to small $L$) is described as follows:

$$\begin{aligned} p(S) &\sim S^{-\tau}, \\ p(T) &\sim T^{-\alpha}, \\ \langle S\rangle(T) &\sim T^{1/z}, \end{aligned} \tag{11}$$

Moreover, the scaling theory requires the following exponentiation relationship[38,66]:

$$\frac{\alpha-1}{\tau-1} = \frac{1}{z} \tag{12}$$

in which the mean field prediction for the scaling exponents are $\tau = 3/2, \alpha = 2.0$, and $1/z = 2.0$[65]. We perform this analysis on the neural avalanche patterns for networks in which 5%, 10%, 15%, and 20% of the neurons are inhibitory.

Fig. 4 shows neural avalanches for inhibition percentage of 20 that follow a scaling relationship and collapse into a single function. A value of $\approx 2.0$ for $\mu$ suggests that the avalanche size grows directly to the lattice size.

Moreover simulations show that inhibitory neurons broaden control parameter's domain, corresponding to critical behavior (Table. 1). Neural avalanches show power-law behavior over a broad range of $K$ values, especially when the inhibition percentage $I$ is set to 20%. Furthermore, the parameters that describe the phase transitions vary for each inhibitory percentage.

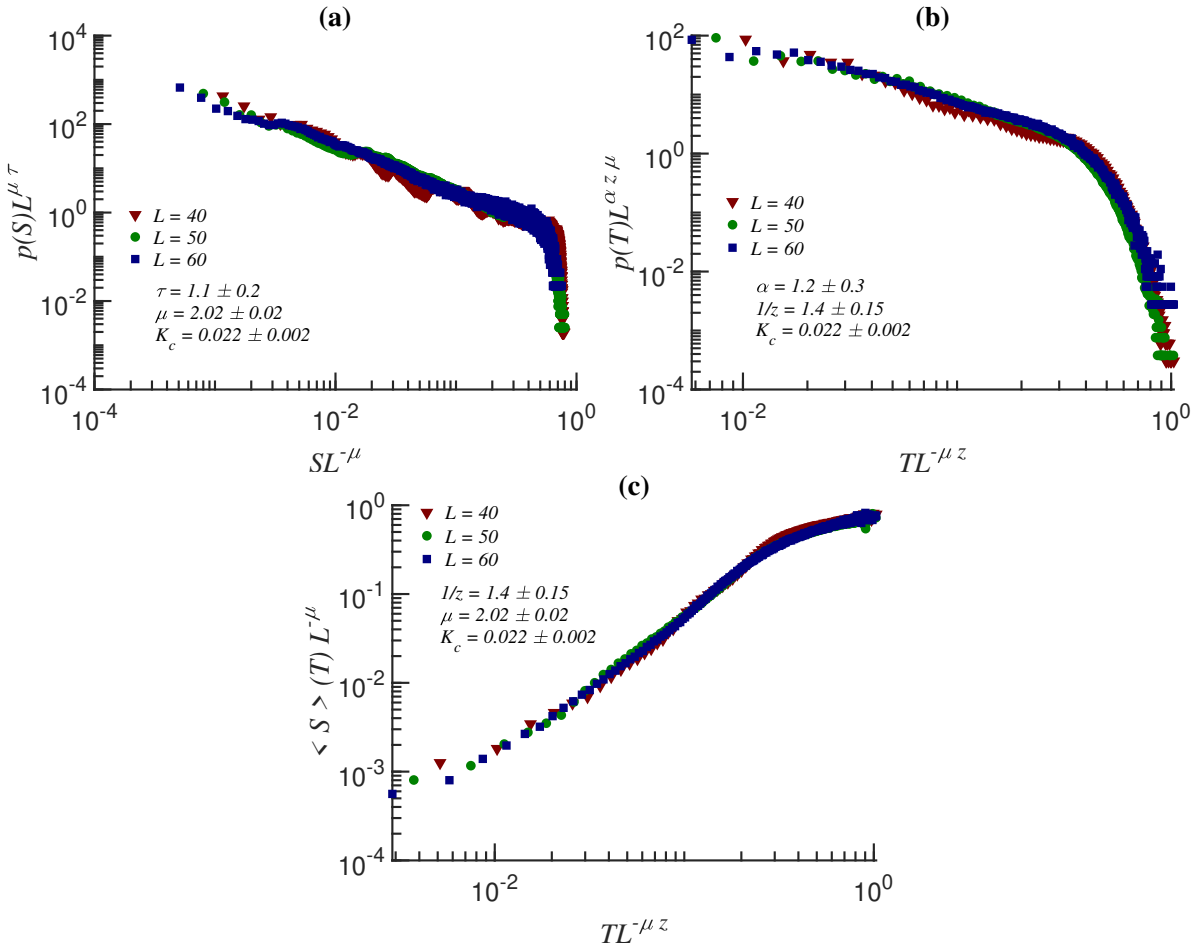


**Fig. 4.** The figure displays the collapse of avalanche data through the scaling relation. Panel (a) display the plotted avalanche sizes whereas panels (b) present the duration probabilities $p(T)$ and the conditional average of avalanche size versus duration shown as (c). The results are presented at the critical point $K$ of square lattices with linear sizes of $L = 40$, 50, and 60, and inhibitory percentages of $I = 20\%$. The slope of maximum avalanche size vs. lattice size was used to obtain $\mu$..

| | $I = 5$ | $I = 10$ | $I = 15$ | $I = 20$ |
|---|---|---|---|---|
| $\nu$ | $1.05 \pm 0.05$ | $1.85 \pm 0.15$ | $1.78 \pm 0.05$ | $3 \pm 0.1$ |
| $\beta$ | $0.32 \pm 0.17$ | $0.55 \pm 0.05$ | $0.33 \pm 0.03$ | $0.85 \pm 0.05$ |
| $K_c$ | $0.0052 \pm 0.0001$ | $0.0072 \pm 0.0005$ | $0.0115 \pm 0.001$ | $0.022 \pm 0.002$ |

**Table 1.** Exponents for data collapsing for different inhibitory percentages.

## Discussion

Inhibitory neurons and neuronal avalanches play a crucial role in understanding complex neural networks. In our previous research, we studied a purely excitatory network and showed a dynamic transition of neuronal behavior from an asynchronous state to a fully synchronized state, with a distinct and complex critical phase between these two phases. Furthermore, we quantified this transition using the Kuramoto order parameter.[56]

Moreover, previous research emphasizes the importance of the E/I ratio in network dynamics, especially at high connectivity levels[67] and have shown that the local excitation-inhibition ratio strongly influences whole-brain dynamics, the structure of spontaneous activity and information transmission[68].

In this context, our primary focus in this study was to examine the impact of different E/I ratios on the emergence of criticality and phase transition. It is shown that an optimal ratio (20%) facilitates critical behavior in the network. Inclusion of 20% inhibitory neurons expands the coupling parameter domain in which neural avalanches satisfy the scaling relation, increasing the probability of finding the network in a critical state and maximizing the dynamic range.

The observed effects might be associated with a subset of inhibitory neurons that are in the same phase as excitatory neurons. This prevents synchronization at larger connectivity values ($K$) compared to networks with different inhibitory neuron percentages. As a result, the difference between $K$ that leads to synchronized and desynchronized states expands, resulting in a more extensive range of dynamic behavior. However, excessive levels of inhibition can prevent the emergence of synchronization. In such scenarios, the system can be pushed into a permanent desynchronized state. This might emphasize the intricate balance necessary for optimal control parameter between excitatory and inhibitory neurons.

The study results, although they concentrate on a particular computational model, also provide insight into broader principles that may apply to other network topologies, especially in the context of criticality, which manifests itself as transitions between desynchronized and synchronized states. Fundamentally, different levels of inhibition can significantly modify the network's dynamic range. The degree of inhibition could, for example, limit the dynamic range at low percentages of inhibition and possibly lead to a lack of transitions in networks dominated by inhibitory activity. It is possible that for another topology, another optimal inhibitory percentage exists, maximizing the dynamic range. This indicates that modulation of neural activity via E/I ratios is a complex process, with different network topologies leading to different outcomes. However, the evolutionarily precise objective function that results in this specific E/I ratio in the cortex is still a matter of further investigation. However, this objective function might drive neural systems toward critical points[69,70], the dynamic behavior of the order parameter despite synaptic plasticity needs to be investigated.

Taken together, although the results of this study are derived from a model with a defined set of parameters and lattice structure, the identified patterns in the model suggest a likely framework for understanding how E/I ratios might modulate cortical scale-free dynamics and contribute to the broader discussion of brain dynamics.

## Methods

### Model description

In this study, we employ the Leaky Integrate and Fire Model (LIFM) [56,62–64,71,72]. The dynamic of the membrane potential of a single neuron $x_i(t)$, which is residing on a two-dimensional square lattice of linear size L with the periodic boundary condition, is

$$\dot{x_i} = -\gamma x_i(t) + S + \sigma\xi_i(t), \tag{13}$$

where $1/\gamma$ is the membrane time constant, assumed to be the same for both excitatory and inhibitory neurons for simplicity. $S$ denotes a constant that drives the membrane potential to the steady-state $x_i = S/\gamma$ in the absence of the third term on the right side of the equation, and $\xi(t)$ is a continuous Gaussian noise having a mean of zero and a variance of one, as defined by

$$\begin{aligned} \langle\xi(t)\rangle &= 0, \\ \langle\xi(t)\xi(t')\rangle &= \delta(t-t'), \end{aligned} \tag{14}$$

where $\sigma$ represents noise intensity, which can drive $x(t)$ to the threshold, in this case $S < \gamma$, and leads the neuron to fire. In this context, $(S + \sigma\xi_i(t))/\gamma$ can be interpreted as the input to each neuron. We randomly distribute $N_E$ excitatory and $N_I$ inhibitory neurons, $N = N_E + N_I$, on the lattice. In principle, inhibitory neurons could have two types of inhibitory-inhibitory, inhibitory-excitatory, and excitatory-inhibitory connections. Here, however, there is no link between inhibitory neurons, i.e., no inhibitory-inhibitory connections exist.

The initial membrane potential for all neurons in the network is a random value between 0 and 1 from a uniform distribution.

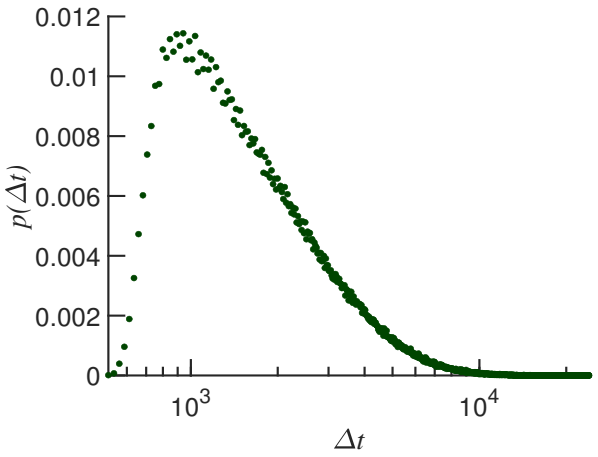


**Fig. 5.** The probability distribution function for the spike time intervals of a single neuron. The simulation time is $10^9$ steps.

Considering the reset mechanism by setting the threshold to one; whenever the membrane potential reaches or passes the threshold, i.e., $x = 1$, it jumps back to the resting state, $x = 0$. If the firing neuron is inhibitory, $K$ (control parameter) is subtracted from the membrane potential of its adjacent neurons, and if it is excitatory, $K$ is added to the membrane potential of its adjacent neurons. The quantity $K > 0$ controls whether the system is in a sub-critical, critical, or super-critical state. We refer to $K$ as a control parameter in which $K_c$ leads to power-law behavior in the model. The simulations in the current paper are based on the following parameters: $S = 0.001$, $\gamma = 0.001005$, and $\sigma = 0.0001$, and the lattice with linear sizes of $L = 40,\ 50$, and $60$. The integration time step for the numerical solution was $\Delta t = 0.01$ (Euler method), and the simulations lasted for $2 \times 10^7$ steps.
Implementing the above parameter concludes that only noise and control parameter make neurons pass or reach the threshold. However, for the case of a single neuron, as illustrated in Fig. 5, the neuron preferentially fires within a particular time called $T_p$, the peak in the figure, and spike time intervals follow the Poissonian distribution. Considering a single neuron in the network leads to a change in the amount of this peak per phase with different $K_c$.

### Neural Avalanches

The term "neural avalanche" refers to the sequential propagation of neuronal firing activity within a network in a correlated manner, initiated by firing a single neuron or a small group of neurons. This activity can cause a network to behave in a synchronized manner. To identify neuronal avalanches, we identify time points where there is an absence of firing activity across all neurons in the system for a continuous duration of at least five time steps ($\delta t = 5$). As shown in Fig. 6, the initiation of an avalanche is marked by the first firing event within the network, indicated by the dashed lines. In this context, a neural avalanche is defined by two key parameters: its size, represented by the number of spikes within the avalanche, and its duration, representing the time span from the initial firing to the last firing event. To comprehensively analyze these neural avalanches, we assess the probability of their occurrence over different sizes, $P(S)$, and durations, $P(T)$.

## Acknowledgements

All authors gratefully acknowledge financial support from their affiliated institutions.

## References

1. Isaacson, J. S. & Scanziani, M. How inhibition shapes cortical activity. *Neuron* **72**, 231–243 (2011).
2. Denève, S. & Machens, C. K. Efficient codes and balanced networks. *Nat. neuroscience* **19**, 375–382 (2016).
3. Zhou, S. & Yu, Y. Synaptic ei balance underlies efficient neural coding. *Front. Neurosci.* **12**, 46 (2018).
4. Van Vreeswijk, C. & Sompolinsky, H. Chaos in neuronal networks with balanced excitatory and inhibitory activity. *Science* **274**, 1724–1726 (1996).
5. Brunel, N. Dynamics of sparsely connected networks of excitatory and inhibitory spiking neurons. *J. computational neuroscience* **8**, 183–208 (2000).

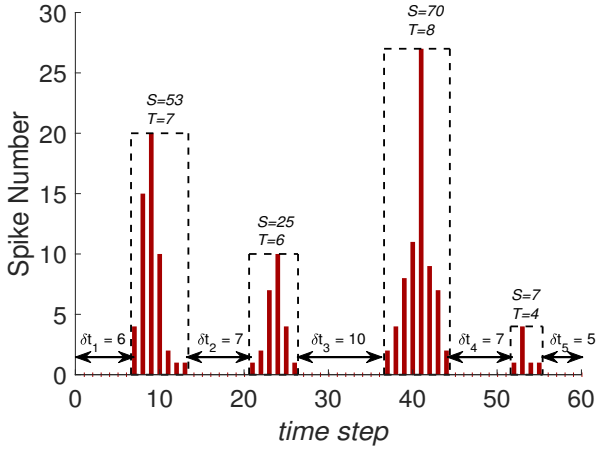


**Fig. 6.** A schematic representation of the process for calculating neuronal avalanches The steps include: 1. Simulating Neuronal Activity: Neuronal firing patterns are generated and observed over time within the model. 2. Identifying Silent Periods: Silent periods where there is no firing activity across all neurons for at least five time steps ($\delta t = 5$) are identified. 3. Detecting and Analyzing Avalanches: The regions between consecutive silent periods are considered avalanches. The size of an avalanche is determined by the number of spikes during its duration. The figure demonstrates how the sequential propagation of neuronal firing activity within a network results in the formation of distinct avalanches of various sizes and durations.


**6.** Wehr, M. & Zador, A. M. Balanced inhibition underlies tuning and sharpens spike timing in auditory cortex. *Nature* **426**, 442–446 (2003).

**7.** Shu, Y., Hasenstaub, A. & McCormick, D. A. Turning on and off recurrent balanced cortical activity. *Nature* **423**, 288–293 (2003).

**8.** Murphy, B. K. & Miller, K. D. Balanced amplification: a new mechanism of selective amplification of neural activity patterns. *Neuron* **61**, 635–648 (2009).

**9.** Zhang, L. I., Tan, A. Y., Schreiner, C. E. & Merzenich, M. M. Topography and synaptic shaping of direction selectivity in primary auditory cortex. *Nature* **424**, 201–205 (2003).

**10.** Froemke, R. C., Merzenich, M. M. & Schreiner, C. E. A synaptic memory trace for cortical receptive field plasticity. *Nature* **450**, 425–429 (2007).

**11.** Brenner, R. P. Eeg in convulsive and nonconvulsive status epilepticus. *J. Clin. Neurophysiol.* **21**, 319–331 (2004).

**12.** Llinás, R. R., Ribary, U., Jeanmonod, D., Kronberg, E. & Mitra, P. P. Thalamocortical dysrhythmia: a neurological and neuropsychiatric syndrome characterized by magnetoencephalography. *Proc. Natl. Acad. Sci.* **96**, 15222–15227 (1999).

**13.** Singer, H. S. & Minzer, K. Neurobiology of tourette's syndrome: concepts of neuroanatomic localization and neurochemical abnormalities. *Brain Dev.* **25**, S70–S84 (2003).

**14.** Rubenstein, J. & Merzenich, M. M. Model of autism: increased ratio of excitation/inhibition in key neural systems. *Genes, Brain Behav.* **2**, 255–267 (2003).

**15.** Yizhar, O. *et al.* Neocortical excitation/inhibition balance in information processing and social dysfunction. *Nature* **477**, 171–178 (2011).

**16.** Wassef, A., Baker, J. & Kochan, L. D. Gaba and schizophrenia: a review of basic science and clinical studies. *J. clinical psychopharmacology* **23**, 601–640 (2003).

**17.** Murray, J. D. *et al.* Linking microcircuit dysfunction to cognitive impairment: effects of disinhibition associated with schizophrenia in a cortical working memory model. *Cereb. cortex* **24**, 859–872 (2014).

**18.** Froemke, R. C. Plasticity of cortical excitatory-inhibitory balance. *Annu. review neuroscience* **38**, 195–219 (2015).

**19.** Dehghani-Habibabadi, M. & Pawelzik, K. Synaptic self-organization of spatio-temporal pattern selectivity. *PLOS Comput. Biol.* **19**, e1010876 (2023).

**20.** Bateup, H. S. *et al.* Excitatory/inhibitory synaptic imbalance leads to hippocampal hyperexcitability in mouse models of tuberous sclerosis. *Neuron* **78**, 510–522 (2013).

**21.** Sillito, A. The contribution of inhibitory mechanisms to the receptive field properties of neurones in the striate cortex of the cat. *The J. physiology* **250**, 305–329 (1975).

**22.** Sillito, A. Functional considerations of the operation of gabaergic inhibitory processes in the visual cortex. *Cereb. Cortex.* 91–117 (1984).

**23.** Hendry, S. H., Schwark, H., Jones, E. & Yan, J. Numbers and proportions of gaba-immunoreactive neurons in different areas of monkey cerebral cortex. *J. Neurosci.* **7**, 1503–1519 (1987).

**24.** DeFelipe, J. Neocortical neuronal diversity: chemical heterogeneity revealed by colocalization studies of classic neurotransmitters, neuropeptides, calcium-binding proteins, and cell surface molecules. *Cereb. cortex* **3**, 273–289 (1993).

**25.** Somogyi, P., Tamas, G., Lujan, R. & Buhl, E. H. Salient features of synaptic organisation in the cerebral cortex. *Brain research reviews* **26**, 113–135 (1998).

**26.** Markram, H. *et al.* Interneurons of the neocortical inhibitory system. *Nat. reviews neuroscience* **5**, 793–807 (2004).

**27.** Huang, Z., Di Cristo, G. & Ango, F. Development of gaba innervation in the cerebral and cerebellar cortices. *Nat. Rev. Neurosci.* **8**, 673–686 (2007).

**28.** Kepecs, A. & Fishell, G. Interneuron cell types are fit to function. *Nature* **505**, 318–326 (2014).

**29.** Buzsaki, G. & Draguhn, A. Neuronal oscillations in cortical networks. *science* **304**, 1926–1929 (2004).

**30.** Dichter, M. A. & Ayala, G. Cellular mechanisms of epilepsy: a status report. *Science* **237**, 157–164 (1987).

**31.** Okun, M. & Lampl, I. Instantaneous correlation of excitation and inhibition during ongoing and sensory-evoked activities. *Nat. neuroscience* **11**, 535–537 (2008).

**32.** Beggs, J. M. & Plenz, D. Neuronal avalanches in neocortical circuits. *J. neuroscience* **23**, 11167–11177 (2003).

**33.** Atallah, B. V. & Scanziani, M. Instantaneous modulation of gamma oscillation frequency by balancing excitation with inhibition. *Neuron* **62**, 566–577 (2009).

**34.** Shew, W. L., Yang, H., Yu, S., Roy, R. & Plenz, D. Information capacity and transmission are maximized in balanced cortical networks with neuronal avalanches. *J. neuroscience* **31**, 55–63 (2011).

**35.** Shew, W. L., Yang, H., Petermann, T., Roy, R. & Plenz, D. Neuronal avalanches imply maximum dynamic range in cortical networks at criticality. *J. neuroscience* **29**, 15595–15600 (2009).

**36.** Yang, H., Shew, W. L., Roy, R. & Plenz, D. Maximal variability of phase synchrony in cortical networks with neuronal avalanches. *J. neuroscience* **32**, 1061–1072 (2012).

**37.** Poil, S.-S., Hardstone, R., Mansvelder, H. D. & Linkenkaer-Hansen, K. Critical-state dynamics of avalanches and oscillations jointly emerge from balanced excitation/inhibition in neuronal networks. *J. Neurosci.* **32**, 9817–9823 (2012).

**38.** Friedman, N. *et al.* Universal critical dynamics in high resolution neuronal avalanche data. *Phys. review letters* **108**, 208102 (2012).

**39.** Petermann, T. *et al.* Spontaneous cortical activity in awake monkeys composed of neuronal avalanches. *Proc. Natl. Acad. Sci.* **106**, 15921–15926 (2009).

**40.** Socolar, J. E. & Kauffman, S. A. Scaling in ordered and critical random boolean networks. *Phys. review letters* **90**, 068702 (2003).

**41.** Beggs, J. M. & Timme, N. Being critical of criticality in the brain. *Front. physiology* **3**, 163 (2012).

**42.** Bertschinger, N. & Natschläger, T. Real-time computation at the edge of chaos in recurrent neural networks. *Neural computation* **16**, 1413–1436 (2004).

**43.** Rämö, P., Kauffman, S., Kesseli, J. & Yli-Harja, O. Measures for information propagation in boolean networks. *Phys. D: Nonlinear Phenom.* **227**, 100–104 (2007).

**44.** Chialvo, D. R. Emergent complex neural dynamics. *Nat. physics* **6**, 744–750 (2010).

**45.** Kinouchi, O., Diez-Garcia, R. W., Holanda, A. J., Zambianchi, P. & Roque, A. C. The non-equilibrium nature of culinary evolution. *New J. Phys.* **10**, 073020 (2008).

**46.** Gireesh, E. D. & Plenz, D. Neuronal avalanches organize as nested theta-and beta/gamma-oscillations during development of cortical layer 2/3. *Proc. Natl. Acad. Sci.* **105**, 7576–7581 (2008).

**47.** Hahn, G. *et al.* Neuronal avalanches in spontaneous activity in vivo. *J. neurophysiology* **104**, 3312–3322 (2010).

**48.** Priesemann, V. *et al.* Spike avalanches in vivo suggest a driven, slightly subcritical brain state. *Front. systems neuroscience* **8**, 108 (2014).

**49.** Krauth, W. *Statistical mechanics: algorithms and computations*, vol. 13 (OUP Oxford, 2006).

**50.** Prignano, L., Sagarra, O. & Díaz-Guilera, A. Tuning synchronization of integrate-and-fire oscillators through mobility. *Phys. review letters* **110**, 114101 (2013).

**51.** Politi, A. & Rosenblum, M. Equivalence of phase-oscillator and integrate-and-fire models. *Phys. Rev. E* **91**, 042916 (2015).

**52.** Ratas, I. & Pyragas, K. Noise-induced macroscopic oscillations in a network of synaptically coupled quadratic integrate-and-fire neurons. *Phys. Rev. E* **100**, 052211 (2019).

**53.** Kuramoto, Y. International symposium on mathematical problems in theoretical physics. *Lect. notes Phys.* **30**, 420 (1975).

**54.** Acebrón, J. A., Bonilla, L. L., Vicente, C. J. P., Ritort, F. & Spigler, R. The kuramoto model: A simple paradigm for synchronization phenomena. *Rev. modern physics* **77**, 137 (2005).

**55.** Kuramoto, Y. & Kuramoto, Y. *Chemical turbulence* (Springer, 1984).

**56.** Safari, N., Shahbazi, F., Dehghani-Habibabadi, M., Esghaei, M. & Zare, M. Spike-phase coupling as an order parameter in a leaky integrate-and-fire model. *Phys. Rev. E* **102**, 052202 (2020).

**57.** Abeles, M., Bergman, H., Margalit, E. & Vaadia, E. Spatiotemporal firing patterns in the frontal cortex of behaving monkeys. *J. neurophysiology* **70**, 1629–1638 (1993).

**58.** Hahnloser, R. H., Kozhevnikov, A. A. & Fee, M. S. An ultra-sparse code underliesthe generation of neural sequences in a songbird. *Nature* **419**, 65–70 (2002).

**59.** Esghaei, M., Daliri, M. R. & Treue, S. Local field potentials are induced by visually evoked spiking activity in macaque cortical area mt. *Sci. reports* **7**, 17110 (2017).

**60.** Esghaei, M., Daliri, M. R. & Treue, S. Attention decouples action potentials from the phase of local field potentials in macaque visual cortical area mt. *BMC biology* **16**, 1–13 (2018).

**61.** Wang, J., Zhou, Z., Liu, Q., Garoni, T. M. & Deng, Y. High-precision monte carlo study of directed percolation in (d+ 1) dimensions. *Phys. Rev. E* **88**, 042102 (2013).

**62.** Zare, M. & Grigolini, P. Cooperation in neural systems: Bridging complexity and periodicity. *Phys. Rev. E* **86**, 051918, DOI: 10.1103/PhysRevE.86.051918 (2012).

**63.** Zare, M. & Grigolini, P. Criticality and avalanches in neural networks. *Chaos, Solitons & Fractals* **55**, 80 – 94, DOI: https://doi.org/10.1016/j.chaos.2013.05.009 (2013). Emergent Critical Brain Dynamics.

**64.** Dehghani-Habibabadi, M., Zare, M., Shahbazi, F., Usefie-Mafahim, J. & Grigolini, P. Neuronal avalanches: Where temporal complexity and criticality meet. *The Eur. Phys. J. E* **40**, 101, DOI: 10.1140/epje/i2017-11590-8 (2017).

**65.** Sethna, J., Dahmen, K. & Myers, C. Crackling noise. *Nature* **410**, 242–250, DOI: 10.1038/35065675 (2001).

**66.** Scarpetta, S., Apicella, I., Minati, L. & de Candia, A. Hysteresis, neural avalanches, and critical behavior near a first-order transition of a spiking neural network. *Phys. Rev. E* **97**, 062305 (2018).

**67.** Baumgarten, L. & Bornholdt, S. Critical excitation-inhibition balance in dense neural networks. *Phys. Rev. E* **100**, 010301 (2019).

**68.** Deco, G. *et al.* How local excitation–inhibition ratio impacts the whole brain dynamics. *J. Neurosci.* **34**, 7886–7898 (2014).

**69.** Lombardi, F., Herrmann, H. J. & de Arcangelis, L. Balance of excitation and inhibition determines 1/f power spectrum in neuronal networks. *Chaos: An Interdiscip. J. Nonlinear Sci.* **27** (2017).

**70.** Zeraati, R., Priesemann, V. & Levina, A. Self-organization toward criticality by synaptic plasticity. *Front. Phys.* **9**, 619661 (2021).

**71.** Luccioli, S. & Politi, A. Irregular collective behavior of heterogeneous neural networks. *Phys. Rev. Lett.* **105**, 158104, DOI: 10.1103/PhysRevLett.105.158104 (2010).

**72.** Mafahim, J. U., Lambert, D., Zare, M. & Grigolini, P. Complexity matching in neural networks. *New J. Phys.* **17**, 015003 (2015).

## 2.5 Effects of optogenetic and visual stimulation on gamma activity in the visual cortex

**Title**: ”Effects of optogenetic and visual stimulation on gamma activity in the visual cortex”

**Journal**: Neuroscience Letters, Volume 816, Pages 137474, Published 2023

**DOI**: https://doi.org/10.1016/j.neulet.2023.137474

**Authors**: Fereshteh Araba, Sareh Rostami, Mohammad Dehghani-Habibabadi, Diego M. Mateos, Roisin Braddell, Felix Scholkmann, Mohammad Ismail Zibaii, Serafim Rodrigues, Vahid Salari, Mir-Shahram Safari

**My contribution to this paper**:

Proposing the idea
Formal analysis:
Main text: Fig. 4 (A and C), Fig. 5.
Supplementary material: Fig. A, A1, A2, and A3

Writing - original draft

# Chapter 3

# Discussion

## 3.1 Learning of Spatio-Temporal Spike Patterns

This part of the discussion refers to the papers presented in 2.1 and 2.2.
To achieve balance in neural networks, the interplay of Hebbian mechanisms in both excitatory and inhibitory synapses appears to be crucial. While Hebbian plasticity at excitatory synapses could lead to escalating and potentially unstable neural activity, its simultaneous presence at inhibitory synapses and the biological upper limit at excitatory synapses to the maximum amount of a synapse efficacy serve as a counterbalance, leading to a balance between excitation and inhibition. Although this has been suggested before[1], we have shown that Hebbian plasticity can select for synaptic efficiencies that allow neurons to detect spatio-temporal spike patterns. This constraint on the uncontrolled growth of excitatory efficacy is particularly valuable because it provides a plausible path to the stability that is essential for biological neural systems. It prevents the network from diverging into states of an excessive increase in firing, allowing instead the dynamic yet stable behavior that is crucial for complex processes such as learning and memory formation. This further deepens our understanding of the self-organization capabilities of neural networks and offers promising avenues for future research.
Our research has shown how a synergistic combination of realistic neural mechanisms, consisting of membrane potential-dependent Hebbian processes, heterosynaptic competition, and synaptic scaling, contributes to the self-organization of pattern recognition in individual neurons. When a learned pattern is absent, our results confirm that excitatory and inhibitory signals are finely tuned in a global balance.[2] When a previously learned pattern appears, neural mechanisms achieve a detailed balance in which excitatory and inhibitory inputs are tightly balanced over time.[3] These findings extend and confirm the existing literature on the dynamic balance between excitation and inhibition in neural cortices. Furthermore, the results clearly show that this detailed balance is particularly prominent during pattern recognition, further confirming it as a stable state within the neural network. The tight balance allows post-synaptic neurons to fire, albeit minimally, indicating the anti-correlation between excitatory and inhibitory signals. Importantly, our model shows that no supervision is required to tune the synaptic weights essential for pattern recognition. While previous models required careful parameter tuning and were often based on unrealistic assumptions, such as the non-separation of excitatory and inhibitory plasticity or the ignoring of Dale's Law, our framework offers a biologically plausible approach.[4–9] It is important to acknowledge that while our model has its strengths, there are aspects, particularly concerning real data, that could be explored in further research. Here, one illustration involves deciphering patterns from authentic neural spike trains, which can provide insights into how the brain processes speech recognition.

Our study has implications for future research in unsupervised learning of spatiotemporal input spike patterns. Although previous models have examined similar phenomena through the lens of spike-timing dependent plasticity (STDP), they have typically lacked the balanced excitation-inhibition relationship that we show is critical for robust and continuous learning.[5–7] Moreover, by exploring the complex interaction of neural mechanisms and their role in pattern recognition, this study serves as a stepping stone to a more comprehensive understanding of neural self-organization and computational neuroscience.

Indeed, the biologically plausible plasticity mechanisms that can facilitate the self-organization of spatiotemporal pattern recognition in individual neurons lend considerable credibility to the hypothesis that such intricate temporal coding schemes are naturally employed in biological neural networks. This is not only important in the context of computational neuroscience but also suggests ways in which natural systems deal with information and complexity.

Our research shows that these neural networks are more flexible, capable of processing both rate and temporal codes. Remarkably, the ability to learn underlying patterns even in the presence of Poisson spike rates suggests that temporal coding can coexist with, and even function as a complement to, rate-based coding schemes. This generalized coding strategy seems to combine two coding paradigms that are often considered mutually exclusive, suggesting that a more detailed understanding of neural coding may be needed.

In essence, our research reveals the possibility of self-organized pattern detection in biological neurons. This discovery provides a foundation for a more unified understanding of the various coding strategies employed in complex neural architectures.

Our research provides valuable insights into the field of neural networks and machine learning by introducing the first biologically plausible model for incremental self-supervised learning of spatio-temporal spike patterns. Our study highlights the instrumental role of pre-synaptic hetero-synaptic plasticity in the orthogonalization of weight vectors in receiving neurons.[10,11] When patterns are learned sequentially, the weight vectors maintain their orthogonal orientation, especially if the subsequent patterns are stochastic variations of the original. This process of orthogonalization provides two benefits: the preservation of existing memories and the facilitation of the acquisition of new information, thus achieving a balance between neural stability and plasticity.

In greater detail, it was observed that the orthogonal nature of weight vectors remains unchanged when learning patterns are generated through a Poisson process, even when learned incrementally. This finding supports the network's robustness to perturbations of pre-existing weight configurations and is consistent with previous studies that focus on the need for minimal perturbations between old and new learning. A feature of our model is its reliance on a unique balance between excitatory and inhibitory inputs, a harmony that naturally manifests during the learning process. This balance is crucial for memory maintenance, lending credence to earlier work suggesting its importance.[1] While this paper does not delve into the intricate relationship between the stability-plasticity balance and the excitation-inhibition equilibrium, it lays the groundwork for future investigations into this vital area. Our work differs from prior research that mainly focuses on recurrent networks and rate-based models.[12] Although these previous approaches also used orthogonalization mechanisms, they employed different strategies and were not specifically designed for spatiotemporal spike patterns. Moreover, our model is greatly improved by synaptic scaling mechanisms, which is in contrast with other models that depend on scaling with $(w^2)$ and were found not necessary for learning in the context of spatio-temporal spike patterns.[13]

Importantly, we agree with previous research that emphasizes the crucial impact of input noise on incremental learning.[5] In our model, noise not only drives the weight vectors towards or-

thogonality, but also minimizes their overlap across different output neurons, further optimizing the learning process.
In summary, our study presents a solid, biologically accurate resolution to the long-standing stability-plasticity problem in neuronal networks tasked with learning spatio-temporal patterns in a self-organizing manner. We demonstrate that the crucial components for effective incremental learning entail the careful balance of excitatory and inhibitory inputs, as well as the insightful integration of heterosynaptic plasticity and noise. These results lay the groundwork for further research to explore these mechanisms in more detail and to develop more effective and adaptive neural network architectures.

## 3.2 Excitatory / Inhibitory Ratio and Dynamic Range

This part of the discussion refers to the papers presented in 2.3 and 2.4.
While previous research has explored the role of synaptic plasticity in guiding neural systems towards criticality[14,15], our study expands on this by investigating the impact of inhibitory neurons on shaping phase transitions. Though we have gained valuable insights into how inhibition influences the emergence of criticality, further research is needed to examine the interplay between synaptic plasticity and the dynamic behavior of the order parameter.
Although criticality can be seen in a purely excitatory network[16,17], to understand criticality in neuronal systems, it is necessary to quantitatively characterize critical behavior in such systems. This can be done by determining factors such as the order of the transition and its universality class in a locally coupled leaky integrate-and-fire (LIF) network.
We observed a shift in neuronal activity from asynchronous states to synchronization. As we manipulated the inter-neuronal control parameter (synaptic efficacy, $K$), we observed a gradual transition from irregular spiking (subcritical phase) to synchronous spiking (supercritical phase). This shift is characterized by a complex critical phase transition, which we quantified using the Kuramoto order parameter.[18,19] However, the analysis of finite-size scaling led to the estimation of critical exponents for this transition and its resulting universality class, which does not fit into previously established classifications. It differs from that of mean-field directed percolation and directed percolation in 2 + 1.[20] Mean-field directed percolation is a theoretical model that predicts how certain types of processes, such as the spread of a disease, will play out over time in a large-scale, averaged system. Directional percolation in 2+1 dimensions is another model describing similar events, but in a specific framework considering the directions and dimensions of the events.
We showed in our study that the phase locking value (PLV) works as an order parameter in the LIF model, specifically in connecting spikes to PAV phases. This relationship holds true regardless of the system's inclusion of inhibitory neurons. However, the values of the phase transition parameters differ for each inhibitory percentage.
This transition is significant as it demonstrates correlations with frequently observed phenomena in actual neural systems, particularly the emergence of neural avalanches widely considered indicative of critical neural dynamics in the cortex, occurring in both *in vivo* and *in vitro* studies.[14,40,96,146] . Additionally, inhibitory neurons were incorporated to enhance comprehension of the elements that contribute to critical behavior in complex neural networks. Our results indicate that inhibitory neurons play a critical role in enhancing the network's ability to exhibit criticality. Our study demonstrated that an inhibitory neuron ratio of $20\%$ provides optimum enhancement of the system's dynamic range. This suggests that inhibition facilitates two purposes: balancing excitatory activity and creating an environment in which critical behavior can

occur more easily. This means that the critical behavior emerges in a wide range of parameter $K$. Although our focus was on a specific inhibitory ratio in a lattice, future studies could explore its impact on other network types. It is possible that another optimal inhibitory percentage maximizes the dynamic range for another network topology. However, which evolutionarily precise objective function results in this specific E/I ratio in the cortex needs to be investigated. This result could be due to inhibitory neurons being in phase with excitatory neurons, preventing synchronization at substantial connectivity levels ($K$), unlike in networks with a varied percentage of inhibitory neurons. The mechanism expands the leanth between the synchronized and desynchronized states in the phase transiton diagram, presenting a wider range of dynamic behaviors within the system. An important point to note, however, is that an excess of inhibitory influences can suppress the system's ability to synchronize, potentially pushing it into a persistently desynchronized state. Therefore, a well-balanced interplay between excitatory and inhibitory neurons is crucial for enhancing network complexity and critical behavior.

## 3.3 Effects of Optogenetic Stimulation on Gamma Activity in The Visual Cortex

This part of the discussion refers to the paper presented in 2.5.
Our research aimed to understand the role of gamma oscillations in the visual cortex through optogenetic stimulation combined with visual cues. Our findings emphasize the essential role of gamma oscillations, specifically low gamma oscillations, in cortical functioning. We observed a boost in low gamma power in both layers (II and IV) of the visual cortex upon optogenetic stimulation. The concurrent presentation of visual stimuli resulted in varying effects across these layers.
To analyze the experimental data, the Wilson-Cowan model[21] which has previously been used to explain enhanced gamma oscillations[22], and phase-amplitude coupling[23] was utilized, indicating that differences in excitatory currents among these layers could account for the variation in responses.
Our modeling goal was to provide a descriptive approach rather than a quantitative one and a conceptual representation of our empirical findings, focusing on variables contributing to observed gamma oscillation power variations. More specifically, the laser stimulus is considered a source of external current into the neuronal populations and is applied to neurons during laser onset.[24]
Our research indicates that stimulation of excitatory neurons affects gamma oscillations. Although optogenetic stimulation was directed towards excitatory neurons, inhibitory neurons are also likely to be involved, possibly leading to a modulation of gamma power.
More specifically, due to the opsin type utilized in our experiment, optogenetic laser stimulation induces excitation in the excitatory neurons. When both the visual and optogenetic stimuli are present at the same time, the neurons' excitation causes different patterns of activity in the network in layers II and IV. This disparity in activity might be a direct consequence of the distinct network architectures in these layers. The neural networks of the primary and secondary visual cortices differ, revealing various stages of visual processing that take place in these regions. These areas have individual features regarding neuronal subtypes, connections, receptive fields, and reactions to visual stimuli.[25]

## 3.4 Future perspective

**Learning of Spatio-Temporal Spike Patterns**

- Exploring key parameters for applying spatio-temporal spike pattern learning algorithm to real-world data.
  The focus here is on delineating the critical parameters for implementing a spatio-temporal spike pattern (STSP) learning algorithm when dealing with real-world datasets. The goal is to bridge the gap between theoretical STSP models and their practical applications, which is essential for advancing machine learning methods towards real-world complexity. Real-world data often presents challenges such as noise, incomplete information, and dynamic changes over time, which can significantly affect the performance of spike pattern learning algorithms. To address these issues, I propose to investigate a number of parameters, including spike timing, neuronal arrangement, learning rates, and threshold adjustments. Optimizing these parameters could improve the robustness and accuracy of the algorithm in various application scenarios. It may also be helpful to consider cross-homeostatic rules rather than the classical form of homeostatic plasticity.[26] This research has the potential to significantly impact how neural network models are calibrated and implemented to solve complex, time-sensitive, and spatially-oriented problems in various domains.

- Investigation of the rule of E/I balance in the stability/plasticity dilemma. Inhibitory neurons maintain memory by trying to inhibit excitatory activity until the excitatory/inhibitory balance is completely destroyed and neurons burst.
  In more details, inhibitory neurons play a critical role in memory by attempting to suppress the activity of excitatory neurons. This prevents neural networks from becoming overactive or saturated with information, which could lead to forgetting. This delicate balance is an ongoing process in which the network self-regulates to avoid excitatory dominance and maintain functional stability. However, if this balance is tipped too far toward inhibition, excitatory inputs may not be sufficient to maintain circuit activity. This can lead to a loss of information and memory. On the other hand, if inhibitory systems are weakened, runaway excitatory activity may destabilize neural circuits and lead to excessive plasticity, which undermines the ability of the network to maintain long-term memory.
  This research focuses on understanding the mechanisms by which inhibitory control can modulate this balance and how dysregulation leads to bursts of neural activity that potentially erase stored information. This study may shed light on memory disorders and potentially help develop treatments that can restore or improve cognitive function by modulating the E/I balance.

**Excitatory / Inhibitory Ratio and Dynamic Range**

- Consideration of synaptic plasticity and investigation of the dynamic behavior of the order parameter despite synaptic plasticity at each time phase.
  This research is devoted to investigating how the order parameter evolves over time despite the continuous changes induced by synaptic plasticity. At each time step, synaptic efficacy is modified, leading to a change in the overall behavior of the neural circuit. This dynamic interplay poses a challenge for predicting system behavior because traditional models of neural activity often assume static synaptic strengths and may not account for

the continuous adaptation inherent in real neural systems.
This study examines the time-dependent nature of synaptic plasticity and its impact on global patterns of neural activity. This involves tracking the order parameter through different phases of learning and memory, from the initial encoding of information to its long-term consolidation and potential forgetting. Understanding these dynamics can provide insights into the fundamental principles governing the rules of synaptic modification and the functioning of neural circuits.
The incorporation of models of synaptic plasticity into our analyses aims to provide a more accurate and comprehensive picture of how neural systems adapt over time, which is crucial for the development of better learning algorithms in artificial intelligence and for informing therapeutic strategies for neurological disorders characterized by synaptic dysfunction.

**Effects of Optogenetic Stimulation on Gamma Activity in The Visual Cortex**

- Modeling the experiment in a more quantitative rather than descriptive way,
- Designing multi-array experiments and determining the exact rule of inhibition in the gamma power in each layer.
- Investigating how gamma power is modulated in response to preferred and non-preferred stimulus.

The effects of optogenetics on gamma activity in the visual cortex provide a rich understanding of the underlying mechanisms of visual processing and neuronal circuits.
This research approach involves a quantitative analysis of this phenomenon that goes beyond descriptive accounts to model the precise influences that optogenetically induced changes have on the gamma oscillations.
First, I propose to model the experiment using quantitative frameworks that allow precise characterization of gamma activity modulation by optogenetic stimulation. This includes the development of computational models that predict gamma oscillation patterns based on different intensities and frequencies of optogenetic stimuli. The simulation of these models will be used to understand the relationship between optogenetic stimulation parameters and changes in gamma power.
Second, multi-array experiments will be designed to dissect the layer-specific effects of inhibition on gamma power within the visual cortex. Through the application of optogenetic tools to selectively inhibit neurons in different cortical layers, we will be able to characterize the distinct contributions of each layer to the generation and modulation of gamma oscillations. The precise rule of inhibition and its effect on gamma oscillatory activity will be determined by analyzing the changes in gamma power with respect to different spatial and temporal patterns of optogenetic inhibition.
Lastly, this investigates how gamma power differentially responds to preferred versus non-preferred visual stimuli. This involves the presentation of visual cues that are either aligned or not aligned with the known preferences of the stimulated neuronal populations. The differential responses measured will reveal how intrinsic visual processing and attention mechanisms are reflected in the gamma activity and how they can be artificially modulated through optogenetic stimuli. The expected outcomes will significantly advance our understanding of the functional significance of gamma oscillations and their role in sensory perception.

# Bibliography


[1] Tim P Vogels, Henning Sprekeler, Friedemann Zenke, Claudia Clopath, and Wulfram Gerstner. Inhibitory plasticity balances excitation and inhibition in sensory pathways and memory networks. *Science*, 334(6062):1569–1573, 2011.

[2] Sophie Denève and Christian K Machens. Efficient codes and balanced networks. *Nature neuroscience*, 19(3):375–382, 2016.

[3] Michael Okun and Ilan Lampl. Instantaneous correlation of excitation and inhibition during ongoing and sensory-evoked activities. *Nature neuroscience*, 11(5):535–537, 2008.

[4] Robert Gütig. Spiking neurons can discover predictive features by aggregate-label learning. *Science*, 351(6277):aab4113, 2016.

[5] Guo-qiang Bi and Mu-ming Poo. Synaptic modifications in cultured hippocampal neurons: dependence on spike timing, synaptic strength, and postsynaptic cell type. *Journal of neuroscience*, 18(24):10464–10472, 1998.

[6] Bernhard Nessler, Michael Pfeiffer, Lars Buesing, and Wolfgang Maass. Bayesian computation emerges in generic cortical microcircuits through spike-timing-dependent plasticity. *PLoS computational biology*, 9(4):e1003037, 2013.

[7] Henry Markram, Joachim Lübke, Michael Frotscher, and Bert Sakmann. Regulation of synaptic efficacy by coincidence of postsynaptic aps and epsps. *Science*, 275(5297):213–215, 1997.

[8] Timothée Masquelier. Stdp allows close-to-optimal spatiotemporal spike pattern detection by single coincidence detector neurons. *Neuroscience*, 389:133–140, 2018.

[9] Sadique Sheik, Somnath Paul, Charles Augustine, and Gert Cauwenberghs. Membrane-dependent neuromorphic learning rule for unsupervised spike pattern detection. In *2016 IEEE Biomedical Circuits and Systems Conference (BioCAS)*, pages 164–167. IEEE, 2016.

[10] Marina Chistiakova, Nicholas M Bannon, Jen-Yung Chen, Maxim Bazhenov, and Maxim Volgushev. Homeostatic role of heterosynaptic plasticity: models and experiments. *Frontiers in computational neuroscience*, 9:89, 2015.

[11] Rudi Tong, Thomas Edward Chater, Nigel John Emptage, and Yukiko Goda. Heterosynaptic cross-talk of pre-and postsynaptic strengths along segments of dendrites. *Cell reports*, 34(4), 2021.

[12] Christian Leibold. Neural kernels for recursive support vector regression as a model for episodic memory. *Biological Cybernetics*, 116(3):377–386, 2022.

[13] Christian Tetzlaff, Christoph Kolodziejski, Marc Timme, Misha Tsodyks, and Florentin Wörgötter. Synaptic scaling enables dynamically distinct short-and long-term memory formation. *PLoS Computational Biology*, 9(10):e1003307, 2013.

[14] Fabrizio Lombardi, Hans J Herrmann, and Lucilla de Arcangelis. Balance of excitation and inhibition determines 1/f power spectrum in neuronal networks. *Chaos: An Interdisciplinary Journal of Nonlinear Science*, 27(4), 2017.

[15] Roxana Zeraati, Viola Priesemann, and Anna Levina. Self-organization toward criticality by synaptic plasticity. *Frontiers in Physics*, 9:619661, 2021.

[16] Christian W Eurich, J Michael Herrmann, and Udo A Ernst. Finite-size effects of avalanche dynamics. *Physical review E*, 66(6):066137, 2002.

[17] Mohammad Dehghani-Habibabadi, Marzieh Zare, Farhad Shahbazi, Javad Usefie-Mafahim, and Paolo Grigolini. Neuronal avalanches: Where temporal complexity and criticality meet. *The European Physical Journal E*, 40:1–7, 2017.

[18] Yoshiki Kuramoto. International symposium on mathematical problems in theoretical physics. *Lecture notes in Physics*, 30:420, 1975.

[19] Juan A Acebrón, Luis L Bonilla, Conrad J Pérez Vicente, Félix Ritort, and Renato Spigler. The kuramoto model: A simple paradigm for synchronization phenomena. *Reviews of modern physics*, 77(1):137, 2005.

[20] Junfeng Wang, Zongzheng Zhou, Qingquan Liu, Timothy M Garoni, and Youjin Deng. High-precision monte carlo study of directed percolation in (d+ 1) dimensions. *Physical Review E*, 88(4):042102, 2013.

[21] Hugh R Wilson and Jack D Cowan. A mathematical theory of the functional dynamics of cortical and thalamic nervous tissue. *Kybernetik*, 13(2):55–80, 1973.

[22] Jorge F Mejias, John D Murray, Henry Kennedy, and Xiao-Jing Wang. Feedforward and feedback frequency-dependent interactions in a large-scale laminar network of the primate cortex. *Science advances*, 2(11):e1601335, 2016.

[23] Angela CE Onslow, Matthew W Jones, and Rafal Bogacz. A canonical circuit for generating phase-amplitude coupling. *PloS one*, 9(8):e102591, 2014.

[24] Stewart Heitmann, Michael Rule, Wilson Truccolo, and Bard Ermentrout. Optogenetic stimulation shifts the excitability of cerebral cortex from type i to type ii: oscillation onset and wave propagation. *PLoS computational biology*, 13(1):e1005349, 2017.

[25] Tania A Seabrook, Timothy J Burbridge, Michael C Crair, and Andrew D Huberman. Architecture, function, and assembly of the mouse visual system. *Annual review of neuroscience*, 40:499–538, 2017.

[26] Saray Soldado-Magraner, Michael J Seay, Rodrigo Laje, and Dean V Buonomano. Paradoxical self-sustained dynamics emerge from orchestrated excitatory and inhibitory homeostatic plasticity rules. *Proceedings of the National Academy of Sciences*, 119(43): e2200621119, 2022.

# Chapter 4

# Conclusion

This comprehensive study of neural networks, ranging from the learning of spatio-temporal spike patterns to the critical role of the excitatory/inhibitory ratio in neural dynamics and the modulation of gamma oscillations in the visual cortex using optogenetics, has led to several insights.

Firstly, in the domain of spatio-temporal spike pattern learning, it has been shown that neural networks exhibit an intrinsic tendency toward self-regulation and stability through a subtle interplay of Hebbian mechanisms, hetero-synaptic plasticity, and synaptic scaling at both excitatory and inhibitory synapses. This also facilitates the dynamic behavior required for complex processes such as learning and memory. The results highlight the unsupervised learning capabilities of neural systems, thus eliminating the need for external supervision or unrealistic assumptions prevalent in previous models. Additionally, the inherent flexibility of these networks was demonstrated by their dual encoding capabilities for rate and temporal coding.

Secondly, The examination of the fundamental dynamics of neural networks, specifically the occurrence of neural avalanches, highlights the role of the E/I ratio in achieving system criticality. Moreover, the existence of an optimal level of inhibitory neurons expands the range of dynamics in the system.

Lastly, the optogenetic study, particularly in the responses of different layers to combined optogenetic and visual stimuli, explained through the Wilson-Cowan model, indicates a complex modulation of excitatory currents within the cortex that is dependent on the layer.

Across all these investigations, one dominant fact remains: neural networks are complex, self-regulating, and highly adaptive. The self-organized learning of spike patterns, the E/I ratio that might drive critical dynamics, and the delicate modulation of cortical oscillations each highlight the inherent complexity of neural systems. These results are contributions to our understanding of neural networks and computational neuroscience, yet there is still vast uncharted territory that requires further exploration.

In the future, it will be essential to address the limitations of current models and approaches, particularly in the realistic simulation of synaptic dynamics and the more accurate incorporation of biological details. Future research efforts should focus on these aspects and address the unexplored interactions between synaptic plasticity, inhibitory mechanisms, and the resulting neural behaviors. Furthermore, taking a more comprehensive approach and combining these various viewpoints could lead to the development of a unified theory that has the potential to greatly impact both neuroscience and artificial intelligence applications.

In essence, exploring these diverse aspects of neural functionality not only reveals the remarkable complexity and adaptive capabilities inherent in neural systems but also sets the stage for future interdisciplinary research that advances our understanding of both biological intelligence

and its potential synthetic counterparts.

**Acknowledgement**

In the process of writing, I utilized special tools such as ChatGPT and DeepL (https://www.deepl.com) to ensure the clarity, accuracy, and correctness of the English language in this document.